University of Stavanger

Faculty of Science and Technology

MASTER'S THESIS

Study program/ Specialization: Masters of Science in Environmental Offshore Engineering	Spring semester, 2014 Restricted access
Writer: Jonas Ntiako	…… (Writer's signature)

Faculty supervisor:
Professor Torleiv Bilstad

External supervisor(s):
Dr. Ashish Sahu

Thesis title:

Pilot Scale Testing of Salsnes Filter (SF500) for Biofilm Solids Removal from a Full Scale Wastewater Treatment Plant

Credits (ECTS): 30

Key words: Biofilm Solids Coagulation/flocculation MBBR Particle Size Distribution Salsnes Filters Wastewater treatment Zeta potential	Pages: 130 + enclosure: 8 Stavanger, 14th July 2014

DEDICATION

This thesis is dedicated to God, for His favour and grace through my studies. Secondly, I dedicate it to my parents, Mr. and Mrs. Ntiako, for their financial support and words of inspiration.

ACKNOWLEDGEMENT

I would like to show my extreme gratitude to my internal supervisor Professor Torleiv Bilstad for giving me this opportunity for industrial experience with AquateamCOWI and Salsnes Filter AS. A special thanks to my external advisor, Dr. Ashish Sahu for his advice and guidance throughout the study, and also giving me the opportunity to build my self confidence in making decisions.

I would like to thank Charles Otis for his support whenever I needed it. I will like to thank Valeri. A. Razafimanantsoa for his guidance and support.

I would like to thank Dini Adyasari and Mamy Ariniana for being accommodative and making it possible to work effectively as a team. I will like to thank AquateamCOWI for their support, and also making me feel part of their team. I would like to thanks NFR wwtp for giving me their premises, and the required volume of chemicals needed for this thesis.

Finally, I would like to thank my family and friends, for their support and words of motivations.

ABSTRACT

This thesis investigated the performance of Salsnes Filter (SF) as a secondary treatment after biological treatment processes at Nordre Follo Renseanlegg (NFR) wastewater treatment plant. Wastewater from moving bed biofilm reactor (MBBR) from Reactor 5, was coagulated/flocculated and filtered on a prototype pilot scale SF500 filter. The investigation included use of PAX-18 aluminum inorganic coagulant, cationic polymers (C-496, C-490), and anionic polymer (A-130), in conjunction with flocculation. A bench scale SF apparatus was used for predictions and selecting optimum parameters for pilot scale coagulation/flocculation with SF fine mesh sieves sizes 250, 210, 158, 90, 54, 33 and 18 µm. Pilot scale testing on the prototype SF500 and on a SF1000 full scale filter were conducted after bench scale testing. PAX-18 and Superfloc C-496 were selected as optimum chemicals to be used on pilot scale coagulation/ flocculation testing. Optimum G-value and flocculation time were of 67.8 s^{-1} and 10 min respectively were investigated and used. An optimum dosage of 94.6 mg Al/g TSS + 7.1 mg C-496/g TSS was used to achieve filtrate containing TP (< 0.3 mg/L), TSS (< 30 mg/L) and COD (< 50 mg/L), for removal efficiency of 96%, 98% and 88% respectively, using a 33µm fine mesh sieve. The pH change, filtration rate and power consumption in the process were also monitored.

Particle size characterization of raw NFR primary (degritted) wastewater and MBBR biofilm wastewater were also investigated using FlowCAM and Malvern Mastersizer 3000 after bench scale SF apparatus with sieve openings from 350 to 18 µm. The SF1000 was also used for NFR primary (degritted) wastewater characterization investigationswith both 33 µm and 350 µm fine mesh openings.

LIST OF ABBREVIATIONS

BNR	–	Biological Nutrient Removal
COD	–	Chemical Oxygen Demand
EU	–	European Union
MBBR	–	Moving Bed Biofilm Reactor
NFR	–	Nordre Follo Resnseanlegg
SF	–	Salsnes Filter
SS	–	Suspended Solid
TN	–	Total Nitrogen
TSS	–	Total Suspended Solid
TP	–	Total Phosphorus
PAX	–	Polyaluminiumchloride
PSD	–	Particle Size Distribution
wwtp	–	Wastewater Treatment Plant

TABLE OF CONTENT

Page

LIST OF TABLE

LIST OF EQUATIONS

LIST OF FIGURES

OVERVIEW

This thesis consists of five (5) parts. First is the introduction and objectives of the study. Second will be the literature review and theories relating to the above introduced topics. Third will be a presentation of the materials and methodologies employed during the study. The forth part presents the results and observations during the study. The conclusion and future recommendations will be provided in the final part of this thesis. In addition to the main parts of this thesis, supporting data for references, pictures and any standard methods referred will be provided in the appendices and bibliography.

CHAPTER I

1.0 INTRODUCTION AND OBJECTIVES

As the population grows, the scientific community faces new challenges and environmental protection becomes a global concern. The increase in concentration of harmful nutrient compounds, such as phosphorus and nitrogen in municipal wastewater plant discharge, has a negative impact causing eutrophication of surface waters. This problem continues to grow, since conventional biological wastewater processes are not capable of treating and removing phosphorus and nitrogen to an extent needed to protect sensitive surface waters (Headworks, 2014). As laws governing discharge of constituents in wastewater become increasingly strict, wastewater treatment becomes more of a challenge; it is more difficult, and expensive to achieve. This has led to research and implementation of new effective and efficient technologies, as well as efforts to improve existing ones (Artiga et al., 2005; Jiang and Zheng, 2013; Woisetschläger et al., 2013). Other areas of research focus on how to significantly reduce investment costs, energy consumption, and space requirements, compared with other treatment processes (Ruiken et al., 2013; Rusten and Ødegaard; 2006, Webster, 2001).

1.1 Biological Nutrient Removal

Biological Nutrient Removal (BNR) is a process used purposely for removing nitrogen and phosphorus from wastewater, before it is discharged into surface or ground water. BNR is described mainly by three groups of organisms functioning in three different zones. These zones are aerobic, anoxic, and anaerobic in a BNR wastewater-treatment plant (wwtp). These functional organisms are ordinary heterotrophic organisms (OHOs), autotrophic nitrifier organisms (ANOs) and phosphorus accumulating organisms (PAOs). The OHOs break the influent wastewater biodegradable organics (COD). The ANOs nitrifies ammonia to nitrate. The PAOs take up phosphorus in excess and store it intracellularly as polyphosphate chains (Ekama, 2011):

These BNR organisms are utilized in wastewater treatment either by suspended growth (activated sludge), or attached growth (biofilm) process. This thesis considers a wastewater treatment plant (NFR) that uses an attached growth process (MBBR) to remove biological nutrient.

1.2 Nordre Follo Renseanlegg (NFR) wwtp

NFR wwtp uses moving bed biofilm reactor (MBBR) technology for its biological nitrogen removal. It consists of two roll nitrogen removal reactor network lines. Each of these lines consists of seven (7) reactors. These reactors are operated as anoxic, aerobic or anoxic/aerobic as shown in Figure 2-3. Each reactor is partially filled with bio-coated (biofilm) Kaldnes carriers. These reactors are equipped with aerators (aerobic zones) and mechanical power stirrers (anoxic zones). It has been designed and monitored to ensure that at least 70% nitrogen removal is achieved (NFRA, 2014). The biofilm consists mostly of nitrifying bacteria and are formed on Kaldnes carriers (K1). Some of the biomass is active in the anoxic reactors and therefore only stirring is required in those reactors. The stirrers cause the Kaldnes carriers to move around and knock each other, while bacteria consume the organic matter in the water. During this movement, the weak or dead biomass falls off from the Kaldnes carriers and flows with the water to the next reactor. In the aerobic reactors, oxygen is added by pumping air through aerators. Aeration causes the Kaldnes carriers to rotate around the reactor, and the same process occurs as with mechanical stirring. The weak or dead biomass that falls from the MBBR reactors is called 'biofilm solids.' Though NFR has seven reactors in a roll, only Reactor 5 effluent was considered in the current study to remove the biofilm solids using coagulation/flocculation process and filtered using SF500. This reactor was selected based on previous experiments carried out by Ng (2012). This MBBR Reactor 5 as shown in Figure 1-1 is an aerobic reactor, with mechanical stirrer and has pH of 6.5.

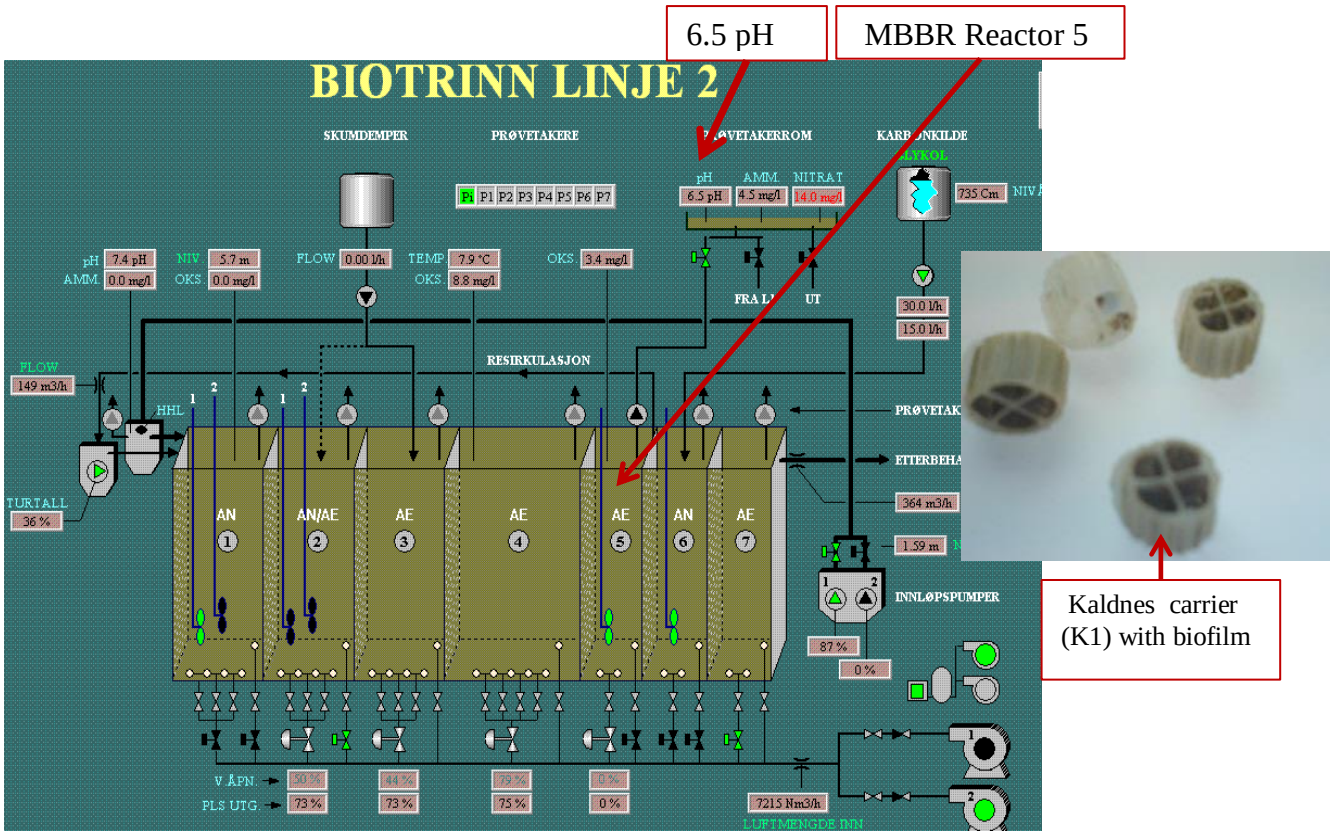

Figure 1-1: NFR MBBR process flow and Kaldnes carrier (NFRA, 2014)

Following the BNR process, it is necessary to remove the fallen off dead bacteria (biofilm) from the treated wastewater for final discharge. Secondary clarifiers are typically installed in conventional treatment plant for this purpose. The secondary clarifier has the specific purpose to separate and remove solids/biomass from biological process from effluent water in order to meet the discharge limit. Other processes include thickening solids for recirculation or storing biomass to buffer treatment process. Figure 1-2 shows the traditional wwtp with the use of secondary clarifier for biofilm solid separation.

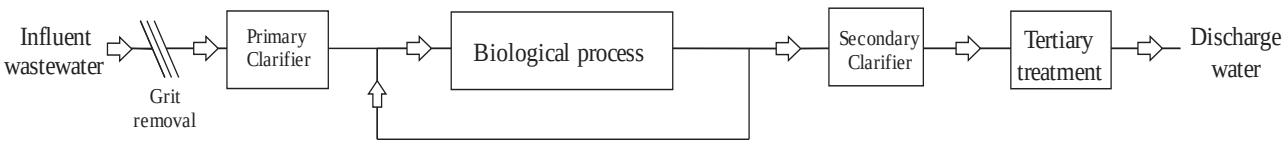

Figure 1-2: Traditional wwtp use of secondary clarifier for biofilm solids separation

The biofilm solids from the MBBR are in the order of 150 – 250 mg SS/l in normal municipal wastewater, therefore making it possible to combine the MBBR treatment with any of the commonly used separation technologies, settling, flotation, micro-screening, media filtration and membrane filtration (Ødegaard et al., 2010). NFR wwtp currently uses coagulation/flocculation process before dissolved air flotation (DAF) for removing the biofilm solids.

The thesis' purpose is to try Salsnes Filter filtration (SF500) after the NFR MBBR technology to separate excess biofilm from effluent water. DAF is a mechanically intensified system, which requires constant presence of an operator and equipment parts (Alemayehu, 2010). Because DAF uses a large foot print and high energy, the goal is to investigate if Salsnes Filters can potentially replace DAF units (and other clarifiers) for clarification purposes.

1.3 Salsnes Filter (SF)

Salsnes Filter (SF) is an eco-efficient solid separation technology developed in Namsos, Norway. The company Salsnes Filter AS has been operating since 1991 with research and development to produce a highly efficient and reliable filter that maximizes solids separation, while dramatically decreasing costs including capital, operating, maintenance, and foot print. The SF machine is a rotating belt filter is a system that incorporates solids separation, sludge thickening and dewatering in a single unit, drastically reducing transportation and disposal costs (Salsnes Filter, 2014). Research and testing performed by Rusten and Ødegaard (2006) confirms that this compact unit technology is more efficient and fulfils all EU primary treatment when a sieve rates below $200 m^3/m^2$-h is normally used. The average removal efficiencies of SF is > 50% for SS and > 20% for BOD_5 (Salsnes Filter, 2014). Figure 1-3 shows SF possible use in wwtp.

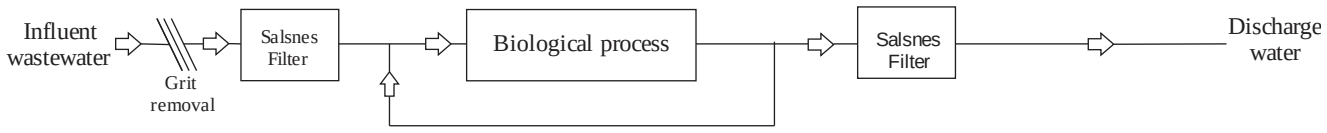

Figure 1-3: Use of SF in wwtp

The company has various models with different specifications for different purposes and wastewater capacities to handle. These models includes; SF1000, SF2000, SF4000, SF6000, SFK 200, SFK 400 and SFK 600, with the main difference being size of the unit. However for this study a newly designed (prototype) SF500 and SF1000 were used in the filtration and particle characterization test respectively. Figure 1-4 shows the general SF fine mesh rotating belt sieve machine with its various components.

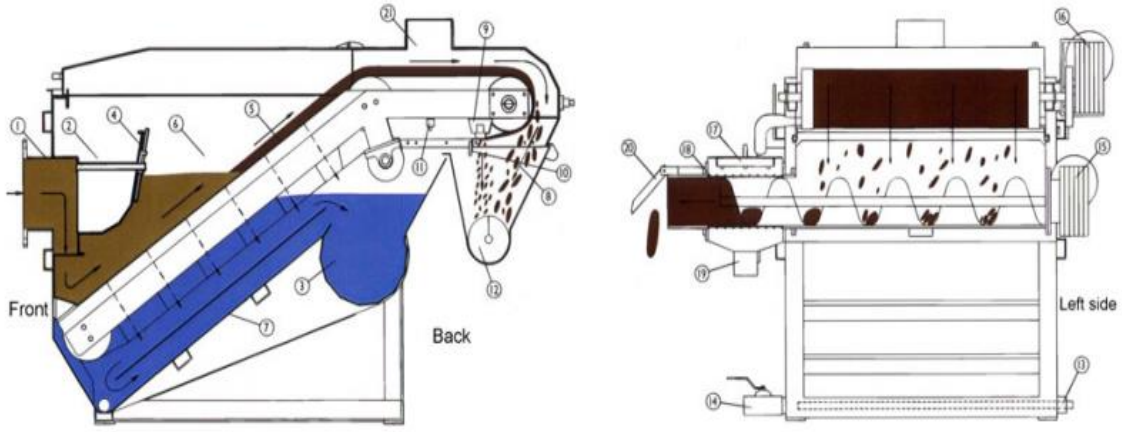

1. Inlet
2. Overflow
3. Outlet
4. Level indicator
5. Wire cloth
6. Wastewater
7. Filtered water
8. Sludge compartment
9. Air-Knife cleaning device
10. Rubber scraper
11. Hot water nozzles
12. Screw
13. Cold water pipe for settled waste removal
14. Drain valve for settled waste
15. Gear/motor for screw press
16. Gear/motor for wire cloth
17. Hot water nozzles for cleaning press cylinder
18. Press cylinder
19. Reject from press cylinder
20. Spring-loaded lid
21. Ventilation

Figure 1-4: General fine mesh rotating belt sieve machine (Brandy et al., 2006)

However, regardless of the technology employed for treatment, removal efficiency can be improved when one carries out a technical or pilot scale testing of that specific technology to determine various treatment conditions and parameters that ensures a high removal performance for a specific wastewater quality (Luo et al., 2014).

Ødegaard et al. (2004) concluded that biofilm solids separation could be enhanced with the use of chemicals to form flocs followed by filtration. It is with this theory that SF implemented studies (Ng, 2012) to enhance its technology for tertiary wastewater treatment

based on the successes it has achieved on municipal primary wastewater treatment (Rusten and Ødegaard, 2006).

Coagulation/flocculation was the key physicochemical process used to increase the biofilm solids size before SF500 filtration. Coagulation/flocculation is a long established technique for the significant removal of colour, particulate matter including protozoa, viruses, bacteria, and other micro-organisms (Gough et al., 2013; Tzfati et al., 2011). This thesis looks at ways to improve the SF technology performance with chemical addition, for removing biofilm solids from a full scale moving bed biofilm reactor (MBBR) at Nordre Follo Resnseanlegg (NFR) wastewater treatment plant (wwtp). Figure 1-5 shows the current study area for this thesis at NFR wwtp with the use of SF500 after coagulation/flocculation.

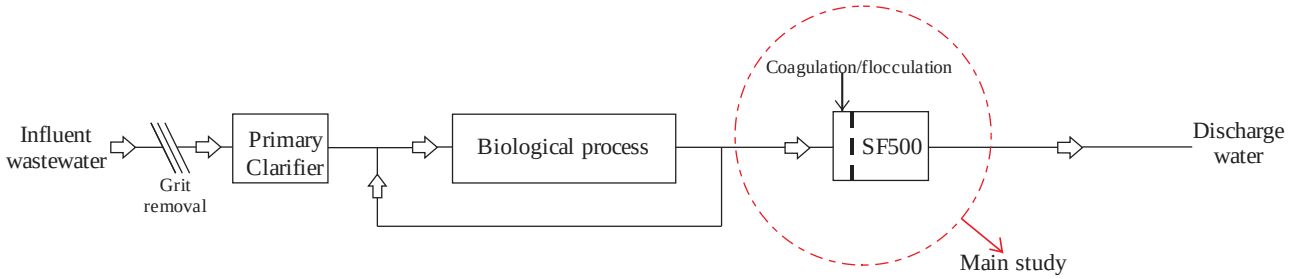

Figure 1-5: Current thesis study

1.4 Particle Size Distribution

Particle size distribution (PSD) is a valuable tool or indicator of quality and performance. Separation steps such as screening and filtering are monitored by measuring PSD before and after the process. The only techniques that can describe PSD using multiple values are microscopy or automated image analysis. Measurements in the laboratory are often made to support unit operations taking place in a process environment (Horiba, 2012).

SF1000 and bench scale SF apparatus (Rusten, 2004) were used to characterize the primary (degritted) wastewater and MBBR Reactor 5 wastewater at NFR wwtp, using particle size distribution (PSD) analysis.

1.5 Objectives

This thesis is a continuation of bench scale studies for the removal of MBBR biofilm solids SF fine mesh sieves (Ng, 2012) at the NFR wwtp. The overall objective of this thesis was to perform a pilot scale testing on SF500 machine with different mesh sieve sizes after biological treatment, with the motive of selecting a mesh sieve size, coagulant and polymer type, coagulant/polymer dosages, and other parameters that can aid in effectively and efficiently removing MBBR effluent biofilm solids. The main aim was to obtain an SF effluent with total suspended solids (TSS), total chemical oxygen demand (COD) and total phosphorus (TP) less than 30 mg/L, 50 mg/L and 0.3 mg/L respectively, with minimum chemical dose and minimal coagulation/flocculation time. SF1000 was also tested with mesh sieves 33µm and 350µm on the NFR primary (degritted) wastewater to characterise its effluent water. The specific objectives for this thesis are listed as follows:

- Conduct jar test experiment and bench scale SF test on NFR MBBR Reactor 5 effluent water for coagulant/polymer screening, coagulant/polymer dosage optimization, and G-value evaluations for floc formation.
- Conduct continuous MBBR Reactor 5 effluent wastewater pilot scale coagulation/flocculation with optimum parameters before SF500 filtration to achieve targeted TSS, TP and COD with high removal efficiencies.
- Characterise NFR primary (degritted/untreated) wastewater, using bench scale SF screening apparatus with 350, 250, 150, 90, 74, 55, 33, and 18µm fine mesh sieves.
- Characterise MBBR Reactor 5 effluent wastewater, using bench scale SF screening apparatus with 350, 250, 150, 90, 74, 55, 33, and 18µm fine mesh sieves.
- Characterise NFR primary (degritted/untreated) wastewater, using SF1000 with 33µm and 350µm mesh sieves.

1.6 Motivation

Though past evaluations performed by Rusten and Ødegaard (2006) showed good performance for SF, there were still some few questions unanswered with regards to this study: Why was there no significant removal efficiency with SF treatment with or without chemically enhanced primary treatment in some wwtp? Why could there be a negative TSS removal when chemical precipitation (coagulant and polymer) was used before SF machine? These questions give an indication of how critical all relating parameters are, to achieving the

target TSS, TP, COD with chemical precipitation (coagulant and polymer) on biofilm solids before SF500.

These questions also raise concerns about the design of the filter and also with the cleaning of the filter mesh after it has captured floc particles, which could have otherwise pass through the TSS analysis filter (GF/C filter 1.2µm) without chemical precipitation. This suggested for critical study on SF, especially with respect to the cleaning procedure at the early stages of the thesis. It was then realised at the beginning of the project, that the targeted effluent TSS and TP can't be achieved if these problems already identified (Rusten and Ødegaard, 2006) persisted. Therefore efforts were put in place to identify some problems through visual observations and effluent particle size distributions (PSD) analysis to identify sizes of particles that made their way to the effluent water after filtration. Possible solutions were suggested to fix some of the identified problems with the SF500 before the main study began.

Another question that came to mind was: could a reliable prediction be made to establish the SF sieve removal efficiencies and filtration rate with the screening test while dealing with floc particles? Studies were also made on the previously designed bench scale SF test apparatus (Rusten, 2004) to try and minimise possible breakdown of flocs which could compromise the prediction on the mesh.

The motivation was to see if the main objective of the thesis could be achieved with SF500 machine, and even beyond the expected values, with minimum cost of coagulant/polymer and power consumption. When these are achieved, it could pave the way for Salsnes Filter AS to increase production and make its product more attractive to the international market, and to put the company a step ahead of other filter technology companies.

CHAPTER II

2.0 LITERATURE REVIEW AND THEORY

This section will seek to justify the relevance of the study base on research made by scholars. As already stated by Ng (2012), there is very little research published literature on using coagulation/flocculation process to separate biofilm solids after biological treatment. However, there is some research has been conducted that is closely related to the subject of the current study. The material relevant to this thesis was used to forecast and predict the quality of MBBR wastewater to be expected, especially the characteristics of biofilm solids. A forecast was also made on the mechanisms of coagulation/flocculation process, factors that can influence better biofilm solids removal as well as what to expect before and after SF filtration. SF filter operation was studied, especially regarding the changing of filter cloths and PLC user interface control. This section of the thesis will demonstrate the knowledge needed to understand the scientific reasons behind each activity performed.

2.1 Characteristics of particles

The nature and behaviour of all particulate suspensions is fundamentally controlled by interfacial properties (particle size, particle shape, surface area, porosity, and morphology) and interfacial chemistry (surface charge, surface tension contact angle). Surface charge usually develops on wastewater particles either by differential ion solubility, direct ionization of surface groups, isomorphous ion substitution, specific ion adsorption, or anisotropic crystals (Fairhurst, 2014). In the case of MBBR biofilm wastewater, one could anticipate most of the surface charge developing processes have already taken place. This is because wastewater typically contains particles and components, which are soluble and react with other substances. Again, ion exchange between particles as well as bacterial activities involved in utilizing organic compounds also result in creating surface charges.

2.1.1 Particle Charge

Particle charge in neutral water is always assumed to be negative, but this is not always the case; it can also be positively charged. Particle charge in any water type is basically determined by various composition of that particular water quality. Components such as ferric hydroxide, aluminium hydroxide, chromium hydroxide, thorium oxide, zirconium oxide, basic dyes and basic proteins give water type with positive surface charges. However components such as silicon dioxide, Au, Ag, Pt, acidic dyes, acid protein, viruses, microbes,

and air bubbles gives water type with negative surface charges (Fairhurst, 2014). MBBR effluent most likely has a negative surface charge due to the microbial activities in the moving bed biofilm reactors.

A negatively charged particle in wastewater does not possess a net charge due to the accumulation of positive counter ions near its surface. This negative charge with its positive counter ions form a double layer (Davis, 2010). The electrical double layer shown in Figure 2-1 makes an important contribution to the stability of the MBBR effluent dispersions.

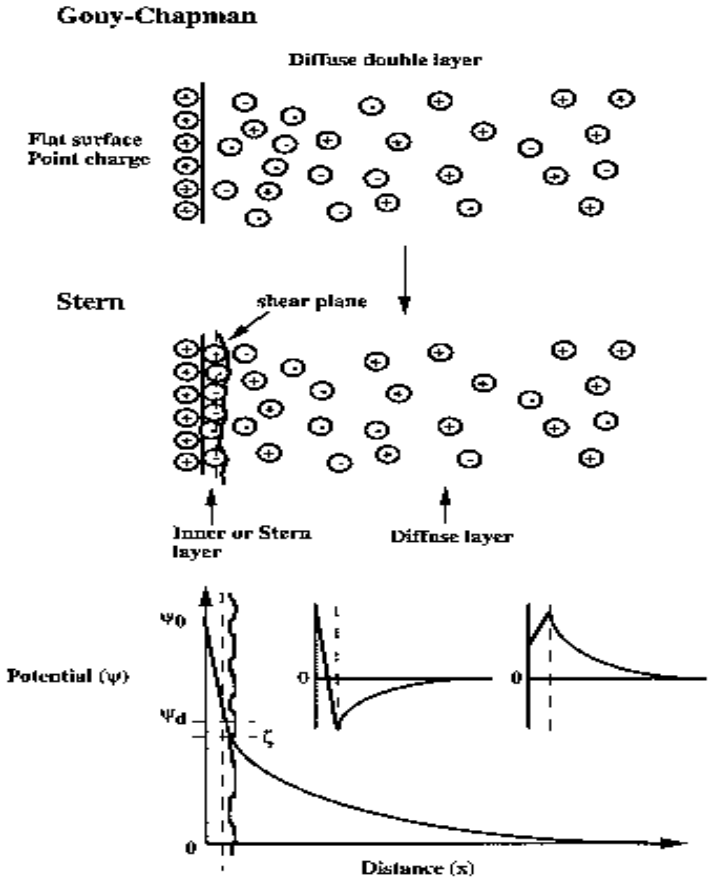

Figure 2-1: An illustration of the basic models proposed to describe the diffuse double layer. The Gouy Chapman model considers a flat surface and point charge. The Stern model adapted this to include a layer of tightly adsorbed ions that can `shear' at a distance from the surface of a particle and the zeta potential (ζ) is an approximate, but experimental, measure of this theoretical shear plane. The inserts also illustrate that the ζ can carry a greater, or opposite charge than would be predicted from the surface charge of the particle (Geoffrey, 2010, Smith et al., 1997)

2.1.1.1 Zeta potential

Zeta potential as shown in Equation 2-1 below is defined as the potential in mV at the shear plane. It is a measure of the charge on a particle surface in a specific liquid medium. It cannot be determined directly and therefore experimentally predicted as an approximate potential at the stern layer. It gives an indication of the stability of dispersions. The larger the value of zeta potential predicts a more stable dispersion. Therefore knowing this potential helps one to know how stable the wastewater is and also have an idea of how many counter ions will be needed to destabilize the particles (Fairhurst, 2014).

Equation 2-1: Relationship between theoretical potential and Zeta potential

$$\Psi = \zeta \exp(kx)$$

Where;

Ψ is the theoretical potential (mV)
ζ is the zeta potential (mV)
k is the Debye-Hückel parameter
x is the distanct (m)

The Debye length (k^{-1}) is a measure of this electric double layer thickness. The electric potential through Debye length depends on the ionic composition of the MBBR effluent water. Hence increasing k, through electrolyte addition, compresses the electric double layer of the medium, thereby decreasing the zeta potential. Therefore coagulating MBBR effluent with electrolyte (aluminium) is expected to reduce the zeta potential so that aggregation can take place. It should also be made clear that the more electrolyte addition may also increase the zeta potential to the opposite polarity which at some point will reverse the surface charge and re-stabilize particles. Figure 2-2 shows an illustration of the effect of cationic electrolyte concentration on the zeta potential of an anionic surface. Again it is seen that as the valence of the electrolyte increase, less concentration will be required to bring zeta potential close to zero and thereby enhancing the aggregation of biofilm particles.

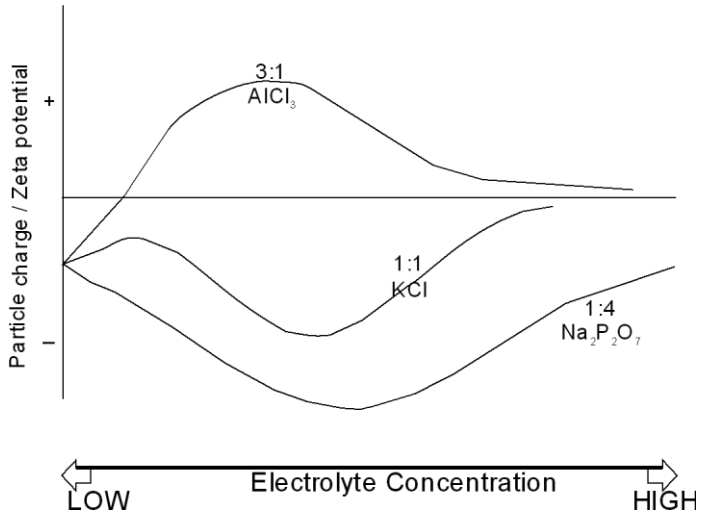

Figure 2-2: Effect of electrolyte concentration on suspension particle charge or zeta potential (Fairhurst, 2014)

Zeta potential depends not only on the fundamental surface sites, but also on the solution conditions (Dougherty et al., 2008) such as temperature, pH and electrolyte concentration (Ntalikwa et al., 2001). Zeta potential is usually derived using electrophoretic mobility, μ, of the particles from Equation 2-2 below. However it should be noted that the relationship between zeta potential and electrophoretic mobility is non-linear.

Equation 2-2: Relationship between zeta potential and electrophoretic mobility

$$\zeta = \frac{\eta}{2\varepsilon f(kr)}\mu$$

Where;

ζ is the zeta potential (mV)
η is the viscosity, (N s/m^2)
ε is the relative permittivity of the medium and
μ is the electrophoretic mobility
f(kr) is a numerical correction term that varies from 1 – 1.5 as *kr* varies from 0 to ∞ (Hunter, 1993).

Solutions with a zeta potential between +10 mV and -10 mV are described as within a critical range and therefore unstable. Solutions outside this range are stable and will require some concentration of electrolyte for coagulation to start or bring them within unstable range. This minimum concentration is known as critical coagulation concentration (CCC) and approximated in Equation 2-3 (Fairhurst, 2014). For the case of the NFR MBBR biofilm

solids the zeta potential measured in this thesis was outside the critical range (< -10 mV), therefore zeta potential analysis was performed with the coagulant (PAX-18) to bring the biofilm solid suspension to the critical range for coagulation to begin. This helped to minimize the aluminium dose as well as determining which polymer (cationic or anionic) to use at any point during flocculation process.

Equation 2-3: Critical coagulation concentration

$$\mathbf{CCC} \approx \frac{\boldsymbol{\zeta}^{\mathbf{4}}}{\mathbf{z}^{\mathbf{2}}}$$

Where;

CCC is the critical coagulation concentration (mol/L)
ζ is the zeta potential of suspension (mV)
z is the electrolyte valence

The zeta potential analysis was very useful in this thesis, to help predict the biofilm solid-solution interface, and to lower coagulant dose to obtain the right floc size for SF filtration.

2.2 Physicochemical treatment techniques for wastewater

Physicochemical processes are mostly employed on primary wastewater to achieve effluents of satisfactory inorganic and/or organic content, to be further treated by biological processes (Santo et al., 2012). However this is not the only location for chemical separation, but rather based on the purpose for which it is required. This thesis seeks to reduce phosphorus and therefore MBBR effluent was selected based on reasons that are outlined below in Section 2.4. There are different treatment techniques for the removal of inorganic and organic waste in recent years to decrease the amount of wastewater release to streams/rivers and to improve the quality of the treated effluent (Kurniawan et al., 2006; Verma et al., 2011; Woisetschläger et al., 2013). Most of these techniques have advantages and disadvantages (Kurniawan et al., 2006). These techniques include chemical precipitation, coagulation-flocculation, flotation, ion exchange and membrane filtration (Fu and Wang, 2011; Kurniawan et al., 2006; Machenbach, 2007; Wu et al., 2010). However coagulation-flocculation with filtration techniques (SF) was employed in this thesis to remove biofilm solids from MBBR reactor 5 effluent at NFR wwtp.

2.2.1 Coagulation-flocculation

Coagulation–flocculation is a widely used process to greatly enhance aggregation, to develop an increased size colloidal dispersions removal in water treatment works (Duan and Gregory, 2003; Jarvis et al., 2005; Shammas, 2004). As already stated in Section 2.1 any negatively charged particle outside the critical range under normal conditions, requires coagulation/flocculation process to destabilize them to form bigger flocs adequate for mesh filtration.

Principally, coagulation/flocculation process destabilises or reduces the likely negative charge on the MBBR effluent biofilm solids, which then allows the Van der Waals force of attraction to encourage initial aggregation to form microflocs (Ebeling et al., 2006). The terms coagulation and flocculation tend to be used interchangeably in colloid science (Geoffrey, 2010), but a distinction should be made: coagulation involves a close aggregation or even a merging of the particles, while flocculation refers to a loose aggregation of colloidal particles or previously coagulated particles (Geoffrey, 2010; McCurdy et al., 2004). There are two major class of chemicals used in coagulation/flocculation processes (Bratby, 2007; Duan and Gregory, 2003; Gough et al., 2013; Mukherjee et al., 2004):

1. Inorganic and organic coagulants including:
    I. Mineral additives (lime, calcium salts, etc.)
    II. Hydrolysing metal salts (aluminium sulphate, ferric chloride, ferric sulphate, etc.)
    III. Pre-hydrolysed metals (polyaluminiumchloride (PAX), polyaluminosilicate sulphate, etc.)
    IV. Polyelectrolytes (coagulant aids)
2. Organic flocculants including:
    I. Cationic and anionic polyelectrolytes
    II. Non-ionic polymers
    III. Amphoteric and hydrophobically modified polymers
    IV. Naturally occurring flocculants (starch derivatives, guar gums, tannins, alginates, bio-flocculant, chitosan, etc.)

This thesis used pre-hydrolysed metal polyaluminiumchloride (PAX) PAX-18, as the main chemical for coagulating MBBR effluent biofilm solids. PAX-18 inorganic coagulant is nontoxic at the normal working dosage, with high charge density, and insoluble in the neutral

pH range (Kemwater, 2008). For the organic flocculant the thesis considered both cationic and anionic polymers and performed some screening test to select the best to form the right flocs for mesh filtration.

2.2.1.1 Mechanism of coagulation

The mechanisms employed in coagulation of stable particles are listed below (Duan and Gregory, 2003; Davis, 2010).

1. An increase in ionic strength, giving some reduction in the zeta potential and a decreased thickness of the diffuse part of the electrical double layer.
2. Specific adsorption of counter ions to neutralise the particle charge.
3. Adsorption and inter-particle bridging, and
4. Enmeshment in a precipitate.

This thesis used zeta potential analysis to help study the coagulation mechanism with the addition of PAX-18 chemical. PAX-18 coagulant was used to destabilize the MBBR biofilm solids to form micro-flocs, in order to enhance flocculation.

2.2.1.2 Mechanisms of flocculation

Smoluchowski (1917) observed that small particles undergo random Brownian motion due to collisions with fluid molecules, and that these motions result in particle collisions. Langelier (1921) observed that stirring water containing particles created velocity gradients that brought about particle collisions. These observations provided the basis for describing the mechanisms of flocculation. The mechanisms of flocculation of particles by polymers can be described under the following:

1. Polymer bridging – Here long-chain polymers adsorbed on particles, in the manner with loops and tails extending in some way into solution. This gives the possibility of attachment of these ‘dangling’ polymer segments to other particles, thus ‘bridging’ particles together (Bolto and Gregory, 2007).
2. Charge neutralisation, including ‘electrostatic patch’ effects (Kleimann, 2005).
3. Depletion flocculation - which depends on the presence of free, unadsorbed polymer (Jang, 2004)

This thesis used both cationic polymer (C-496 and C-490) and anionic polymer (A-130) as a means to form a bridging point for destabilized particles. These polymers were added after

the wastewater had been destabilised with PAX-18, with the motive to form bigger floc size adequate for mesh filtration.

2.2.1.3 Factors affecting coagulation/flocculation

Coagulation/flocculation according to experiments performed in the past, show that they are mostly influence by conditions of dosage, pH and other operating parameters like mixing speed, time, temperature, G-value, and retention time (Hopkins and Ducoste, 2003; Santo et al., 2012; Shammas, 2004; Thomas et al., 1999). Again, one has to be cautious of the amount and concentration of the coagulant used since excess dosage has be shown to cause a charge reversal and restabilization of stable particles, as stated in Section 2.1 and shown in Figure 2-3 (Bolto and Gregory, 2007; Spicer and Pratsinis, 1996).

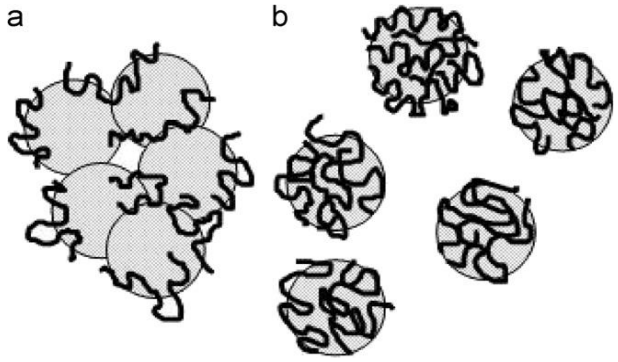

Figure 2-3: Schematic picture of (a) bridging flocculation and (b) restabilization by adsorbed polymer chains **(**Bolto and Gregory, 2007)

Rubin (1979) suggested the following treatment options to overcome restabilization by:

1. Increase the coagulant dosage;
2. Decrease the coagulant dose (settling will suffer, but since turbidity is likely low, flocs will be retained by filters)
3. Raise the pH; and
4. Add coagulant aids (polymers)

2.2.1.4 Coagulant/flocculant dose and pH

Coagulant dosage is very critical, as stated in Section 2.2.1.2. This is the first process, and therefore when not considered carefully, will lead to poor performance of subsequent

processes (flocculation). Effect of the site (location) of coagulant dosage in the coagulation tank have been studied by Kan et al. (2002) and it was concluded that there was no apparent difference among the dosing sites on coagulation performance. However the coagulant dose for this thesis was located in the influent pipe to coagulation as shown in Figure 3.14. Kan et al. (2002) stated that dilution of coagulant during rapid mixing had an effect, and therefore was an important factor to consider when looking forward to improve coagulation performance. Kan recommended a dilution factor of about 5 – 10 to be appropriate. Though from the manual of PAX-18, it was advised not to be diluted, the dosing pump could not deliver the right/optimum dose undiluted, therefore a dilution factor of 6 was used to deliver the optimum dose which provided a good and expected flocs for SF filtration.

Coagulant and flocculant dosages were closely monitored and optimized by settled turbidity, zeta potential measurement, and visual observation of floc formation using conventional jar testing procedures. Davis (2010) observed that using just the optimum dosages were not enough, because metal coagulants hydrolyse to form acid products could affect pH which at some point turns to affect the solubility of coagulant.

This thesis therefore monitored pH closely during coagulant/flocculant dose to avoid problems with solubility, and to ensure SF effluent is not acidic, to corrode steel pipes during discharge.

2.2.2 Jar Tests

Jar Testing is usually conducted using six flat blade paddles and six (1L/2L) mixing vessels, following standard protocols (ASTM, 2003). Jar test results show the treatment efficiency in terms of suspended matter and organic matter removal (Tzfati et al., 2011). Jar tests are performed to assess the effect of different chemicals at varying doses for turbidity removal, colour (UV400nm absorption) and dissolved organic matter (DOC and UV254nm) (Hatt et al., 2011). In spite of using jar tests to assess the above parameters, coagulant selection is not an easy task because one coagulant and polymer combination can remove efficiently the suspended matter but at the same time increase the conductivity, acidity, and potentially clogging filters. This thesis, from the onset, selected one coagulant (PAX-18) base on previous studies (Ng, 2012), therefore the focus was using jar test to select the optimum dose with various polymers to be screened.

2.2.2.1 Mixing theory

Mixing is an important parameter for coagulation/flocculation of wastewater, and therefore its efficiency needs to be considered carefully (Kan et al., 2002). There are generally two mixing regimes in coagulation/flocculation process, namely rapid mixing and slow mixing (Casson and Lawler, 1990). Efficient coagulation is depended on the efficiency of mixing the coagulant, with the raw wastewater normally under rapid mixing regime. On the other hand, efficient flocculation requires a slow mixing regime enough to bring the particles into contact with one another, but low enough to prevent the flocs from breaking apart. Both regimes were considered during this thesis with PAX-18 in the coagulation tank and selected polymer in the flocculation tank.

2.2.2.1.1 G-Value

These mixing regimes are related to the eddy currents created using a stirring device and mostly guided by determining the velocity gradient (G). The G-value is regarded as the amount of shear taking place and therefore shows how violent the mixing is at any instant. It is a function of the power input in a unit volume of water and is usually estimated using Equation 2-4 (Bratby, 2006).

Equation 2-4: G-value

$$\mathbf{G = (\frac{P}{\mu V})^{1/2}}$$

Where;

G = global root mean square (RMS) velocity gradient, s^{-1}
P= Power of mixing input to vessel, W
μ = dynamic viscosity of water, Nms^{-1}
V = volume of liquid, m^3

The G-value was determined empirically in the pilot scale coagulation/flocculation test rig, and correlated with jar-test studies to ensure optimum G-values were used in all tanks. Again, it should be noted that the desired floc size determines the velocity gradient to be used. As floc size becomes bigger, it turns to be weaker and experiences shear stress and result in breakage of flocs. In general, if small floc particles are desired then a high velocity gradient may be required. On the other hand, where larger floc particles are preferred, a lower velocity gradient might be used. This thesis considered forming floc particle of size not too small (less than mesh pore size), but also not too big as not to break flocs and form tiny particles before

it gets to the mesh sieve. Therefore optimum G-value experiment was also crucial in the study.

2.2.2.1.2 GT-Value

Another important parameter considered for the pilot scale coagulation/flocculation process was the dimensionless product of G-value and detention time, which is also termed as GT-value. Though American Water Works Association (AWWA) recommends a typical slow-mixing duration of 20 min and a range of GT-value of 24000-84000 (American Water Works Association, 2000), this thesis considered a constant slow-mixing of 10 min. However efforts were made to ensure the GT-value remained in the range recommended. The 10 min time was considered based on the purpose of the study (direct filtration after flocculation) as suggested by Crittenden et al. (2012). The mixing time is usually approximated as the hydraulic detention time or the theroretical detention time and was calculated using Equation 2-5 below.

Equation 2-5: Theoretical detention time

$$\mathbf{t = \frac{V}{Q}}$$

Where;

t = theoretical detention time, s
V = volume of fluid in reactor, m^3
Q = flow rate into reactor, m^3/s

2.3 Filtration theory

Filtration is a separation technique basically for two main purposes. The first is to remove solid impurities from a liquid, and second, to collect solid from a solution from which it was precipitated. Both purposes were of concern during the thesis period, removing suspended biofilm solids and also precipitating soluble phosphorus (orthophosphate) to facilitate its removal with the use of the SF filter. Two general methods used in filtration include gravity filtration, and vacuum filtration (University of Arizona, 2014). SF machine basically uses the gravity filtration method, to achieve most of its goals as belt rotates in order to draw liquid through mesh sieve to thicken solids before removal. The effectiveness of the filtration process relies on the sizes of the solids as well as the pore size of the filter.

The basic principle is that solid particles greater than the pore size of the filter are retained on the filter. However, when more particles are retained while the filtration process continuous, a new layer with reduced pore size is generated on the original filter. These particles build-up is usually called the filter mat or filter cake. Rusten and Ødegaard (2006) concluded that a more efficient removal can be achieved if the filter is operated with the filter mat on municipal primary wastewater. Though an improvement in performance might be achieved, the filtration rate is affected and the filtration rate decreases to an extent where filtration essentially stops. This filtration process can only continue by changing the filter or removing the deposited solids (filter mat), usually by mechanical means.

SF filters perform very well by ensuring the filtration process is continuous and uninterrupted by rotating the filter belt to remove filter mat and ensuring new filter area is present to continue the process. It also has the capacity of removing any adhering solids which are retained in the pore spaces with either air or water.

During the study, both the SF500 and SF1000 were operated using both phenomenon (with and without filter mat) for the filtration process. Again a sieve rate of range between $20m^3/m^2$-h and $300m^3/m^2$-h as recommended by Rusten and Ødegaard (2006) were used to achieve the needed efficiency required.

2.4 Phosphorus removal

Nutrient accumulation in wastewater poses a threat to freshwater lakes and rivers due to eutrophication (Mainstone and Parr, 2002). Phosphorus is often growth limiting nutrient for plant or algae for eutrophication to occur in these water bodies. Therefore removal of phosphorus from domestic and industrial wastewater discharge could reduce the rate at which eutrophication occurs. Phosphorus removal was the most important parameter considered during the thesis period, since SF500 effluent will be discharged into freshwater without going through any further treatment.

One possible way to remove phosphorus is through metal salt addition and precipitation. Bratby (2006) showed various typical location where chemical addition can be employed in wwtp with respect to removing phosphorus, Figure 2-4. The main objective of phosphorus precipitation is to convert the soluble phosphorus species to an insoluble form to facilitate removal. During biological nutrient removal (BNR), bacterial enzymes convert much of the condensed phosphate species to orthophosphate species. This makes it possible to use less

chemicals after MBBR effluent to convert the soluble orthophosphate into insoluble form for SF removal. Therefore phosphorus removal after BNR (MBBR effluent) is described more efficient and advantageous as compared to upstream in primary clarifiers, where a larger proportion of phosphorus is in the form of organic or condensed phosphate form.

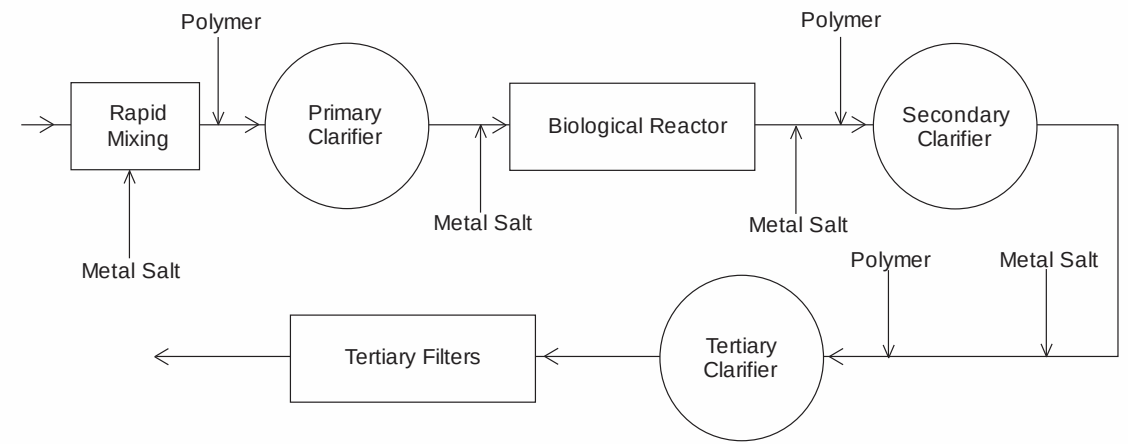

Figure 2-4: Possible chemical dosage points for phosphorus precipitation (Bratby, 2006).

Again coagulant addition after BNR has the benefit of doing both simultaneous phosphorus precipitation and tertiary treatment. This thesis therefore considered this location to achieve a low final phosphorus concentration after SF500 machine while reducing the amount of metal precipitant added, as stated by Bratby (2006).

CHAPTER III

3.0 MATERIALS AND METHODS

This chapter focuses on describing and discussing the equipment and materials used, for this thesis. Below is a list of routine activities, performed in achieving the main objective of this thesis.

1. Jar test experiments were conducted, for chemical screening, evaluation of optimum chemical dose and optimum G-value.
2. Samples with optimum jar test parameter obtained, were then tested, and analysed using bench scale SF screening test.
3. Optimum jar tests, and bench scale SF screening test predictions, were then tested on pilot scale coagulation/flocculation.
4. SF500 with a selected mesh sieve was used for pilot scale filtration.
5. Samples obtained were analysed, for further decisions.
6. Documentation for every experiment conducted, and data obtained were organized.

Figure 3-1 below shows a flowchart, which summarises, how the entire experiment on MBBR Reactor 5 was structured, in other to achieving the main objective of the thesis. Figure 3-2 shows some steps, to obtaining the final SF500 effluent sample for further analysis

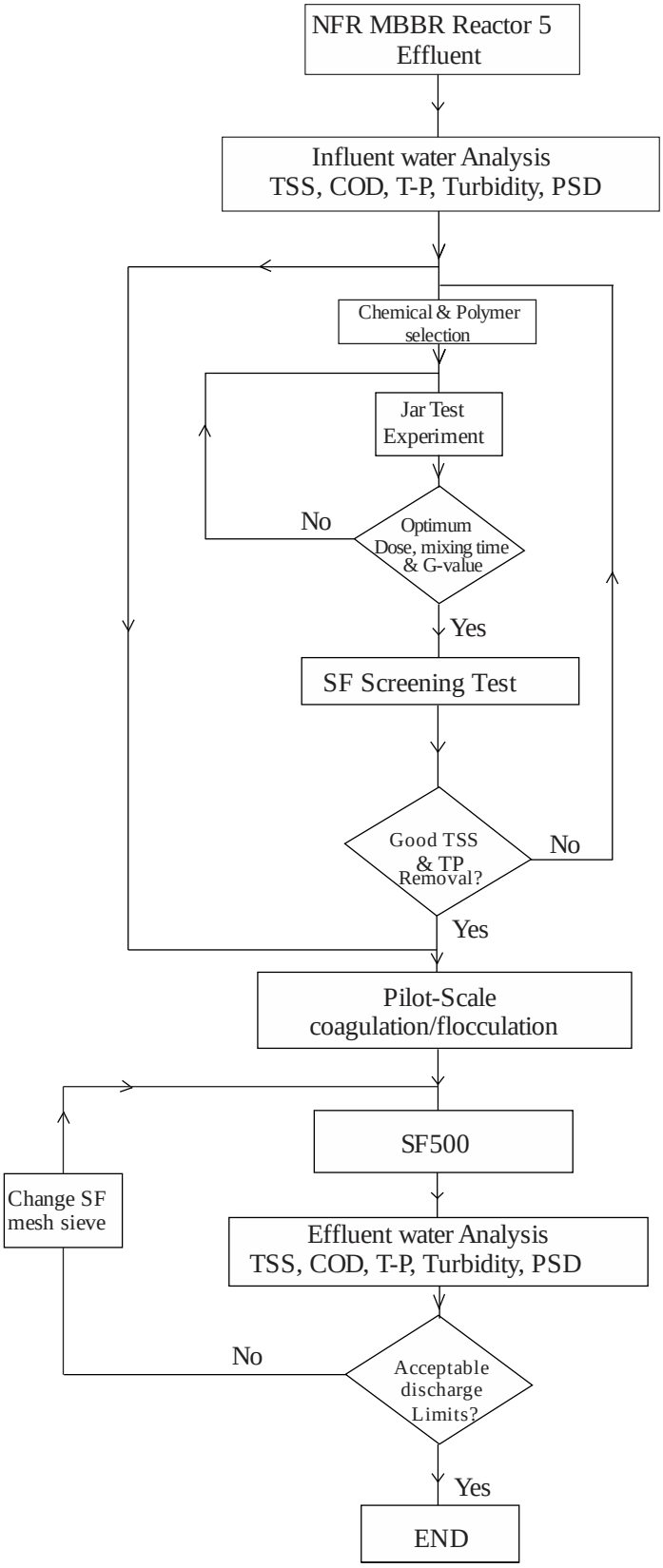

Figure 3-1: Overall experiment flowchart

1. Jar test experiment for optimum parameters

2. Bench scale SF test for mesh sieve screening test

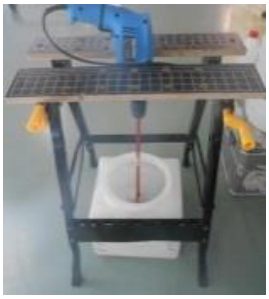

3. Polymer preparation for pilot scale test

4. Mesh sieves to be studied

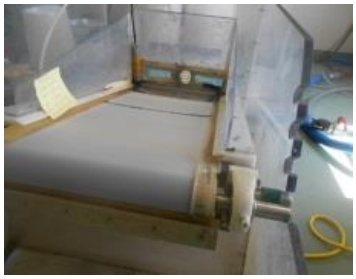

5. Selected mesh sieve fixed to SF500

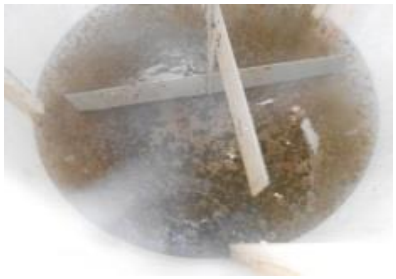

6. Pilot scale coagulation / flocculation is then started

7. Pilot scale coagulation / flocculation tanks with fully formed flocs

8. Pilot scale biofilm flocs ready for SF500 filtration

9. Carrying tube with biofilm flocs to SF500

10. SF500 for flocculated biofilm solids separation

11. Filtered biofilm flocs removed by scraper to the sludge containing basin

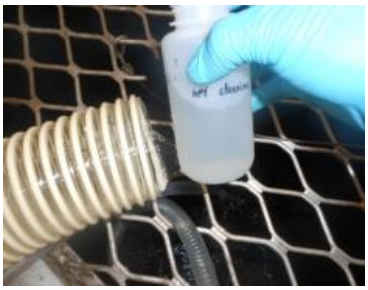

12. SF500 effluent sampled and ready for further analysis

Figure 3-2: Steps to obtain final SF500 effluent sample for further analysis

3.1 Inorganic chemicals and polymers

Some of the chemical and polymers used for this thesis were selected based on recommendations by Ng (2012). Polymer already used by NFR wwtp, was also studied. Inorganic PAX-18 chemical was used for chemical coagulation. Cationic (C-496 & C-490) and anionic (A-130) polymers were used for flocculation. These chemical and polymers were produced by Kemira Kemwater (Sweden) and were obtained from NFR wwtp.

3.1.1 Inorganic chemical – PAX-18

For the thesis, Kemwater PAX-18 was used as a coagulant, and was obtained from the NFR wwtp in bulk quantity. PAX-18 is an iron-free, polyaluminium chloride (PAC), and contains active polyvalent aluminium compounds (Kemwater, 2008). It is usually used as a liquid precipitant. The composition of PAX-18 is found in Appendix A. Table 3-1 shows a conversion, for dosing the precise optimum dose during pilot scale coagulation/flocculation process. This thesis reports all PAX-18 dosages using the active aluminium (mg Al/L) used, as in the third column of Table 3-1.

Table 3-1: Conversion for dosing PAX-18 (Kemwater, 2008)

ml PAX-18/m^3	g PAX-18/m^3	g Al/m^3
20	27	2.43
40	54	4.86
60	81	7.29
80	108	9.72
100	135	12.15
120	162	14.58
140	189	17.01
160	216	19.44
180	243	21.87
200	270	24.30
300	405	36.45
400	540	48.60
500	675	60.75

3.1.2 Polymer preparation

A suitable method as outlined by Bratby (2006b), for preparing powder or micro bead polyelectrolyte stock solutions was followed. Granular cationic (superflocs C-490 polymer, C-496) polymer and anionic (A-130) polymer were obtained, to prepare a stock polymer solution, with a predefined concentration of 1 g/L. During the pilot scale study, about 20 L (1 g/L) polymer was prepared at a time as follows;

1. 20 g of the granular polymer was measured, using analytical mass balance with aluminium dish.
2. A power drill with attached stirrer was fixed to a stand as shown in Figure 3-3. 25 L square tank (to ensure polymer do not spill over during stirring), was then place just below the stand for holding the solution.
3. 20 L of tap water was collected, and poured into the 25 L tank. The stirrer was then immersed into the tap water. After which the drill was started and began to stir the tap water slowly.
4. The 20 g granular polymer was then added slowly over a period of about 1 min. This is to avoid the polymer beads from clumping together.
5. After the granular polymer addition, the stirrer was left to mix the entire solution continuously for about two (2) hours, before ready to use.

Due to the time involved before the polymer was ready, the polymer solution to be used any given day, was prepared the day before in parallel with normal experiments to avoid any delays. Figure 3-3 shows a photograph of the polymer preparation setup.

Figure 3-3: Polymer preparation setup at NFR wwtp

3.2 Jar-Test Kemira Kemwater Flocculator

Kemira Kemwater jar test Flocculator device, developed by kemira kemwater in Sweden, has been used for many experimental studies (Jarvis et al., 2005, Ng, 2012, Yukselen and Gregory, 2004). This comes with six (6) 1 L beakers. The device is semi-automated, consisting of 6 parallel agitators controlled by a microprocessor. It allows each agitator to be operated individually, controlling the times for rapid mixing, slow mixing, and settling time before an alarm sounds. The stirring motors can be operated at varying speeds of 10, 20, 30, 40, or 50 rpm for slow mixing, and 300, 350, or 400 rpm for rapid mixing. Figure 3-4 shows Kemira Kemwater flocculator 90, with MBBR reactor 5 effluent samples during jar-test experiment.

Figure 3-4: Kemira Kemwater flocculator 90

The device was used for all jar test experiment carried out during the study. It was used with all six (1 L) beakers for obtaining the optimum dosage ranges of PAX-18, C-490, C-496, and A-130, according to standard procedures (ASTM, 2003).

Procedure of the jar test experiments was as follows: coagulant (PAX-18) was added to the 1 L sample with a 20-200ml pipette, and immediately after addition the rapid mixing was started for 20 s at 400 rpm. Polymer (C-490, C-496, or A130) was added after the 20 s rapid mixing and allowed to slow mix for 10 min at 50 rpm. After slow mixing, the flocculated

solids were allowed to settle for 10 min. After the settling time, 10 ml samples were taken from 5 cm below the surface for turbidity analysis. Table 3-2 below, shows the dosages range of chemical and polymers studied.

Jar-test apparatus theoretical G-values at each speed were also calculated, using Equation 3-3 and attached in Appendix B.

Table 3-2: Dosage range studied for chemical/polymer

Chemical/Polymer	Dosage Range Studied
PAX-18 (mg Al/L)	3.65 – 19.44
C-490 (mg/L)	0.05 – 1.00
C-496 (mg/L)	0.30 – 1.50
A-130 (mg/L)	0.30 – 1.00

The pH before and after jar test experiment was monitored, using WTW SenTix 41 probe connected to a WTW 340i portable set (WTW GmbH, 2004). Temperature remained almost constant at 18 °C throughout the study. Turbidity of settled supernatant (10 mins), was initially used to select optimum dosing ranges for all chemical and polymers using jar test with all six (1 L) beakers. The turbidity of samples was measured, using Hach 2100P turbidity meter.

3.2.1 Hach 2100P portable turbidity meter

The Hach Model 2100P portable turbidimeter as shown in Figure 3-5 was used in evaluating the turbidity of samples throughout the study. It measures a range of 0.01 to 1000 NTU in automatic mode, with automatic decimal point placement. It has manual range mode, which measures turbidity in three ranges, thus 0.01 to 9.99, 10.0 to 99.9 and 100 to 1000 NTU. It is designed primarily for field work, and has a rechargeable battery (Hach, USA, 2008). This instrument comes with nine sample cells and three stabilized formazin primary standards, 15 mL of silicon oil, oiling cloth, carrying case and instrument manual.

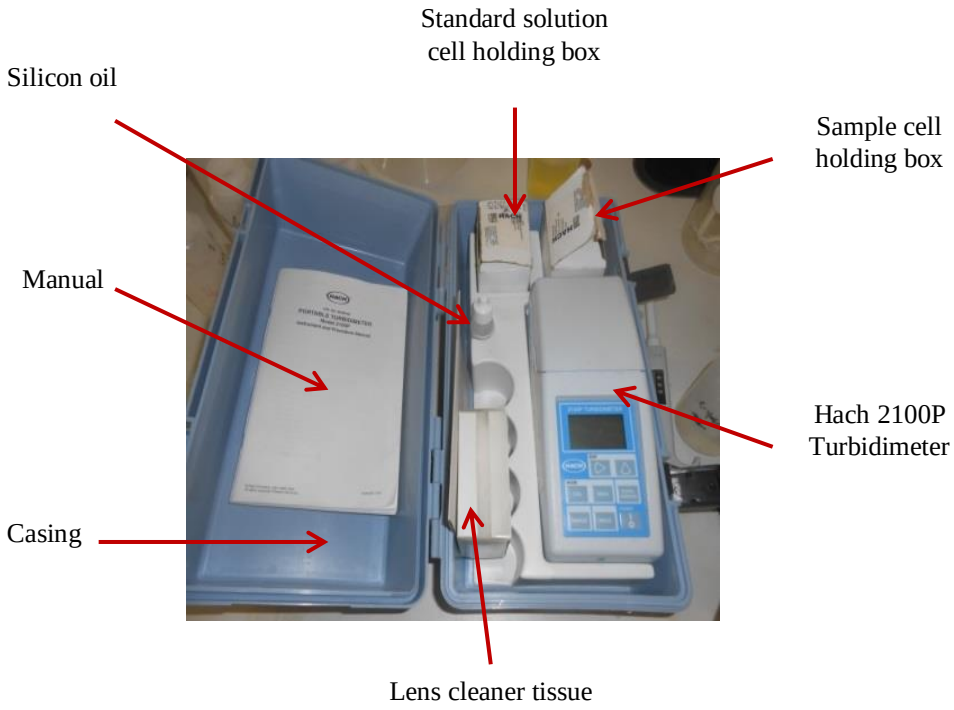

Figure 3-5: 2100P Turbidimeter and Accessories

Calibration of the Turbidimeter was done using stabilized formazin primary standards, which come with it. However, the instrument's electronics and optical design provides long-term calibration stability, and therefore minimizes the need for frequent calibration (Hach, 2008). Due to this, the calibration was done once every two (2) months. It should be noted here that in order to minimize the errors during measurements, only one of the nine sample cuvette cells was used for all sample measurements. Measurement with this instrument was carried out as follows;

1. 10 mL of sample was pipetted from 5 cm below water interface of the settled jar test sample into the sample cuvette cell.
2. The cell was cleaned with a lens cleaner tissue, and immediately inserted into the calibrated instrument, and then the lid closed.
3. The Read button was pushed to evaluate the sample.

Again, all samples collected outside jar-test experiments, were measured the same way but first stirring or shaking sample for some time, to keep particles in suspension before taking 10 mL for turbidity measurements.

3.2.2 Multi 340i meter

Handheld Multi 340i meter was used with WTW SenTix 41 probe to measure the pH of all samples studied. This instrument was calibrated each time the probe was connected, and also when signal (sensor symbol flashes) was displayed on the screen. The calibration was done using three buffer solutions of pH 4, 7 and 10, according to guidelines provided in its manual (WTW GmbH, USA, 2004). After Multi 340i meter pH calibration, each sample was measured by immersing the pH probe (WTW SenTix 41 probe) in the test sample, and pH displayed on screen was recorded. Though this probe measures pH and temperature at the same time, pH was of most concern while temperature was assumed to be constant throughout the study. Figure 3-6 below shows the Multi 340i meter used.

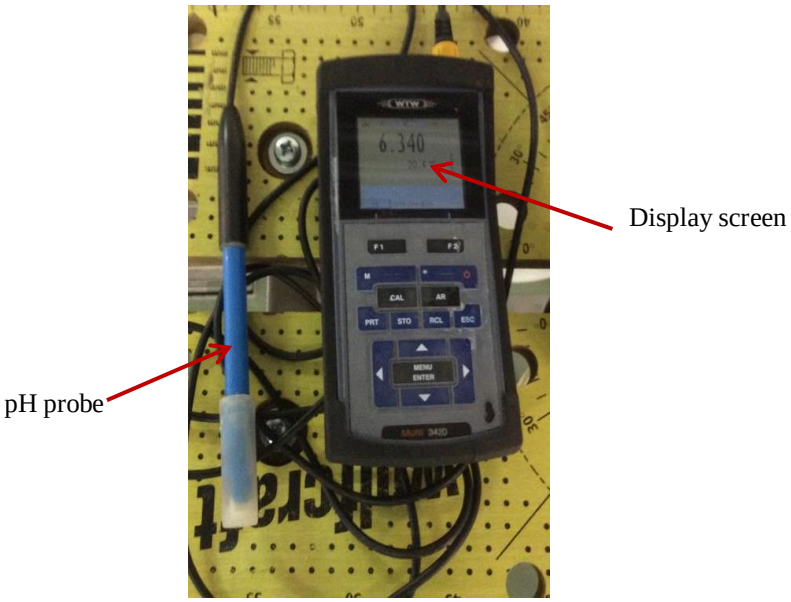

Figure 3-6: Multi 340i meter with WTW SenTix 41 probe

3.3 Bench scale SF test apparatus

A simple bench scale SF test apparatus developed by Rusten (2004) for the testing of SF fine mesh sieves on primary (untreated/degritted) wastewater, was used in determining the pilot scale optimum parameters. This was also used to predict the removal efficiencies and estimate filtration rate, which can be expected for a given sieve. However in order to minimize any possible shear, breakage of formed flocs, during the pouring of samples into the PVC sample holder, the tube height from the standard apparatus (Rusten, 2004) was

modified from 550 mm to 210 mm. SF mesh fine sieves, with pore sizes of 18, 33, 55, 74, 90,150, 250 and 350 µm each of filtering area 0.0077 m^2 were used. Figure 3-7 shows some photographs of bench scale SF fine mesh sieves. Figure 3-8 shows a sketch of the bench-scale SF apparatus used. This same apparatus was used in the NFR primary wastewater characterisation test, and NFR MBBR biofilm wastewater characterisation test as stated in Section 3.13.

Figure 3-7: Photograph of bench scale SF fine mesh sieves

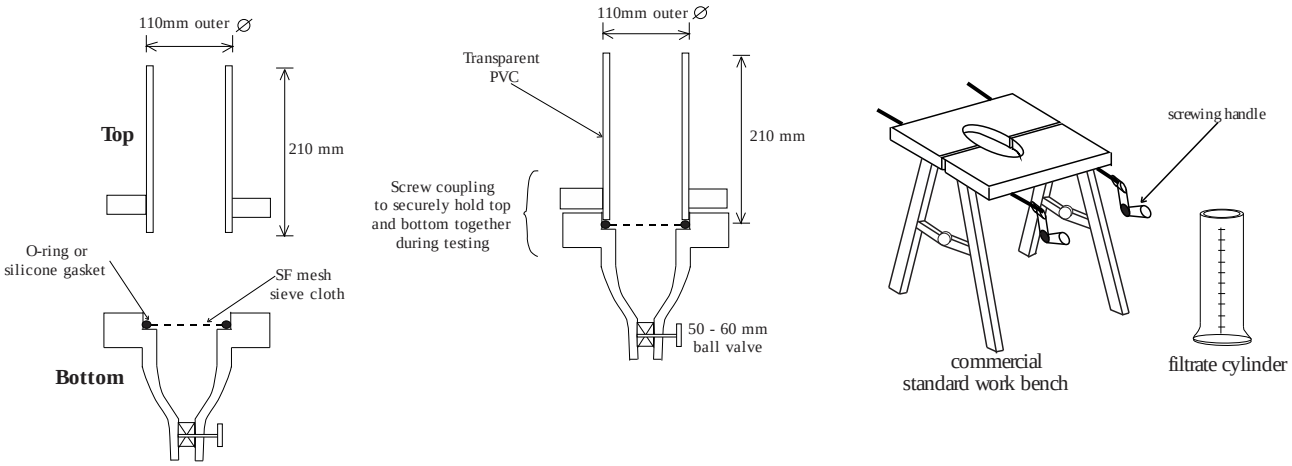

Figure 3-8: Simplified sketch of bench-scale SF apparatus for characterization and testing of wastewater with regards to treatment by fine mesh sieves (Rusten, 2004)

3.3.1 Bench scale SF screening test procedure for pilot scale optimum parameters determination

About 30 L of MBBR (Reactor 5) effluent was collected at a time, stirred vigorously, and pH recorded. TSS and TP were then analysed according to Section 3.4 and 3.5.3 respectively. SF fine mesh sieve of a particular size (µm), was selected and fixed into the bottom part of the test apparatus (Rusten, 2004), which is already fixed to the work bench. The top and bottom parts were securely screwed, to couple them (Top and Bottom) together. A filtrate cylinder was placed at the bottom of the commercial standard work bench, to collect the filtrate through the filter fine mesh sieve. Procedures as outlined by Rusten (2004) were strictly followed.

1 L MBBR biofilm wastewater was then sampled from 30 L MBBR wastewater containing tank, for jar test experiment, with a constant rapid speed of 400 rpm for 20 s and any varying parameter (chemical, dose, G-value, slow mixing time) to be considered, selected. However, during each jar test experiment, sample was allowed to flocculate for 10 min at 50 rpm before ready for screening. Sample from the jar test experiment (1 L) just after slow mixing and without settling, was transferred to the bench scale SF test apparatus. While the bottom ball valve was closed, the sample was poured into the transparent PVC sample holding tube. The valve was then opened, and the volume of filtrate collected for a certain period of time was recorded. Further analyses (TP, TSS) were then performed on the filtrate. The filtration rate (m^3/m^2-h) for each mesh was evaluated using Equation 3-1. Figure 3-10 below shows a flow chart of how both jar test and bench scale SF test apparatus were used, to obtain various optimum parameters, to be used in the pilot scale coagulation/flocculation studies. Figure 3-9 shows a photograph showing the bench scale SF test setup.

Equation 3-1: Mesh filtration rate

$$\text{Filtration rate}\left(\frac{\text{m}^3}{\frac{\text{m}^2}{\text{h}}}\right) = \frac{\text{Flow rate } \left(\frac{\text{m}^3}{\text{h}}\right)}{\text{Mesh sieve area } (\text{m}^2)}$$

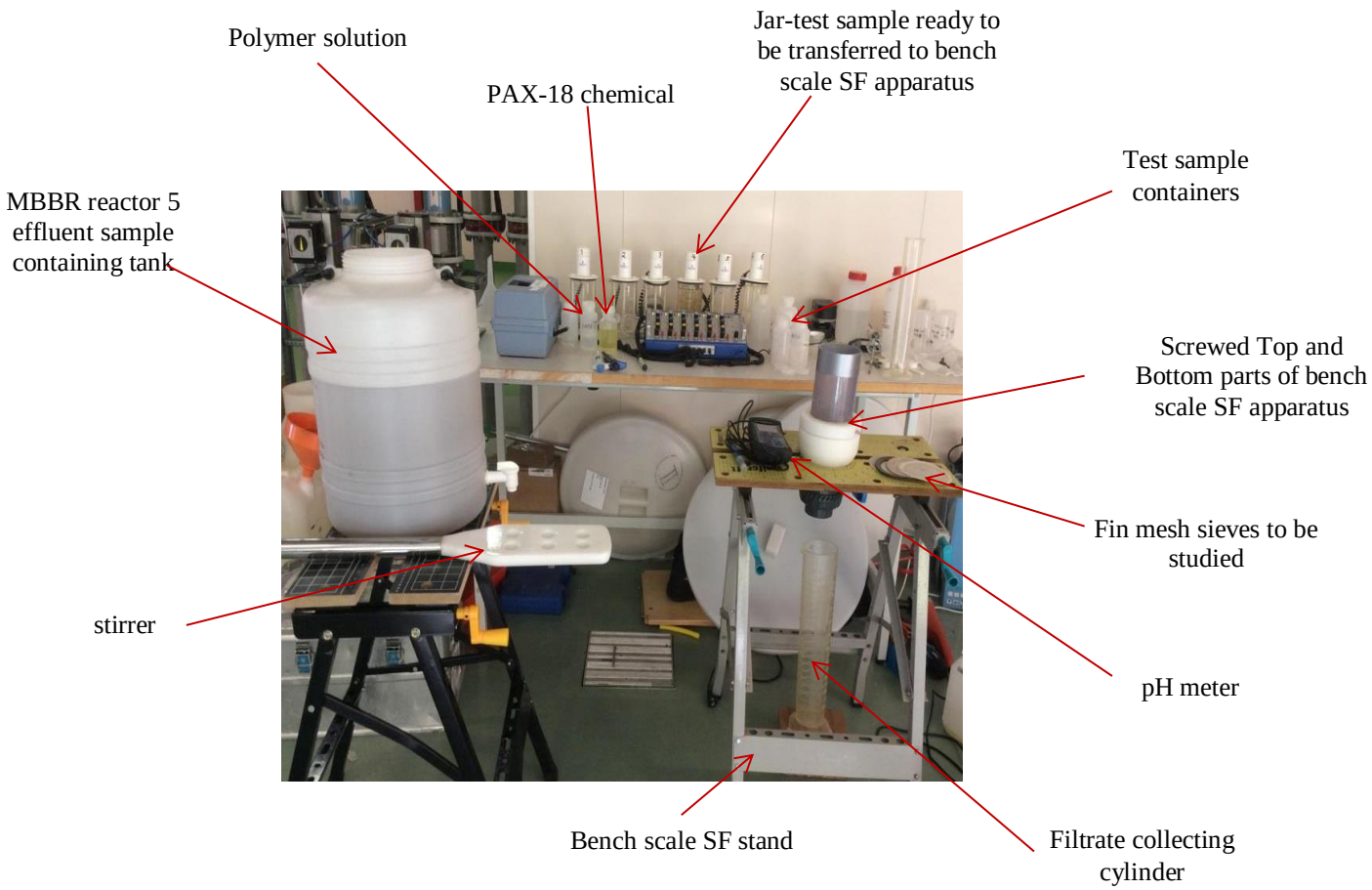

Figure 3-9: Bench scale SF screening test setup at NFR wwtp

3.4 Total suspended solids (TSS) apparatus

Total suspended solid (TSS) was one of the most important measurement performed during the study. All needed apparatus, as stated in Section 2540 D of the Standard Methods for Examination of Water and Wastewater (AWWA, 1999), were used to evaluate the TSS concentration. All water samples collected at various sampling points were analysed for TSS. TSS concentration was calculated using Equation 3-2 (AWWA, 1999).

Equation 3-2: TSS evaluation

$$\frac{\boldsymbol{mg\ total\ suspended\ solids}}{\boldsymbol{L}} = \frac{(\boldsymbol{A}-\boldsymbol{B})\times \mathbf{1000}}{\boldsymbol{sample\ volume, mL}}$$

Where;

A = weight of filter + dried residue, mg, and
B = weight of filter, mg.

3.5 Chemical analysis

Chemical analyses were performed on both influent and effluent samples. These analyses were used as a monitoring tool for increasing the removal efficiency, and also obtaining effluent water with parameters below the discharge permit. This helped as a guide, to limit chemicals in other to make the technology the most preferred, attractive, and economical to the society and environment as a whole. These analyses were also performed on both NFR primary wastewater (untreated/degritted) and MBBR biofilm wastewater characterization tests, as stated in Section 3-13 and Section 3-14. Among these analyses were total chemical oxygen demand (COD), total phosphate (TP) and total nitrogen (TN). These parameters were analysed, using Dr. Lange cuvette test kits, and also measured using Dr. Lange 2800 spectrophotometer. Figure 3-10 shows the setup for conducting the chemical analysis.

3.5.1 DR 28000 spectrophotometer

This analytical instrument as shown in Figure 3-10, has both tungsten (visible) and deuterium (UV) lamps for evaluating all Dr. Lange cuvette test kits. It has automatic method detection capability, with TNT plus reagents and thereby reduces test time and potential errors (HACH, 2010). It has been designed to have the following specifications; wavelength range (340 to 900 nm), with accuracy of ±1.5 nm, Wavelength Resolution (1 nm), and its wavelength calibration is done automatically. It automatically detects the cuvette test kit, when inserted and uses the bar codes to adjust the instrument for the required correct measurement parameters. This instrument was used to measure all cuvette test kits, during analysing COD, TN and TP of test samples.

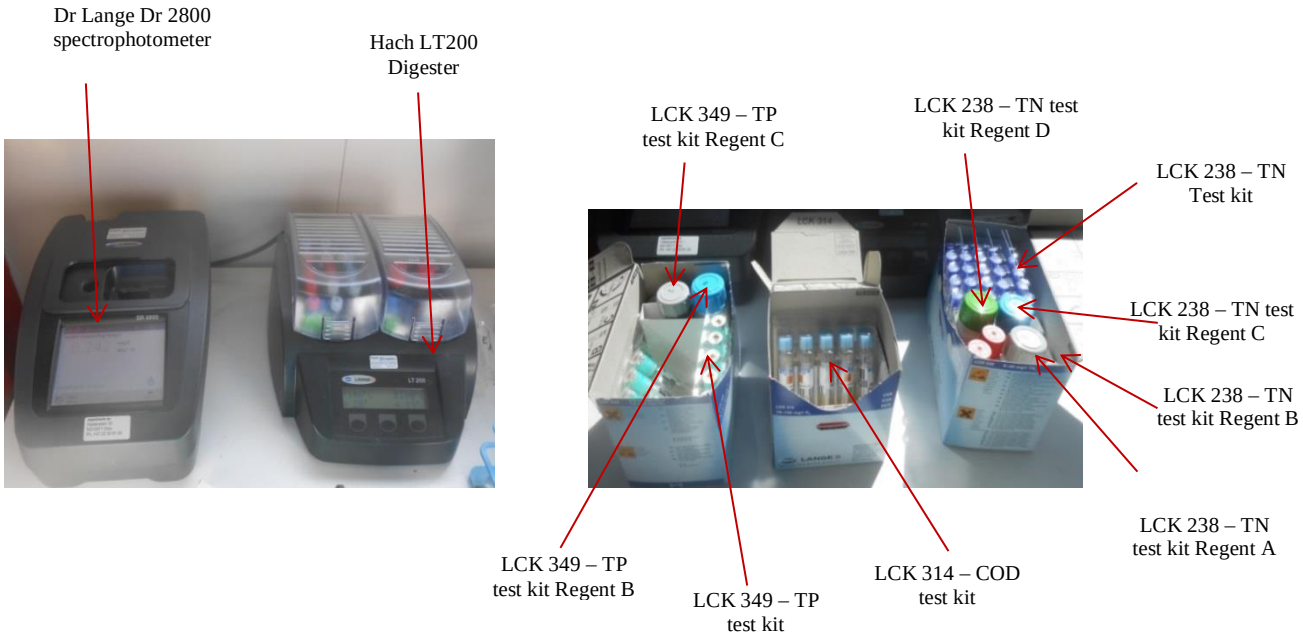

Figure 3-10: Chemical analysis setup at NFR wwtp

3.5.2 Chemical oxygen demand

Chemical oxygen demand (COD) is a measure of oxygen equivalent, of the organic matter in a sample, which is susceptible to oxidation by a strong chemical oxidant. This is measured in mg O_2 /L, to correspond the mass of oxygen required oxidizing the compounds in a liter of water sample. COD analysis is usually performed in wastewater examination to evaluate this volume of oxygen equivalent, when the oxidizable substances react with potassium dichromate solution in acidic solution (usually sulphuric acid) when digested at 148 °C for two (2) hours (COD classic). Chloride is masked by mercury, and the green coloration of Cr^{3+} is evaluated when cooled. The organic carbon in the sample is finally oxidized to CO_2 and H_2O.

All water samples collected during SF1000 wastewater characterisation with 350 µm and 33µm, were tested for COD. Again samples from the influent to the pilot scale coagulation/flocculation process, and effluent of SF500 machine were also analysed for COD using LCK 314 Dr. Lange cuvette test kits, and measured with Dr. Lange DR 2800 spectrophotometer. LCK 314 test kit is usually for measuring low ranges COD of 15 mg/L to 150 mg/L. For this reason all samples with the exception of SF500 effluent, were diluted before analysis, to minimize errors and to be within range of the test kits. The final

measurement was then multiplied, by the respective dilution factor. COD analysis was performed as follows (Lange, 2001);

1. LCK 314 test kit sediments were brought to suspension, by inverting the kit several times.
2. Test sample (diluted or undiluted) was shaken, to also bring particles in suspension and 2 mL sample was carefully pipetted into the test kit.
3. The cuvette test kit was then covered, with its zip cap and the outside thoroughly cleaned with a lens cleaner tissue.
4. The test kit was digested in Hach LT200 thermostat shown in Figure 3-9 for two (2) hours at 148 °C.
5. After digestion, the hot cuvette was removed, and inverted twice and allowed to cool down in a cuvette test kit stand, to room temperature (20 °C).
6. When all sediments had settled down after cooling, the outside of the cuvette was cleaned and evaluated using DR2800 spectrophotometer and recorded.

3.5.3 Phosphorus

Phosphorus exist in two forms; soluble or particulate forms. Particulate form is easy to remove, but the soluble form presents a challenge. Therefore the most objective of phosphorus removal, is basically using chemical (metal coagulant) precipitation to convert soluble phosphorus species to an insoluble form, to facilitate removal. An operational definition of soluble phosphorus is that which can pass through 0.45 micron filter. Among the soluble phosphorus are orthophosphate, polyphosphates, pyrophosphates, and organophosphates. There are various forms of phosphorous reported in literature (Bratby, 2006);

i. Soluble reactive phosphorus (SRP). This is the orthophosphate content of a sample prepared by filtering through 0.45 micron filter, and conducting a direct colorimetric analysis, without sample digestion.
ii. Total dissolved phosphorus (TDP). These samples are obtained by filtering through 0.45 micron filter and then preserving them by using sulphuric to a pH of 2. Samples are later digested with strong acid solutions.

iii. Total phosphorus (TP). Samples are not filtered and immediately preserved to pH 2 or even less using sulphuric acid.

Total phosphorus (TP) removal efficiencies from SF500, was of most concern throughout the study, with a goal to achieve a level below 0.3 mg/L. Samples from SF1000 (33 and 350 μm characterization test), NFR primary (degritted) and MBBR wastewater characterization test were also tested for TP. TP of all water samples was evaluated, using LCK 349 test kit. LCK 349 test kit has a TP measuring range of 0.15 mg/L PO_4 to 4.50 mg/L PO_4. It works on the principle that, phosphate ions react with molybdate and antimony ions in an acidic solution, to form an antimonyl phosphomolybdate complex, which is reduced by ascorbic acid to phosphomolybdenum blue (Lange, 2001). All samples with the exception of SF500 effluent samples were diluted before analysis. TP analysis with LCK 349 was performed as follows;

1. LCK 349 test kit foil on the DosiCap Zip was carefully removed and then DosiCap Zip unscrewed.
2. The test sample (diluted or undiluted) was inverted several times to keep particles in suspension and then 2 mL pipetted into the LCK 349 test kit.
3. The DosiCap Zip was screwed back tightly, fluting at the top after which the kit was shaken firmly for some time.
4. The test kit was then digested in Hach LT200 thermostat at 100 °C for one (1) hour.
5. After digestion, the test kit was removed and allowed to cool down to room temperature in the cuvette test kit stand.
6. The cooled test kit was then shaken firmly and 0.2 mL of reagent B (LCK 349B) was pipetted and added.
7. A grey DosiCap C (LCK 349C) was then screwed on to the cuvette and inverted a few times and allowed to rest for about 10min or more.
8. After 10 min, the cuvette was inverted some few times and the outside cleaned thoroughly with a lens cleaner tissue. It was then evaluated using DR2800 spectrophotometer. Measurements were then multiplied with their respective dilution factors before recording.

3.5.4 Total Nitrogen

Total Nitrogen as already stated above requires nitrifying bacteria activities for removal. However as part of this thesis, total nitrogen (TN), removal efficiency of the fine mesh sieve was also studied. TN on both influent and effluent of SF1000 (33 and 350 μm mesh characterisation test) were evaluated. TN throughout these experiments was determined and measured using LCK 238 test kit as shown in Figure 3-10. This test kit had a measuring range of 5 – 40 mg/L. It works on the principle that inorganically and organically nitrogen will be oxidizing to nitrate by digestion with peroxodisulphate. These nitrate ions then react with 2, 6-dimethylphenol in a solution of sulphuric and phosphoric acid to form nitro phenol. TN analysis was performed on the field as follows;

1. 0.5 mL sample (diluted or undiluted) was pipetted into a dry reaction tube that comes with the test kit box. 2 mL of reagent A and 1 tablet from reagent B was then added. This tube was then closed immediately and digested with Hach LT200 for 1 hour at 100 °C.
2. After digestion, the reaction tube was removed and allowed to cool down to room temperature (20 °C) after which 1 microCap from reagent C was added. The reaction tube was then closed and inverted a few times.
3. The reaction tube was opened and 0.5 mL of the digested sample slowly pipetted into the LCK 238 cuvette test kit. 0.2 mL of reagent D was also pipetted and added to the cuvette test kit and finally closed and inverted for a few times.
4. The cuvette test kit was left in a stand for over 15 min before the outside cleaned with lens cleaner tissue and then evaluated using DR2800 spectrophotometer.

The respective dilution factors were then multiplied to the spectrophotometer measurement and recorded for further interpretations and discussion.

3.6 Selecting chemical/polymer and determining optimum coagulation/flocculation parameters

During this thesis, both jar test and bench scale SF apparatus were used to select both chemical/polymer and optimum coagulation/flocculation parameters, to be used in the pilot scale coagulation/flocculation. This was performed as shown in Figure 3-11. Optimal dosages which were determined by settled turbidity in the jar tests were used.

About 30 L MBBR reactor 5 effluent wastewater was taken and kept in a storage tank shown above in Figure 3-8. This wastewater was stirred vigorously before 1 L sample was taken each time for jar test experiment. A chemical (coagulant), polymer (flocculant) or combination of both, each at its already determined optimum dose was selected to perform 1 L jar test experiment at a time with constant parameters (rapid speed, rapid time, slow speed, and slow mixing time). After the slow mixing time, this 1 L flocculated biofilm sample was transferred to the bench scale SF apparatus. Using a particular mesh sieve, the filtrate collected was further evaluated for TSS and TP. This process was repeated until all the mesh sieves (158, 90, 74, 33, and 18 μm) were evaluated using the particular selected chemical or polymer. The aforementioned process was again repeated until all combinations of coagulants and polymer, and mesh sieves were studied. Based on the results obtained, a chemical & polymer combination was selected for further studies.

The optimum dose of this selected chemical & polymer combination to be used on the pilot scale was then determined. Above procedure but with 33 μm mesh sieve was repeated, but varying the selected coagulant & polymer dosages. The determined optimum pilot scale chemical & polymer doses were then used, through the same process, to obtain the pilot scale optimum G-value and flocculation time by varying slow mixing speed and slow mixing time respectively. It should be noted that the previously determined pilot scale optimum parameter was kept constant, before the next optimum parameter was determined.

These selected parameters (chemical & polymer, optimum dose, optimum G-value and optimum flocculation time) were then replicated to be used in the pilot scale coagulation/flocculation process. Figure 3-11 summarises the entire process used to obtain the pilot scale coagulation/flocculation parameters.

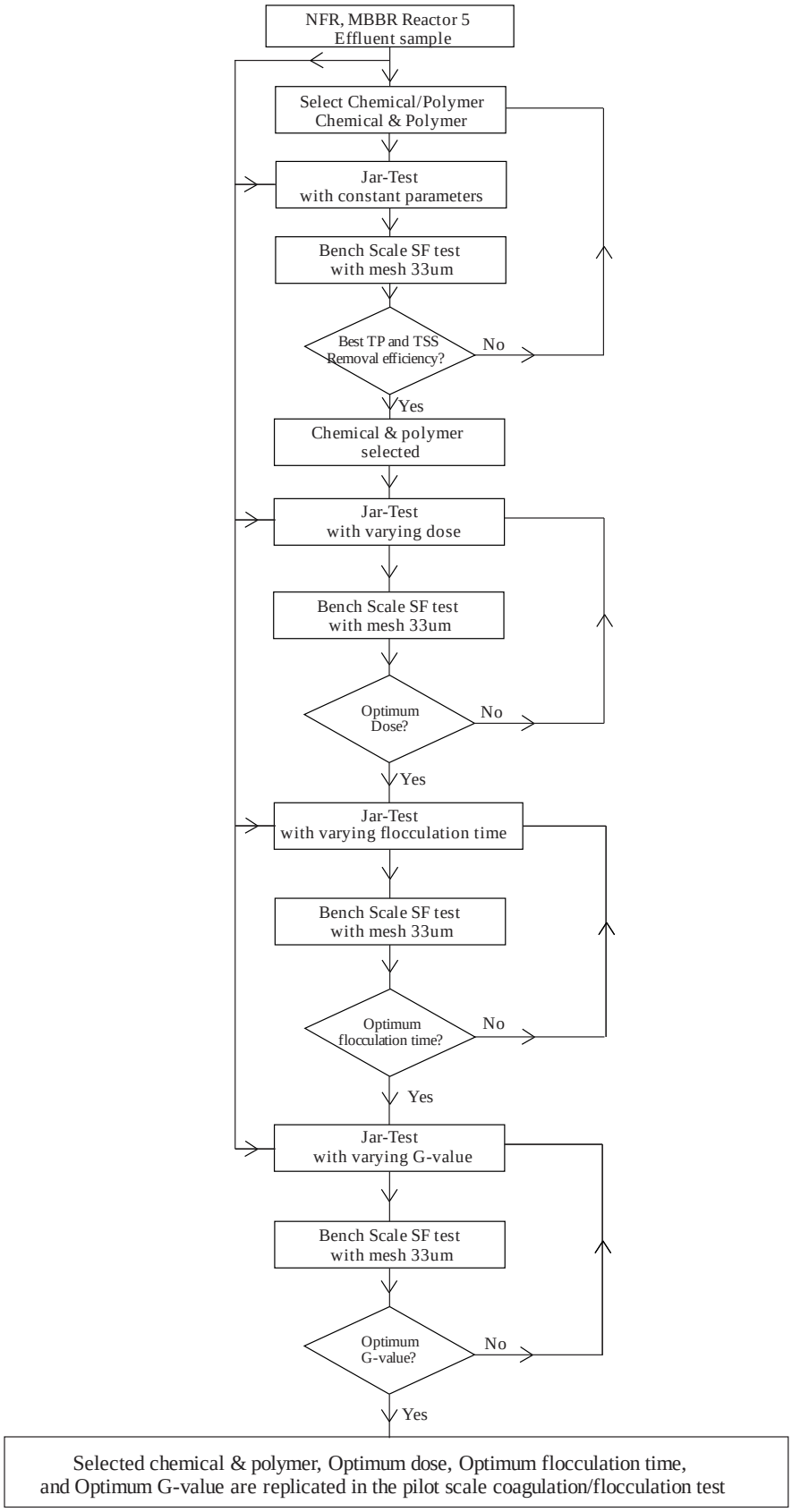

Figure 3-11: Flow chart for using bench scale SF apparatus in obtaining the optimum parameters for pilot scale coagulation/flocculation test

3.7 Pilot scale coagulation/flocculation

The pilot scale coagulation/flocculation setup was integrated as shown in Figure 3-14. Karcher SD14000 (Q_{max} 14000 L/H, H_{max} 8 m, P 800W) with a maximum water pumping capacity of about 3.8 L/s was used as feed pump, to deliver NFR MBBR effluent (Reactor 5) water to the pilot scale coagulation/flocculation tanks. Distance of the carrying hose from Reactor 5 to pilot scale tanks was 40 m. Due to the carrying distance (40 m) to tanks, there was head loss, and thus ~ 1.21 L/s was received at the tanks. However a regulating valve was connected to the carrying hose, to help regulate the flow rate to 1 L/s biofilm wastewater to the rapid mixing tank. This flow rate ensured a constant flocculation time of 10 min in pilot scale flocculation tanks. A peristaltic dosing pump (CIR/P, P_{max} 2.5 bar, Q_{max} 4.5 L/H) was used for transferring optimum PAX-18 dose, to the coagulation tank. This pump based on its location to the rapid mix tank, could deliver a dosing range of 0.3 mL/s to 1.25 mL/s. Another pump from Aqua water system (HC797) with a dosing range of 0.1 mL/s to 2.25 mL/s based on its location, was used for dosing polymer to flocculation tank.

A small tank of volume 55 L was used as rapid mixing tank, to receive NFR MBBR effluent from Reactor 5. The outlet of the 55 L tank was placed at 20 L mark, to ensure a solid retention time of 20 s during coagulation. This rapid mix tank had a propeller stirrer connected to a micro motor (2 Nm torque, 1380 rpm max), to rotate at a varying speed range of 0 rpm (0 V) to 1380 rpm (24 V). Two bigger tanks, each of volume 320 L (base diameter 680 mm, height 100 cm) were used for slow mixing. Each flocculator had a stirrer connected to a micro motor (2 Nm torque, 60 rpm max), and was operated with a variable speed control device (0 V to 12 V). Each stirrer had 8 flat blades, each of 27 cm length, 8 cm width and connected to 8 mm shaft diameter. Figure 3-13 shows the dimension of the flocculator stirrer and the flocculation tank with stirrer, used for the pilot scale experimental setup. Each flocculation tank had three (3) square baffles (2 cm x 2 cm) fixed on its walls to avoid rolling over of particles on tank wall during stirring. Each of the two tanks carried 300 L of water during the continuous mix coagulation/flocculation.

These flocculation tanks were originally designed, to be used with SF1000, due to its higher capacity. However, due to biofilm floc cleaning difficulty with SF1000, SF500 was

Figure 3-12: SF1000 biofilm flocs initial filtration (left) and during air knife cleaning (right)

used for this purpose. Therefore part of the flocculated biofilm solids had to be by-passed, before a portion gets to SF500 to be filtered. Figure 3-12 shows the air knife cleaning difficulty with SF1000. This change in SF (SF1000 to SF500) resulted in a difficulty of regulating the by-passed valve, to get the require flow rate for SF500 to operate properly.

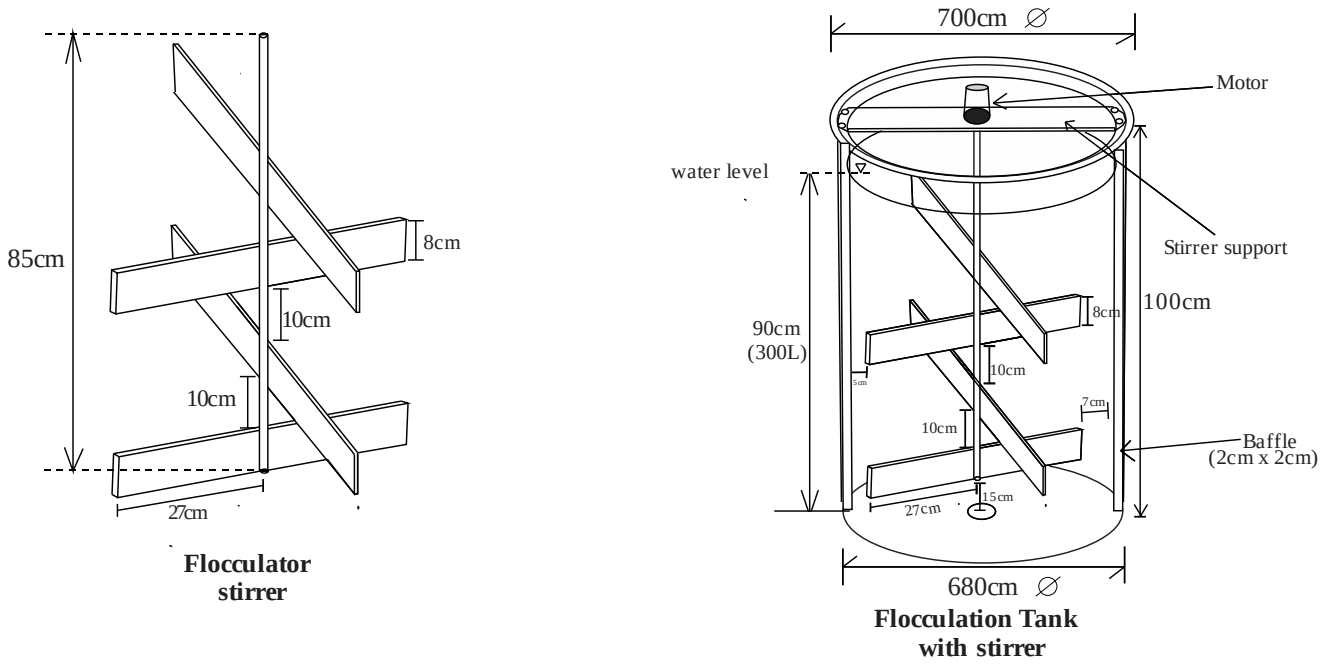

Figure 3-13: Dimensions of flocculation stirrer (left) and flocculation tank with stirrer (right)

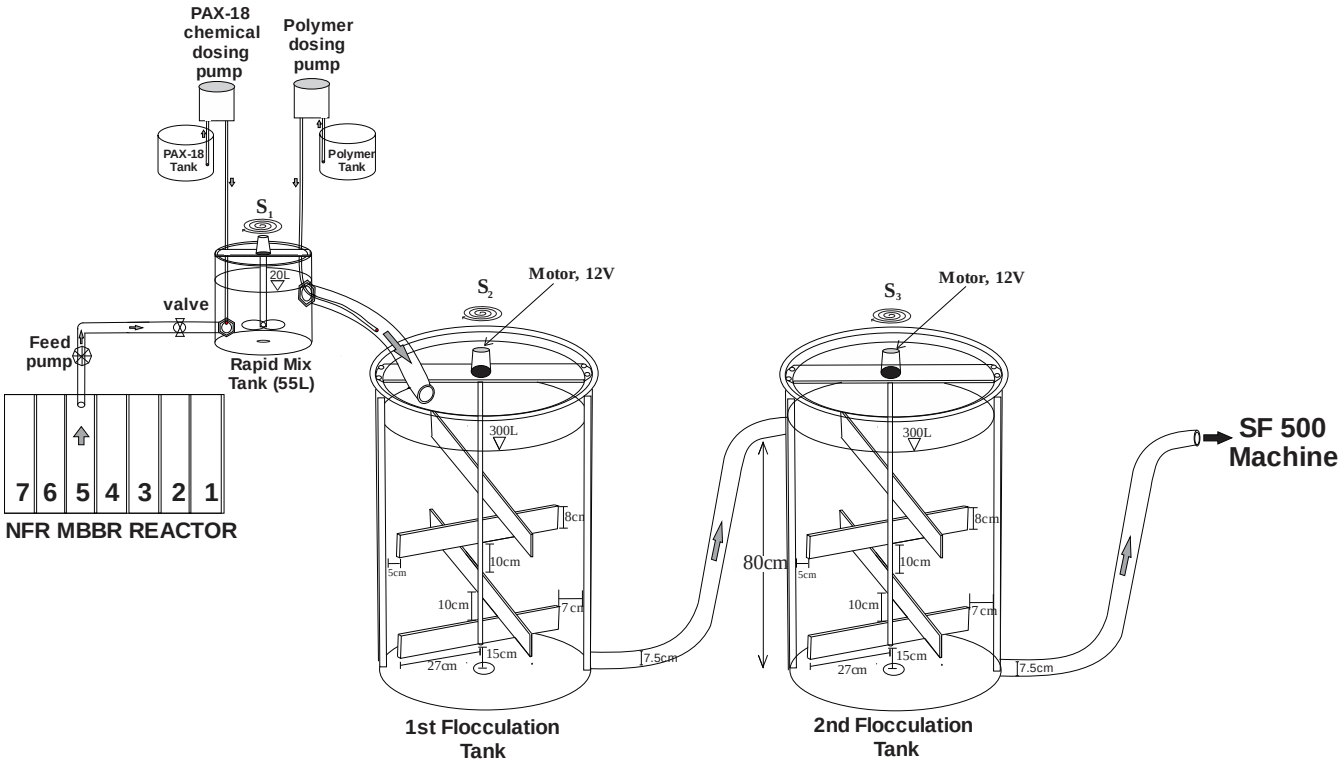

Figure 3-14: Pilot scale coagulation/flocculation setup integration with the SF500 machine.

The G-value of the flocculator stirrer during the coagulation/flocculation, was estimated as shown in Table 3-3 using the procedure by Camp (1955). The ratio of speed of rotation of water to speed of rotation of stirrers (*k*) was assumed as 0.24. Camp's expression used is as shown in Equation 3-3;

Equation 3-3: Camp's expression for G-value calculation

$$\mathbf{G} = \left(\frac{\boldsymbol{P}}{\boldsymbol{\mu V}}\right)^{\frac{1}{2}} = \sqrt{\frac{\mathbf{1.24.10^5.C_D(1-k)^3 S_s^3}}{\mathbf{V.\mu}} \sum \mathbf{A.r_b^3}} \ (\mathbf{s^{-1}})$$

Where;

C_D = drag coefficient = 2.0 for flat blades
S_s = speed of rotating of shaft (rev/s)
kS = speed of rotation of water (rev/s)
V = volume of water in tank (m^3)
A = cross sectional area of each blade in the plane perpendicular to direction of motion (m^2)
r_b = distance from center of each blade from shaft (m)
μ = absolute viscosity of water (Ns/m^2)
P = Power (W)

Table 3-3: Calculated G-value at various voltages across the flocculator stirrer motor.

Voltage (Volt)	Speed in water (rpm)	G-value (s^{-1})
3	9.5	46.38
4.5	12	65.84
6	14	82.97
7.5	16.5	106.16
9	18	120.96
12	20	141.67

G-value of the flocculation tanks were also calculated practically and attached in Apendix C.

During pilot scale coagulation/flocculation, optimum doses obtained in the jar-test experiments as stated above were replicated using a scale factor depending on the flow rate. One of the dosing pumps was used to transfer the coagulant (PAX-18) to the rapid mixing tank just at the tank influent to ensure effective chemical mixing. It should be noted that due to the lowest dosing rate of the pump, which was far more than the required optimum dose, PAX-18 chemical was diluted using a dilution table prepared and attached in Appendix D, to dose the precise optimum dose of the chemical. This was stirred continuously with a particle retention time of about 20 s. The polymer dosing pump transferred optimum polymer dose, directly into carrying hose to first flocculation tank. Same optimum G-value was selected for both flocculation tanks, during the flocculation process. In the first flocculation tank biofilm flocs began to form, and continuous to grow in the second flocculation tank. Fully grown biofilm flocs, then leave the tank to SF500 machine through a 75 mm pipe tube. A portion of biofilm flocs was by-passed unfiltered. Figure 3-15 shows a photograph of the pilot scale coagulation/flocculation setup.

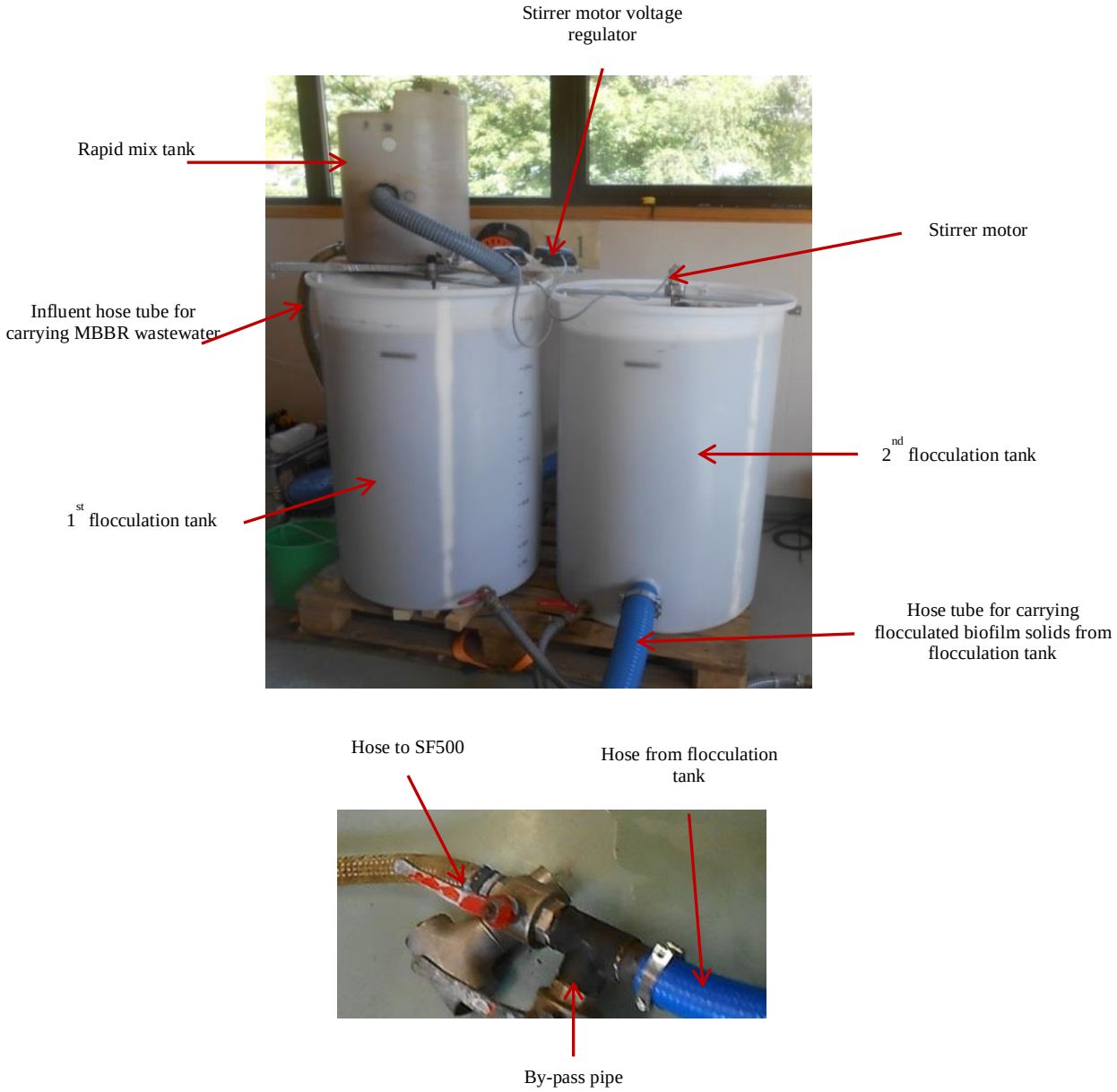

Figure 3-15: Pilot scale coagulation/flocculation setup

3.8 SF500

A newly designed SF500 which was previously used in Spain (Barragán, 2014), and has gone through various modifications, was used for the pilot scale test. Both manual and automatic modes were used with the machine to achieve the objectives of the study. Various SF fine mesh sieves of sizes 250, 210, 158, 90, 54, and 33µm, were evaluated. Flocculated MBBR biofilm wastewater was filtered using SF500 machine.

SF500 like any other SF model comes with a fully automated programmable logic controller (PLC), as shown in Figure 3-16. SF500 with a particular filter fine mesh sieve was operated, using the accompanied PLC panel. Figure 3-16 shows the front view of the control panel and various buttons for safe control of SF500.

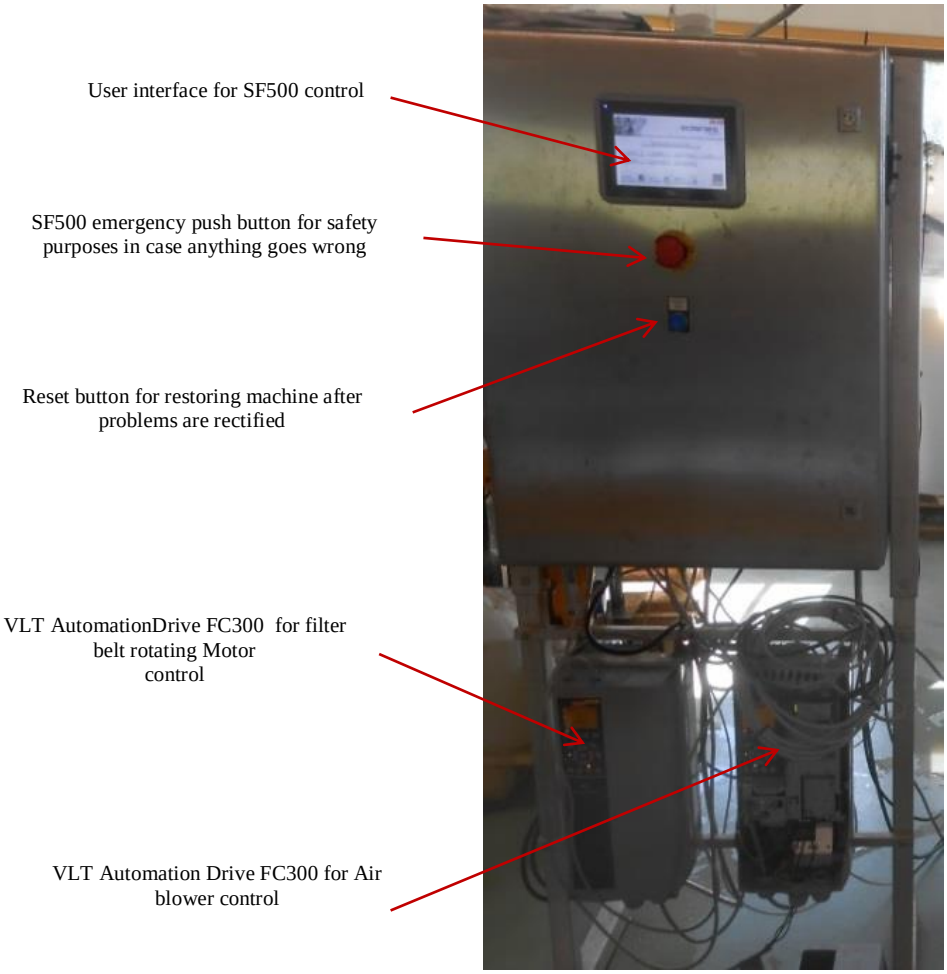

Figure 3-16: Front view of SF500 PLC control panel

The PLC controls the filter through a touchscreen, as a user interface. The user interface is shown in Figure 3-17. All settings whether in the automatic or manual mode were preselected, using the touchscreen for preferred performance of SF500.

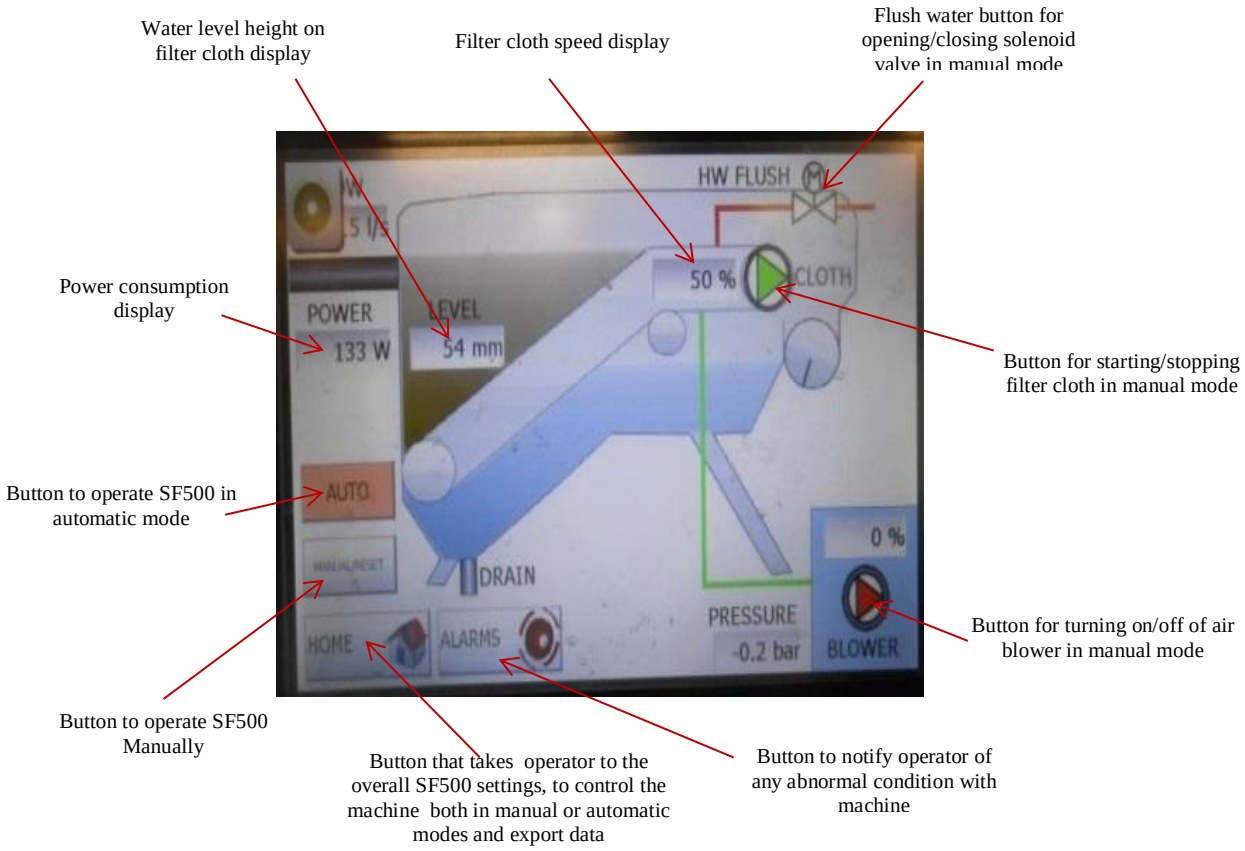

Figure 3-17: PLC touch screen user interface

SF500 as shown in Figure 3-18 has five important components for a better performance in filtering biofilm flocs. These are as follows;

1. **Inlet Pipe**: This pipe is made of plastic PVC, on which the influent hose can be connected. This segment provides an interconnection between SF500 and pilot scale coagulation/flocculation tank.
2. **SF500 Cartridge**: The filter frame/cartridge made of stainless steel, which houses both air and water knives, as well as the connections to the blower and water solenoid valve. It has two rollers (upper and lower) for rotating the SF fine mesh sieve. The upper roller has a shaft that is coupled to a three (3) phase motor. The roller has metal gears that are coupled to the lower inner rubber teeth edges of the mesh sieve. The lower roller however, has no gears but helps to facilitate the rotation of the mesh sieve. The mesh sieve is fixed on the cartridge by the two rollers by tension. The cartridge also has a stainless steel plate, which is designed with the motive to carry

filtered water contacting the back side of the mesh. The cartridge is also the mounting point for the scraper, which removes filtered biofilm from the mesh sieve to the sludge collection basin. The scraper is made of both stainless steel and flexible rubber. The flexible rubber lies static on top of the mesh sieve, and begins to remove filtered solids as the mesh sieve on the cartridge rotates.

3. **Effluent Basin**: This compartment receives the filtered water from the mesh. It also has a circular hole with PVC pipe on its side. The PVC pipe is connected to a hose, for discharging filtered water from SF500.
4. **Washwater Compartment**: This compartment is design to collect all back water, which has been used to clean the mesh sieve. A solenoid valve controls the wash water to SF500 wash nozzles. One part of this valve is connected to a clean tap water, while the other part connected to a 10 mm diameter tube. This 10 mm diameter tube is fitted to the water knife. The PLC for SF500 controls the valve, and can be operated in manual or automatic mode with a level threshold delay. The wash water contains high solids and polymer, so this compartment prevents wash water from coming into contact with filtered effluent. Figure 3-19 shows SF500 solenoid valve.
5. **Sludge Collection Basin**: This basin is designed to collect all sludge from the mesh sieves as it rotates. It is located below the upper roller of SF500 cartridge. As the mesh rotates, the scraper on the cartridge removes any filtered biofilm solids into the sludge collection basin. This basin however does not have a screw press, for dewatering and removing sludge like any other SF.

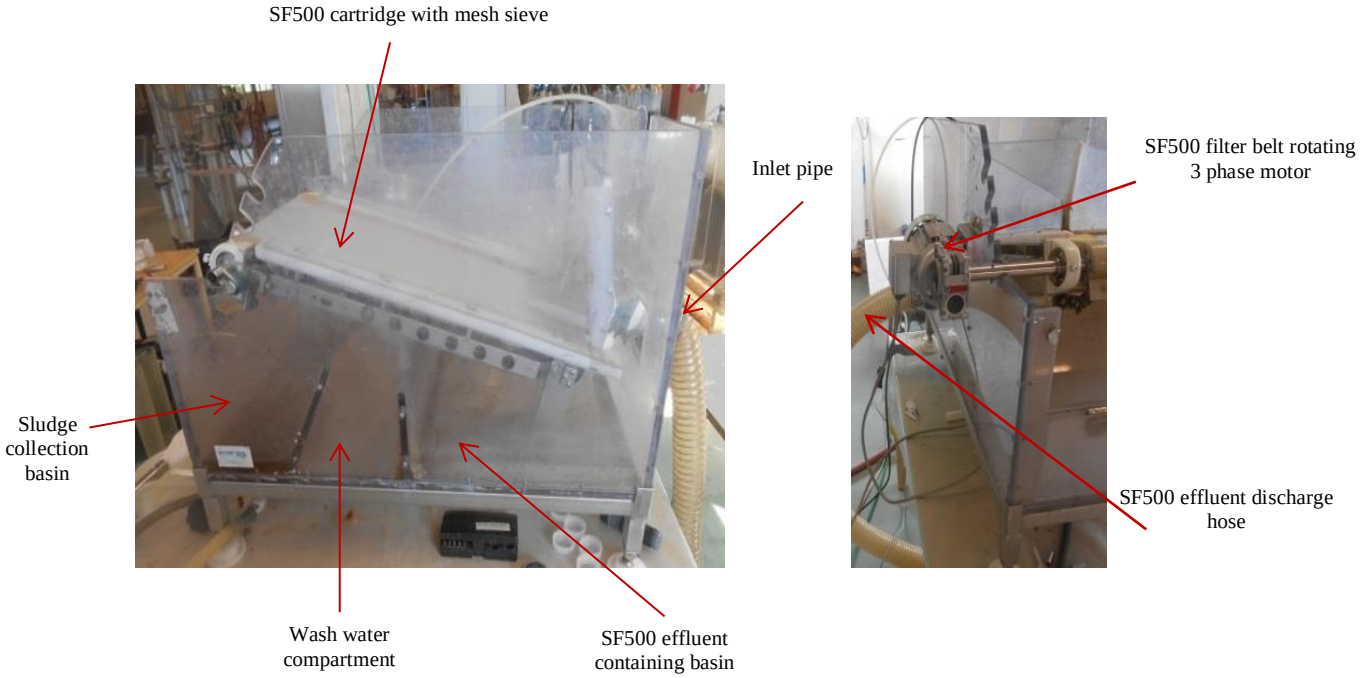

Figure 3-18: SF500 machine and its various compartments

3.8.1 SF500 operation

The flocculated MBBR Reactor 5 effluent biofilm solids leave the pilot scale coagulation/flocculation tank to the SF500 machine. As already stated in Section 3.7, only a portion of the flocculated water was filtered with SF500, while the remaining was by-passed unfiltered. The flow rate of the portion to be filtered was measured, using an electromagnetic flow meter as shown in Figure 3-19. This water then enters the inlet pipe to SF500 fine mesh sieve. Flocculated biofilm solids with sizes greater than mesh sieve size, initially settle above the filter mesh, and create a "filter mat". The mat enhances separation performance as particles build-up on the mesh, creating progressively smaller holes that retain increasingly smaller particles. Water that is filtered past the mesh exits through the outlet to the effluent basin. When the newly created pore size becomes too small, flocculated water level on the mesh sieve rises to a certain set point level. This height of water on mesh sieve is automatically measured with a level sensor. The three phase motor is then triggered to rotate at a set speed predetermine, in order to lower the water level below the set point level. The filter cloth starts to rotate like a conveyor belt, and moves the mesh sieve already covered with flocs, for new and cleaned mesh to begin the filtration process. During this same period

the filtered biofilm solids are transported to enable the thickening process by gravity. Sludge or filtered flocs are then removed from the mesh sieve, by the scraper which then drops into the sludge collection basin. The filtration process continuous until the entire mesh sieve size is clogged. At this point the solenoid valve shown below is triggered, to begin washing of the mesh sieve for one belt rotation. This wash water is then collected and discharged from the machine. The solenoid valve can also be pre-set to operate in a time sequence or manually when needed. The above mentioned process can continue to filter any amount of flocculated biofilm wastewater. When the right parameters are set on the PLC, the presence of an operator is not needed during filtration process. The PLC then logs all data (cloth speed, flow rate, power consumed, time of operation, and cleaning times) and stores these data, which can be exported in excel file for further analysis. Figure 3-20 shows SF500 scraper removing flocculated biofilm solids.

SF500 wash water solenoid valve

MagFlux Electromagnetic flow meter

Figure 3-19: Solenoid valve for SF500 washwater control (left) and Electromagnetic flow meter (right) for SF500 influent flow measurements

Figure 3-20: SF500 scraper removing flocculated biofilm solids

3.8.2 SF500 problems identified and immediate solutions provided

Though SF500 is a prototype and had gone through various modification, some problems were identified which made it very difficult for the machine to be operated the same way as it is operated on municipal primary wastewater. The problems were with the prototype design, and it was difficult to provide solutions for them in the short period of the study. Regardless, to avoid any delays in research, some temporary solutions were provided to fixe as much as possible and to meet the deadline of the project. For some of the problems, nothing could be done without complete overhaul of the machine, and many likely did not make much negative impact on the study. A few materials that were available were used to help fix some of the issues.

During the filtration process, as flocculated biofilm water entered SF500, shear currents were seen on the mesh sieve which broke up some of the biofilm flocs. This also allowed most of the water to be filtered at the same point. This problem was always seen each time filter cloth rotates to make way for clean mesh sieve to begin filtration. A critical look at SF500 showed the problem was as a result of a gap between the lower roller and the inner cartridge plate. This gap is shown on the left of Figure 3-21.

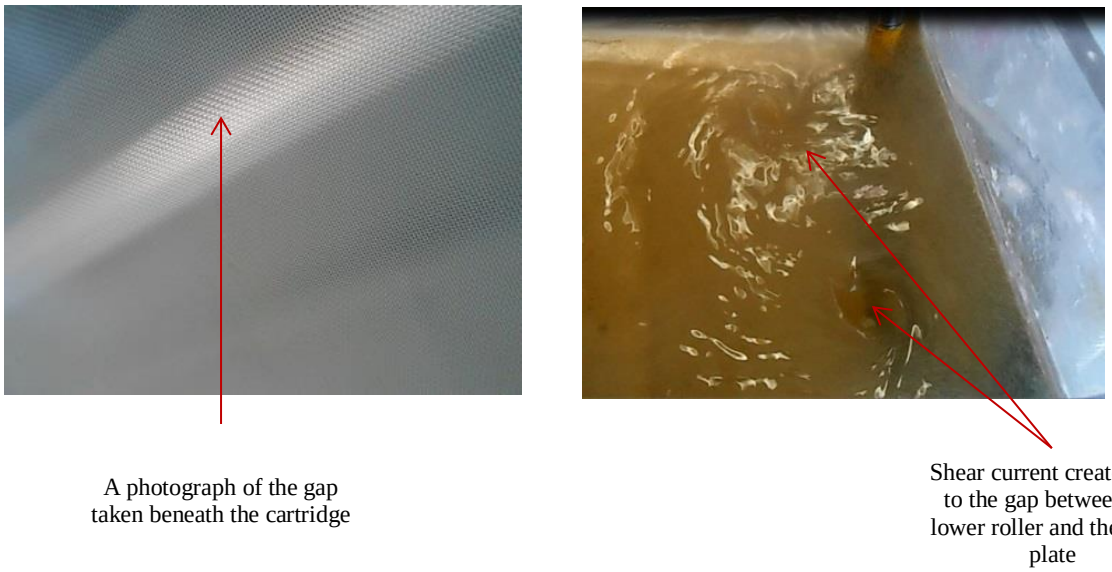

Figure 3-21: Gap identified (left) and shear current on mesh (right) on SF500

Another problem was identified with the cleaning of the mesh. This was identified when the machine was made to operate with only scraper. Some of the filtered flocs were left on the mesh sieves and carried to the next cycle. The air blower and air knife that came with the machine were also not efficient in cleaning capture flocs on mesh sieve. This problem worsened with higher mesh sieve sizes (> 90µm) were used. Figure 3-22 shows a photograph of a slightly cleaned mesh sieve by the scraper.

Figure 3-22: Slightly cleaned mesh sieve by scraper with SF500

The combination of the above two problems, lead to a third problem. This problem was solids being washed to the effluent water as shown in Figure 3-23. This problem was suggested to have risen from the fact that, there was a gap between the lower roller and the inner plate. And this gap made it possible for the filtered water to move through this gap to wash solids on the other side of the unclean mesh. Again these problems worsen when the machine was operated at higher flow rate, where the filtrate was enough to wash more solids to the effluent water.

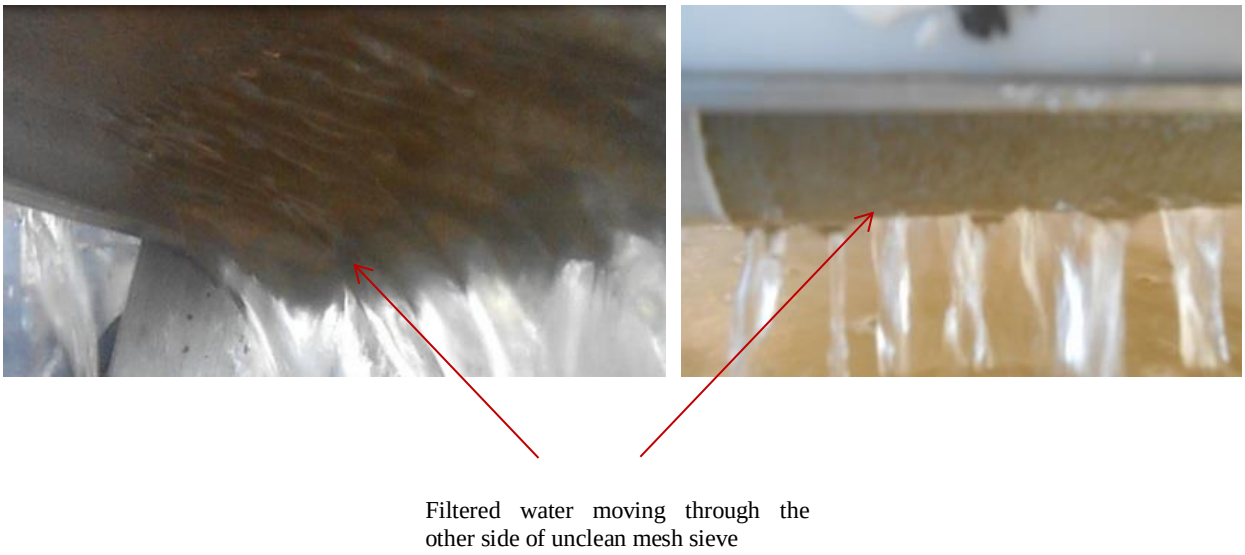

Figure 3-23: Photographs of filtered water washing solids to effluent water in SF500

The fourth problem was a build-up of flocs beneath the mesh sieve as it began to rotate. This problem was identified when floc sizes far bigger than the pore sieve size was identified in the effluent water. A critical look at the process and SF500 cartridge design helped to link the problem with a plastic support, which was originally intended to support the mesh sieve, when the water level increases and also to avoid bending in of the sieve under high water levels. Figure 3-22 shows a photograph of the problem identified.

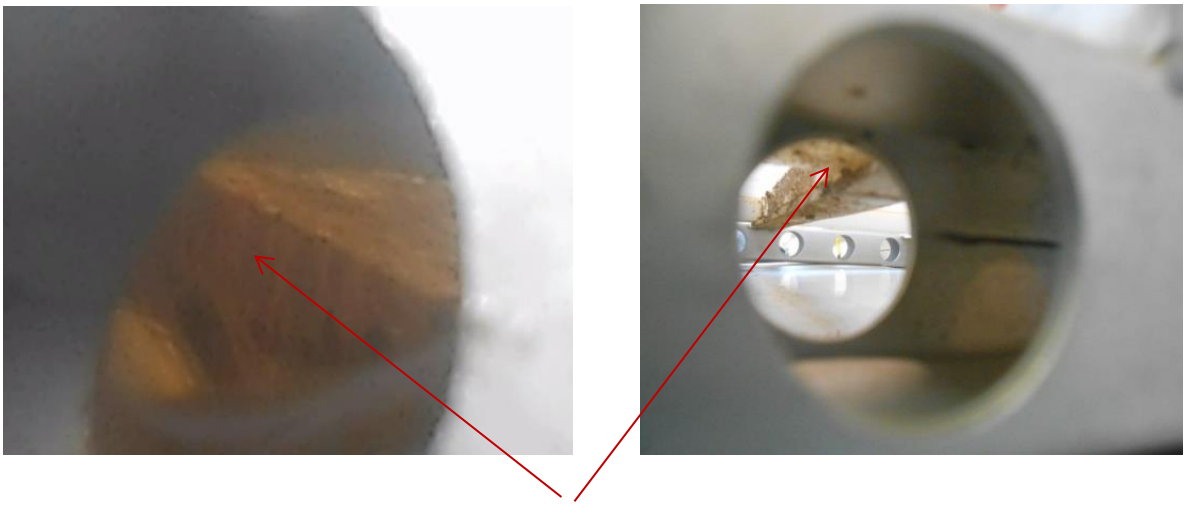

Figure 3-24: Solids build-up on mesh sieve plastic support inside the cartridge in SF500

The fifth problem was the design of the effluent collecting basin. This was made rectangular with limited slope angle, to facilitate easy discharge of filtered water. It should be made clear that any solid that finds its way to the effluent basin is not a stable suspension, since it had gone through coagulation/flocculation and will therefore settle at the shortest possible time. This basin was big and kept water for a longer time, which made some solids settle at certain parts of the basin. Figure 3-25 shows a photograph of the fifth problem identified.

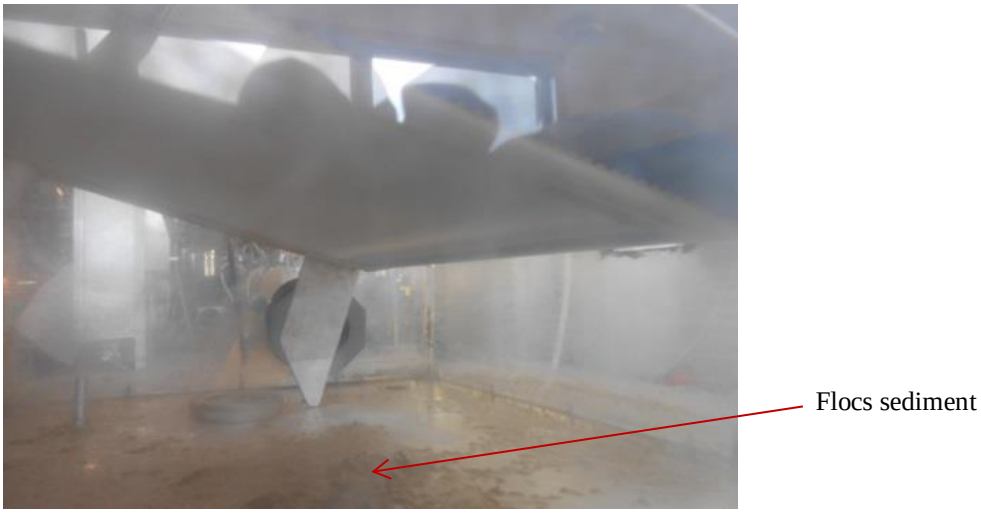

Figure 3-25: Floc sediment in effluent containing basin in SF500

In order to avoid any delays some immediate solutions were provided to some of the problems mentioned. Efforts were made to either reduce or remove the shear currents created on the mesh. A rectangular rubber plate shown in the top left of Figure 3-26 was fixed to the upper frame, which lies on top of the mesh sieve. Again with the help of a heat gun, plastic plate was designed and fixed on top of the inner plate of the cartridge. A flexible rubber cover was fixed to the edge of this plate, and made to lie on top of the lower roller to close the gap. This flexible rubber was used due to the contact it made with the mesh and therefore will avoid any rip-up of mesh sieve as it rotates. This flexible rubber was to prevent filtered water from moving to the other side of the mesh. These provided solutions were not enough to eradicate the problem completely but was able to reduce its effects. However the flexible rubber also generated a secondary problem of producing some frictional movement on the lower roller. This secondary problem was considered as minor and therefore no further solution was provided to that. Figure 3-26 shows various solutions that were provided to fix some of the problems identified.

Figure 3-26: Rubber plate fixed to SF500 upper frame (top left) and the designed plastic plate fixed inside SF500 cartridge/frame (top right)

Considering the forth problem stated above, the mesh sieve plastic support was removed. This totally rectified that problem. However a secondary problem that was associated occurred, when the water level on mesh sieve increased. Therefore machine was operated in a way to avoid higher water level on mesh sieve. Relating to the fifth problem, nothing could be done and also it did not have much negative impact on the study. Apart from these solutions that were provided to facilitate the thesis process, further recommendation on the design has been provided in Section 6 of this thesis.

These problems and solutions however affected the normal operation of the machine, and at some point in time much water wash cleaning was used to help clean the mesh sieves (> 90µm) before it begins another cycle. This resulted in either diluting samples or making the technology less efficient, because more cleaned water had to be used to clean the mesh sieve. Again the washwater contained more solids and cannot be discharged but had to be recycled. Unfortunately a recycled pump was not available for this purpose. Therefore during the pilot scale study, TSS of the wash water and the sludge was measured. Samples were also taken from inside the mesh sieve (filter water) and compared to the actual designed effluent of SF500. This was to determine the effects the identified problems had on the performance of SF500 with regards to achieving the objective of the study. TSS, TP, COD, pH and Turbidity of all SF500 effluent samples were evaluated.

3.9 SF1000

SF1000 as shown in Figure 3-29 was used with fine mesh sieves 350 and 33 µm for characterizing the primary degritted wastewater at NFR. SF1000 as any other SF had its own PLC with a front view same as that of SF500. However the user interface for machine control had additional control buttons for other functionalities (screw press, cold, and hot flush water). This user interface also displays the influent wastewater flow rate. Figure 3-27 shows the user interface control for SF1000 machine.

The machine is 415kg by weight, and design for an average operating power consumption of 3.5kW. It has the capacity for 31m^3/h or above depending on the mesh sieve size used. Again depending on the design (flow rate) and wastewater constituents, TSS and biological oxygen

demand (BOD_5) removal efficiency of about 40 – 80% and 20 – 35% respectively can be achieved (Salsnes, 2014).

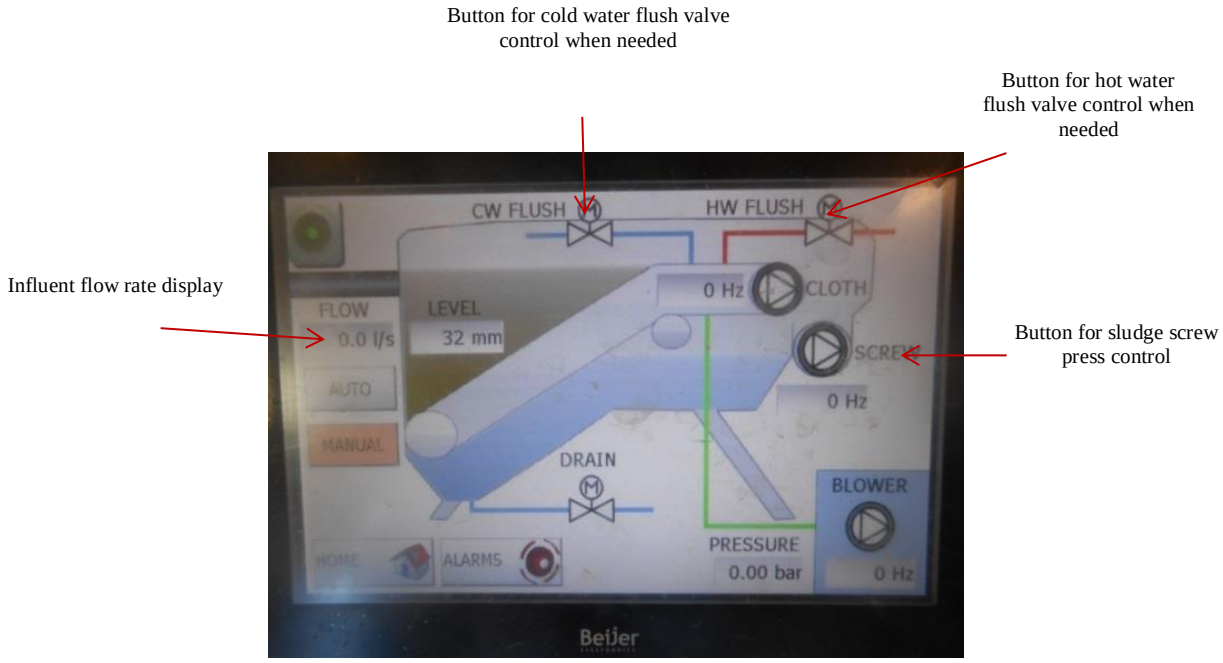

Figure 3-27 : PLC user interface for SF1000 machine control

3.9.1 SF1000 screening test with 33 µm and 350 µm fine mesh sieves

The NFR primary wastewater to be filtered entered the inlet chamber, and solid particles (usually toilet papers) with sizes greater than mesh sieve size, initially settle above the filter sieve and creates a "filter mat". The mat enhances separation performance as particles build-up on the mesh, creating progressively smaller holes that retain increasingly smaller particles. Water that is filtered past the mesh exits for collection. When the newly created pore size becomes too small wastewater level rises to a certain set point level (measured by a sensor when it's operated in automation mode). The filter cloth, blower, and screw press are triggered to start operation, with some set delay points. The filter cloth starts to rotate like a conveyor belt, transporting sludge and enabling the thickening process. Gravity thickens the sludge to 3– 8%. With the help of an air knife or scraper, sludge is removed from mesh into the sludge collection area. A screw press further dewaters the sludge to 20–30% (Salsnes, 2014) dry mass (DM) before it exits the unit . Figure 3-28 and 3-29 shows a photograph of SF fine mesh sieves (350 and 33um) and SF1000 respectively, used for the NFR primary (degritted) characterization test.

Figure 3-28: 350 and 33 µm fine mesh sieve on SF1000 cartridge

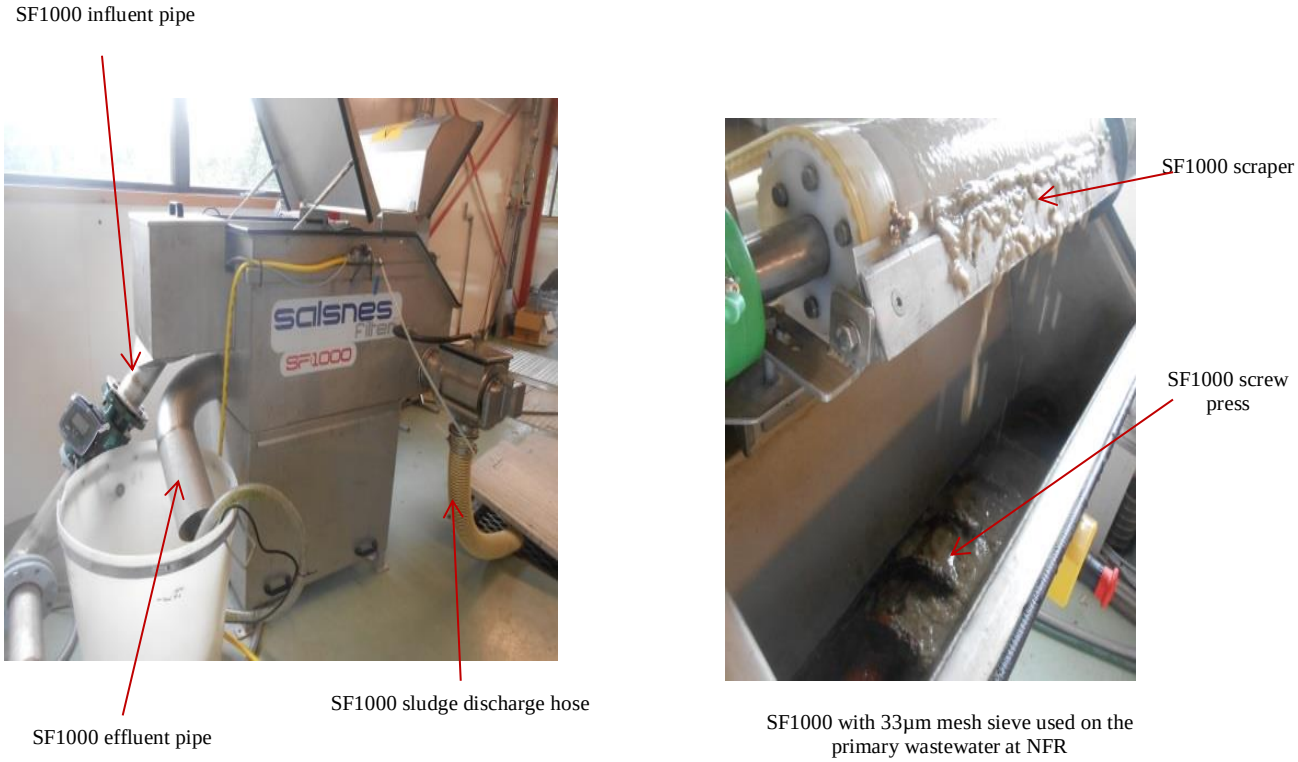

Figure 3-29: SF1000 machine (left) and scraper on 33µm mesh (right)

The SF1000 PLC user interface shown above was used to change any variable such as water level limits, cloth speeds, and many parameters for preferred performance especially in the manual mode. However during this test, cloth speed variation and filter mat formation were of most importance. SF1000 with 350 µm mesh sieve was operated in automatic mode where filter mat formation and air knife cleaning were used in the filtration process. However SF1000 with 33 µm mesh sieve was operated in manual mode, where only the scraper cleaning was used and machine operated at constant speed without filter mat formation.

During this SF1000 screening test both influent and effluent samples were evaluated for TSS, TP, TN, and COD. PSD analysis was also performed on these samples using portable series FlowCAM shown in Figure 3-30 of Section 3.10.

3.10 FlowCAM

Portable series FlowCAM (Fluid Imaging Technology, USA) shown in Figure 3-30 was used for analyzing the particle size distributions (PSD) of samples. It is an integrated system for rapidly analyzing particles in a moving fluid. It combines selective capabilities of flow cytometry, microscopy, and fluorescence detection for its operations. It automatically counts images captured by a camera, and analyze (count base on sizes and shapes) the particles in the sample or in a continuous flow. It uses its attached computer software, to process the raw data and classify them for further analysis Figure 3-31 shows the main window for visual spreadsheet (left) and an example of the separate view window (right) including the particle properties display on the attached computer. This instrument has the following features and capabilities (Fluid Imaging Technologies, 2011);

1. High-speed digital imaging.
2. Particle size, count, and shape.
3. Real-time bulk and individual particle analysis
4. The combined benefits of multiple instruments.
5. Compact and durable packaging.
6. Ability to Image particles 2 µm to 3 mm in diameter.
7. Fluorescence detection providing additional selectivity.
8. Scatter detection for low particle concentrations.

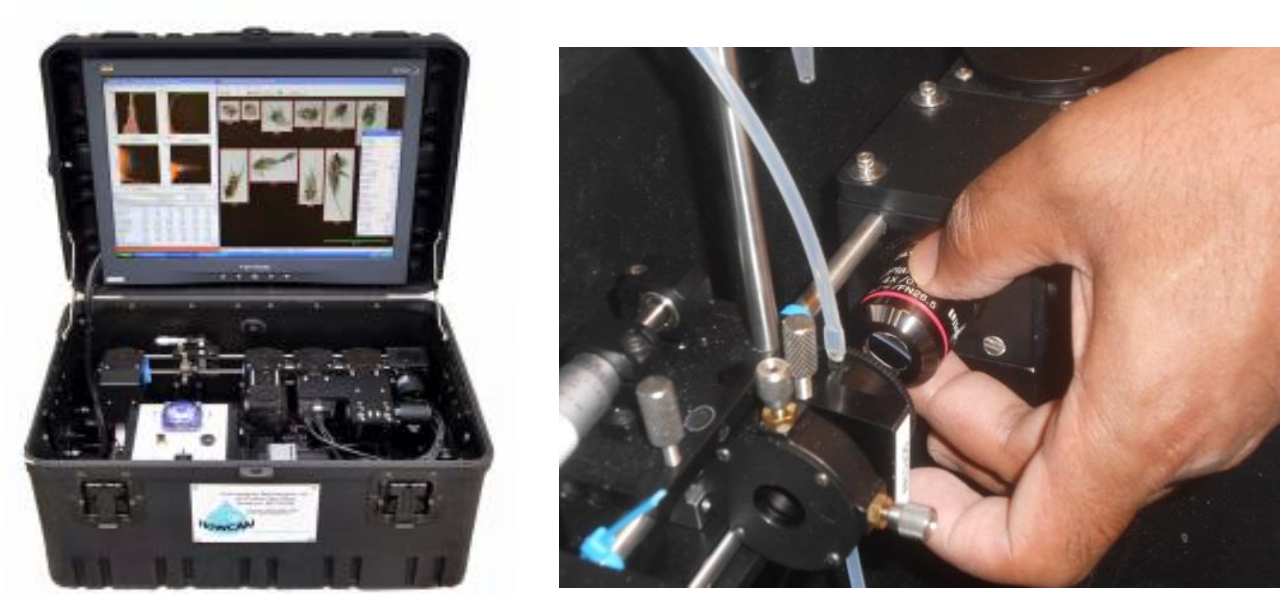

Figure 3-30: Portable Series FlowCAM (left) and 4X zoom camera fixing (right)

The FlowCAM architecture is divided into three distinct systems (Fluid Imaging Technologies, 2011). These are optics, fluidics, and electronics. Figure 3-32 shows a block diagram showing all the various distinct architecture of the FlowCAM.

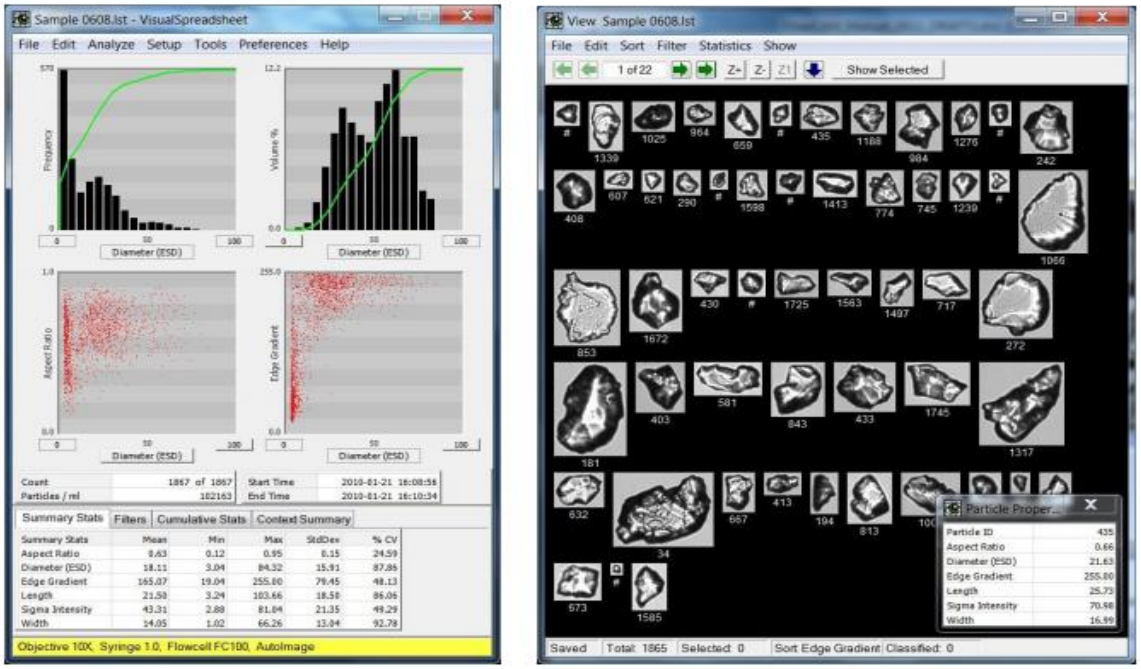

Figure 3-31: The main window for visual spreadsheet (left) and an example of the separate view window (right) including the particle properties display (Fluid Imaging Technologies, 2011)

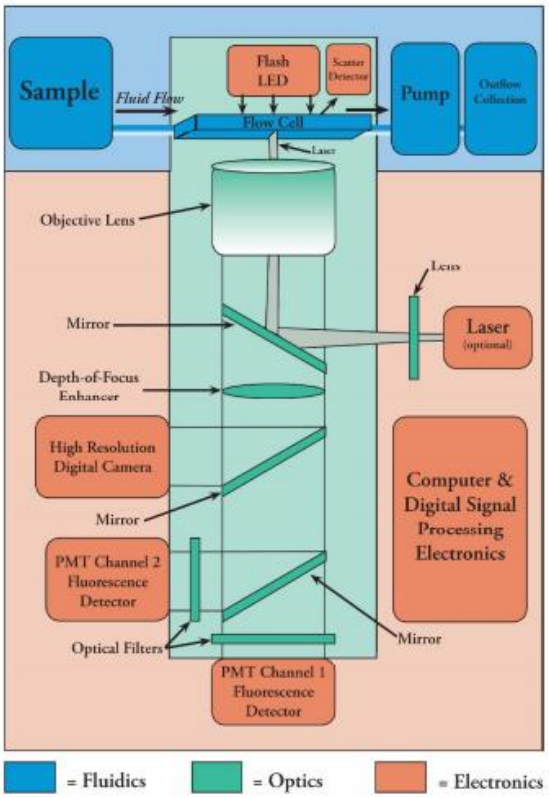

Figure 3-32: Block diagram FlowCAM showing the various distinct architecture in different colures (Fluid Imaging Technologies, 2011).

The FlowCAM with a field-of-view (FOV) flow cell of 300µm inner diameter was used for the evaluations. Test samples from SF1000 and bench scale SF particle characterization tests were analyzed using FlowCAM. All samples were diluted in order to reduce the number particles moving through the flow cell. This measurement for the instrument was performed, according to standard procedure provided in the company's product manual. 4X magnification camera was used to capture particles of different sizes in the samples and then grouped for further counting. These data was then stored in an excel file and later exported for further analysis.

3.11 Malvern Mastersizer 3000 for PSD

Malvern Mastersizer 3000 is analytical instrument developed by Malvern Instrument technology. It was also used for PSD evaluation. The instrument uses both blue and red laser lights of wavelength 470 nm and 630 nm respectively for particle examinations. This instrument has an

optical unit, normally referred to as, the optical bench or just the instrument; it's the core of the Mastersizer 3000 system. Its purpose is to transmit red laser light and blue light through the sample carried in the cell and then uses its detectors to generate data about the light scattering pattern caused by the particles in the test sample. This pattern is then interpreted by the Mastersizer software to provide accurate particle size information (Malvern, 2011). The software is run on a computer and controls the optical unit and dispersion unit hardware. Figure 3-33 below shows the software user interface with a measurement file loaded. The software also processes the raw data gathered by the system, providing flexible data analysis, reporting features and helps the operator for a preferred operation of the instrument. Figure 3-28 below shows a picture of the Malvern Mastersizer 3000 setup.

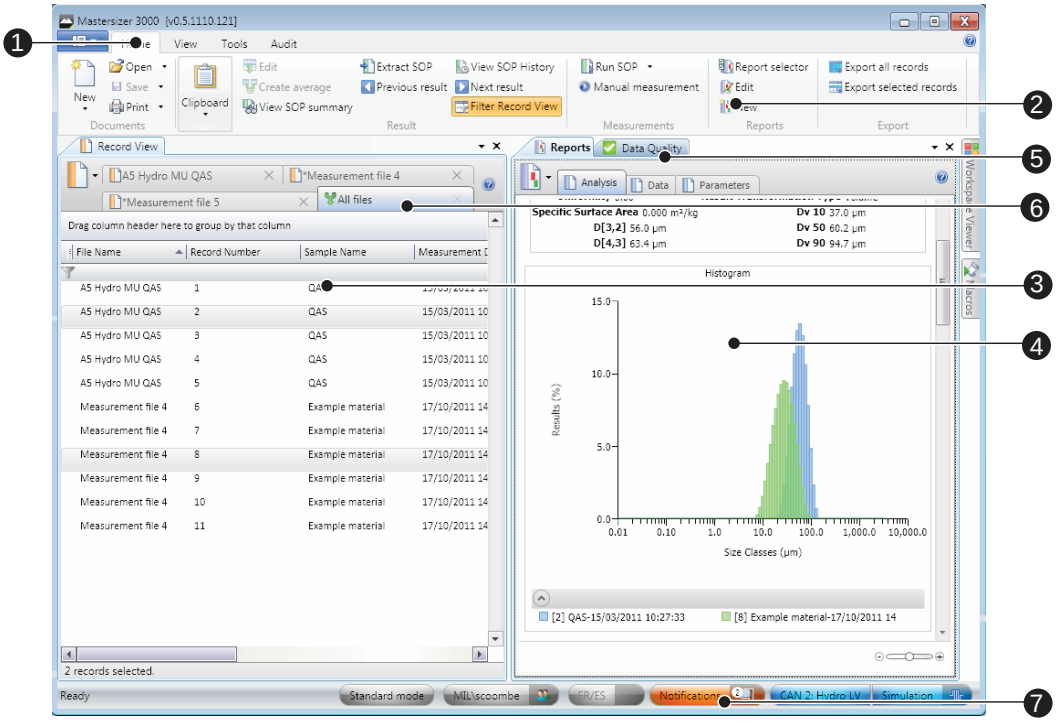

Figure 3-33: Malvern Mastersizer 3000 software user interface with a measurement file loaded (Malvern, 2011b)

Keys:

1. Ribbon selector tab
2. Control ribbon
3. Record view panel
4. Reports tab
5. Data quality tab
6. All files tab
7. Status tab.

Figure 3-34 shows the setup for Malvern Mastersize 3000 measurement. PSD of all samples from SF1000 screening test, and bench scale SF particle characterization tests were evaluated. The correct standard operation procedure (SOP) previously used by AquateamCOWI was used for all analysis.

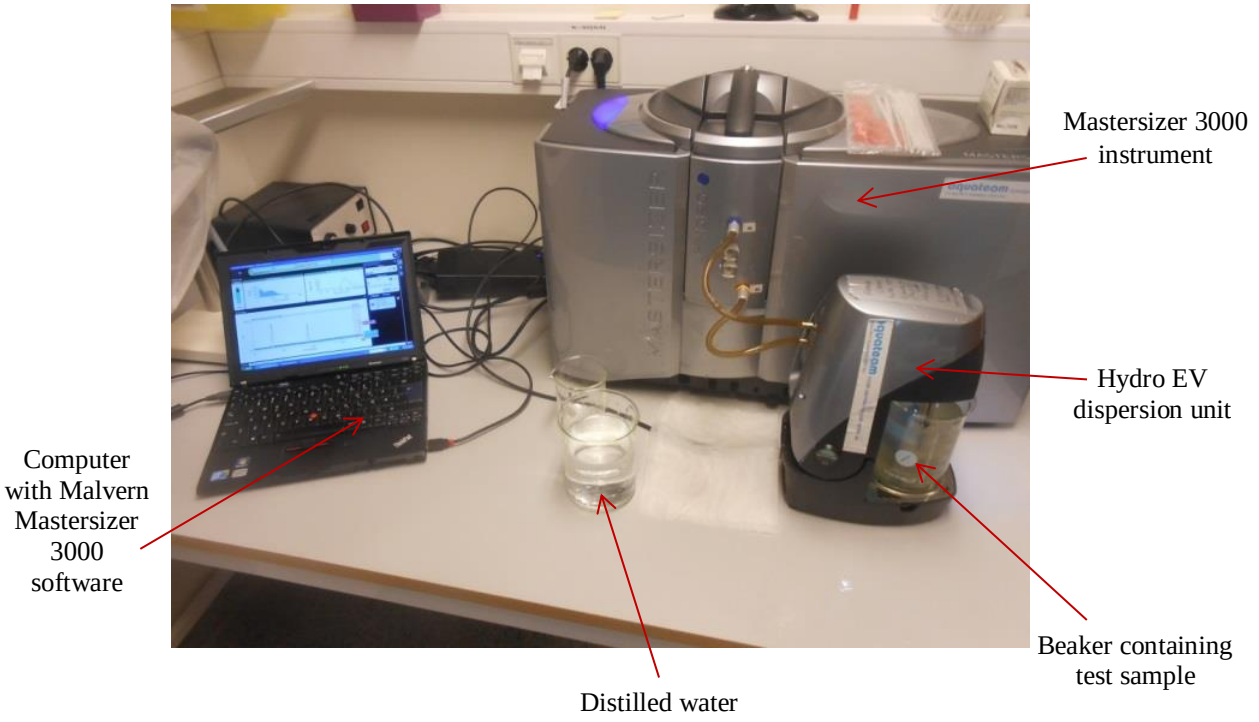

Figure 3-34: Malvern mastersizer 3000 experimental setup for PSD analysis

During the PSD analysis a 600 mL beaker capacity was used to contain the sample prior to circulation. The beaker was filled with about 500mL diluted sample in order to obtain an obscuration less than 20% and also to avoid spillage of sample when the pump begins. Mastersizer 3000 application software was used to initialize instrument and to measure background with distilled water. Again distilled water was used to clean instrument in-between sample measurements and after sample measurement using the same software. PSD analysis data was then exported for interpretation and discussion.

3.12 Zeta potential measurement

As part of the thesis, critical coagulant concentration for the pilot scale coagulation/flocculation process was determined using zeta potential measurement. Figure 3-35 shows optics layout used for Zetasizer Nano ZS for zeta potential measurement. Zeta potential analysis was performed on the MBBR biofilm wastewater using Malvern Zetasizer Nano ZS as shown in Figure 3-36.

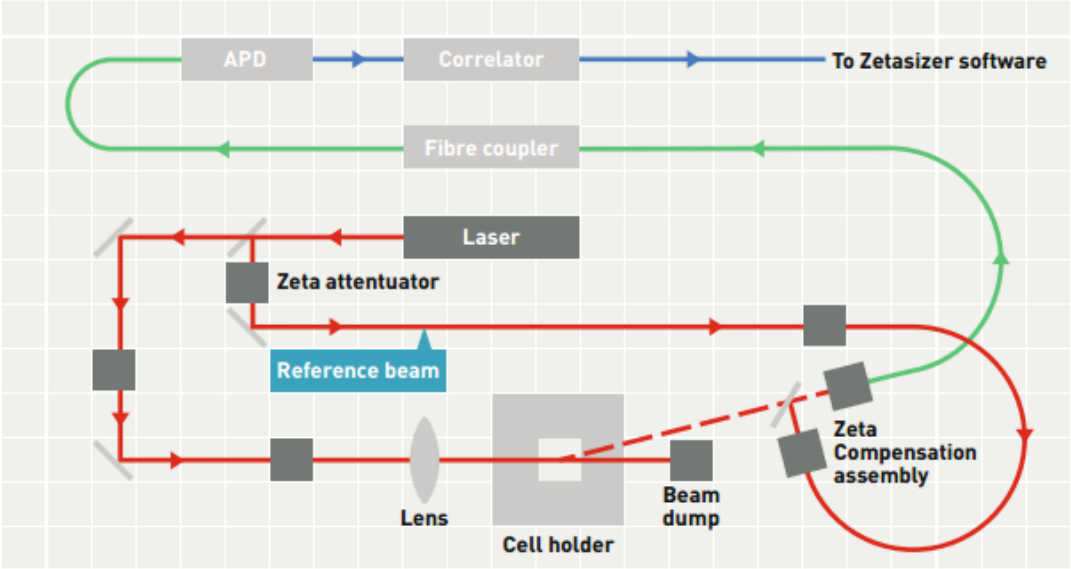

Figure 3-35: The zeta potential optics layout used for all zeta potential measurement (Malvern, 2014b)

The instrument uses a sample cell with two (2) electrodes at its ends. These electrodes are connected to the positive and negative polarities of the instrument. When a potential is applied across this cell the sample particles move either to the negative or positive electrode based on their surface charges. This direction determines the charge on the particle. A laser is used to measure the velocity of the particle with the applied potential and therefore the zeta potential is measured. During start up the instrument was powered up with a switch behind it and the connected laptop turned on and allowed to stabilize for 30mins. The software on the computer with DTS (Nano) icon was then started. A *.dts* file is created for all measurements to be saved (Malvern, 2014a). A standard operating procedure (SOP) for zeta potential

measurement was selected for all sample measurements. The sample to be used for zeta potential measurement was prepared as follows;

1. 1 L of MBBR Reactor 5 effluent sample was taken for jar test coagulation experiment without settling using Karima Kemwater flocculator 90.
2. PAX-18 chemical dose selected was added to the sample and stirred at 400 rpm for 20s.
3. After 20 s, 5 mL of the sample was pipetted and used to fill the sample cell by avoiding air bubble in the cell. Sample cell was cleaned and inserted into the instrument and the lid closed.
4. The start button on the computer software was clicked to measure the zeta potential.
5. The pH and temperature of the remaining sample were then measured and recorded.
6. After the zeta potential measurement the sample cell was removed and cleaned by flushing through it with distilled water. The sample cell was then ready to be used for the next measurement.
7. The experiment from procedure 1 to 6 was repeated for various PAX-18 chemical doses.

After the entire experiment, the saved data on the computer was exported and further analysed together with the recorded temperature and pH measurements.

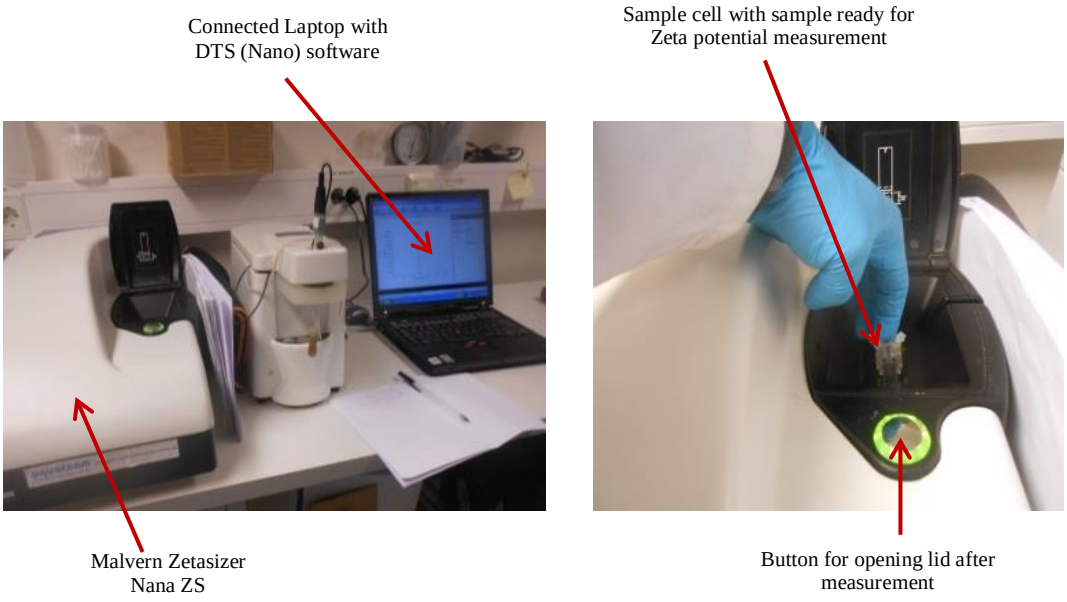

Figure 3-36: Malvern Zetasizer Nano ZS setup for zeta potential analysis

3.13 Characterization of primary (degritted) wastewater and MBBR Reactor 5 effluent wastewater at NFR using bench scale SF apparatus

As part of this thesis, bench scale SF apparatus shown in Figure 3-7 was used to characterize both primary (degritted) wastewater and MBBR biofilm wastewater at NFR. This was done to characterize the particle size distribution of each wastewater, and also to determine the removal efficiency with respect to SF mesh sieve sizes. This experiment was also useful to know the effect of each mesh sieve size upstream the other. It helps one to determine what meshes to select in order to ensure high removal efficiencies while increasing mesh flow rate.

The experiments on primary wastewater and MBBR biofilm water at NFR were performed as shown in Figure 3-37. For Experiment 1, about 30 L of NFR primary wastewater was collected stirred, and sample 1 was taken for further analysis on PSD, TSS, TP, TN, and COD. The remaining water was then filtered using bench scale SF apparatus, using 350 µm mesh sieve without forming filter mat. During the filtration process the mesh was taken out as soon as it began to clog, and then cleaned to continue the filtration process until all remaining wastewater were filtered. The filtrate from 350 µm mesh sieve was then stirred completely and sample 2 was taken for similar analysis as mentioned above. The remaining 350 µm mesh sieve effluent was further filtered with 250 µm mesh sieve using the same procedure as for 350 µm. The 250 µm mesh sieve filtrate collected was stirred completely and sample 3 collected for similar above mentioned analysis. This same filtration process was repeated from one higher mesh sieve size to a lower mesh sieve for 150 µm, 90 µm, 74 µm, 55 µm, 33 µm and 18 µm mesh sieves. After the entire filtration processes nine (9) samples were collected for further analysis and results obtained compared and discussed in chapter 4 of this thesis.

Experiment 2 shown in Figure 3-37 was performed with the same procedure as Experiment 1 outlined above, but using about 30 L of MBBR Reactor 5 effluent at NFR as raw sample.

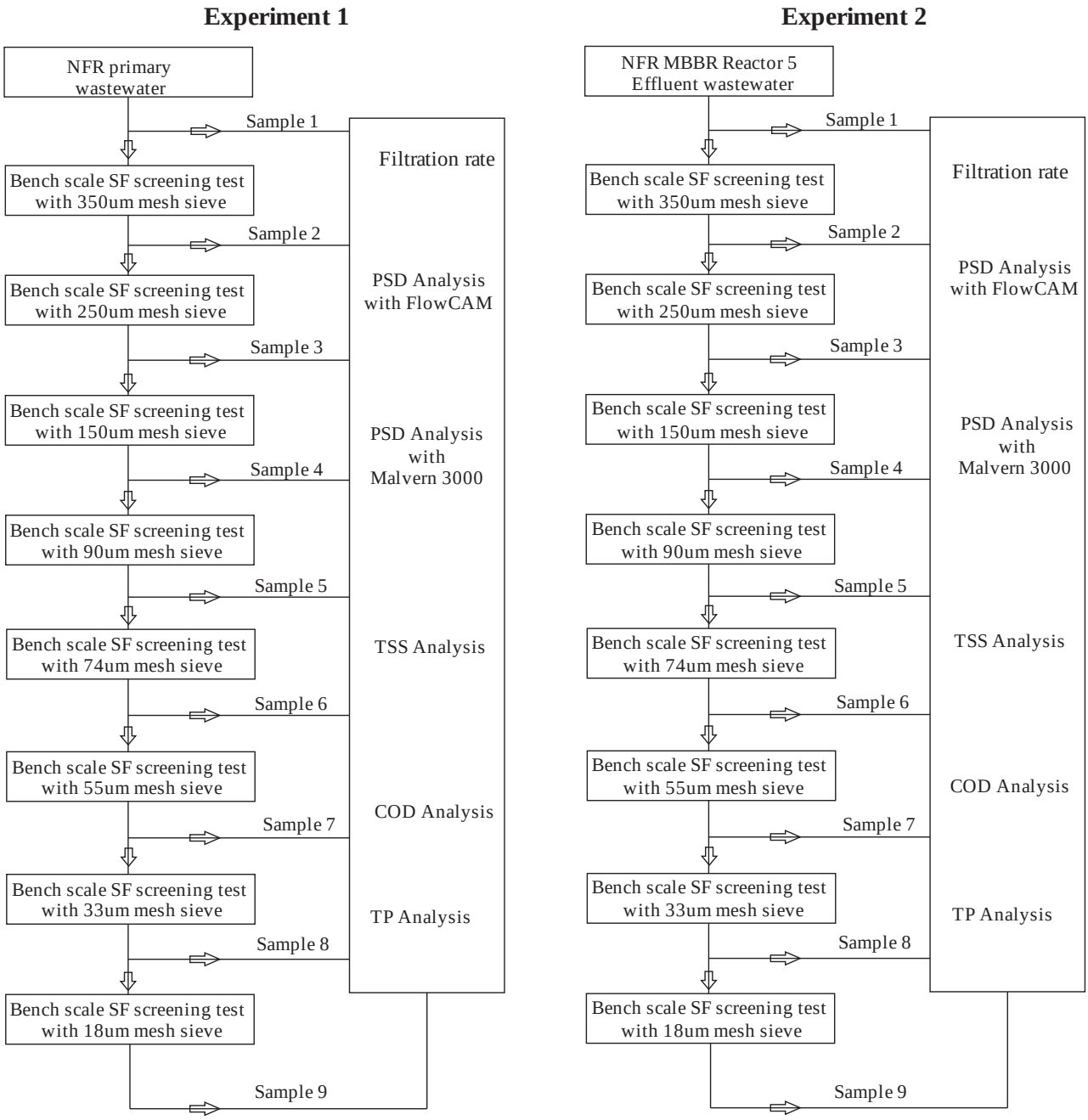

Figure 3-37: Flowchart of primary (degritted) wastewater (left) and MBBR reactor 5 effluent wastewater (right) characterization using bench scale SF apparatus at NFR

3.14 Characterization of NFR primary (degritted) wastewater with SF1000 using 33µm and 350 µm mesh sieves for BNR

This experiment was to characterize the primary (degritted) wastewater at NFR using SF1000 machine with 33 µm and 350 µm mesh sieves. SF1000 machine with 350 µm mesh was operated with filter mat formation at various cloth speeds of 10, 20, and 30Hz while that of 33 µm mesh sieve was operated without filter mat formation at various cloth speeds of 10, 20, and 30Hz. SF1000 with these two mesh sieves were operated at the same SF1000 influent flow rate of 1.5L/s. SF1000 effluent were further analyzed for TSS, TP, TN and COD. PSD analysis was performed with FlowCAM on SF1000 effluent samples. Figure 3-38 shows a flow chart of how the NFR primary wastewater characterization was performed.

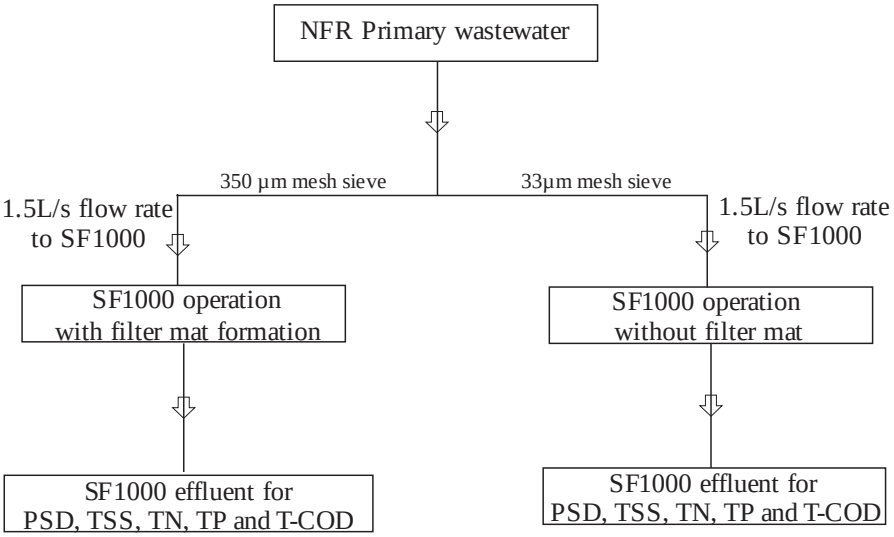

Figure 3-38: Flowchart for NFR primary (degritted) wastewater characterization using 33µm and 350µm on SF1000

CHAPTER IV

4.0 RESULTS AND OBSERVATIONS

This chapter seeks to present all results obtained during the period of study and to discuss them. It is organised in the order at which the entire thesis experiments were structured. This chapter is divided into four (4) main sections. First section will be on results and discussions relating to all experiments on bench scale SF screening test with MBBR biofilm wastewater (Reactor 5). The second section presents pilot scale Coagulation/Flocculation processes and SF500 filtration. The third section will be related to particle size characterization of NFR primary (untreated/degritted) wastewater and effluent from MBBR Reactor 5, using bench scale SF screening apparatus from 350 µm to 18 µm mesh sieve openings. The last section will focus on SF1000 filtration with 33 µm and 350 µm mesh sieves on NFR primary wastewater

4.1 Bench scale SF screening test for chemical/polymer selection

This section presents all experiments, results, and follows with discussion regarding selection of both chemical and polymer to be used on the pilot scale coagulation/flocculation process. It also presents how various optimum parameters were obtained and discusses the reasons for each selection.

4.1.1 Chemical and polymer selection

Based on initially conducted jar test experiments with rapid mixing speed of 400 rpm for 20s, slow mixing speed of 50 rpm for 10 min, and settling time of 10 min, the turbidity of the settled jars was used to obtain Table 4-1 below. The PAX-18 and A-130 combination dose (Sample 6) was selected based on the combination already used by NFR wwtp for their DAF (Dissolved Air Floatation) process.

Table 4-1: Optimum values based on settled turbidity on MBBR reactor 5 effluent and NFR wwtp optimum

Sample	Chemical & Polymer combination	Chemical dose (mg Al/L)	Polymer dose (mg/L)
1	PAX-18 only	17.1	—
2	C-490 only	—	0.2
3	C-496 only	—	0.2
4	PAX-18 and C-490	17.1	0.5
5	PAX-18 and C-496	17.1	0.3
6	PAX-18 and A-130	17.1	0.7
7	MBBR Reactor 5 effluent		

Dosing values presented in Table 4-1 were used on bench scale SF apparatus to perform bench scale SF screening test experiment as described in Section 3.6 with mesh seizes 18, 33, 74, 90, and 158µm. The results obtained are presented in Figure 4-1 using only SS removal efficiencies.

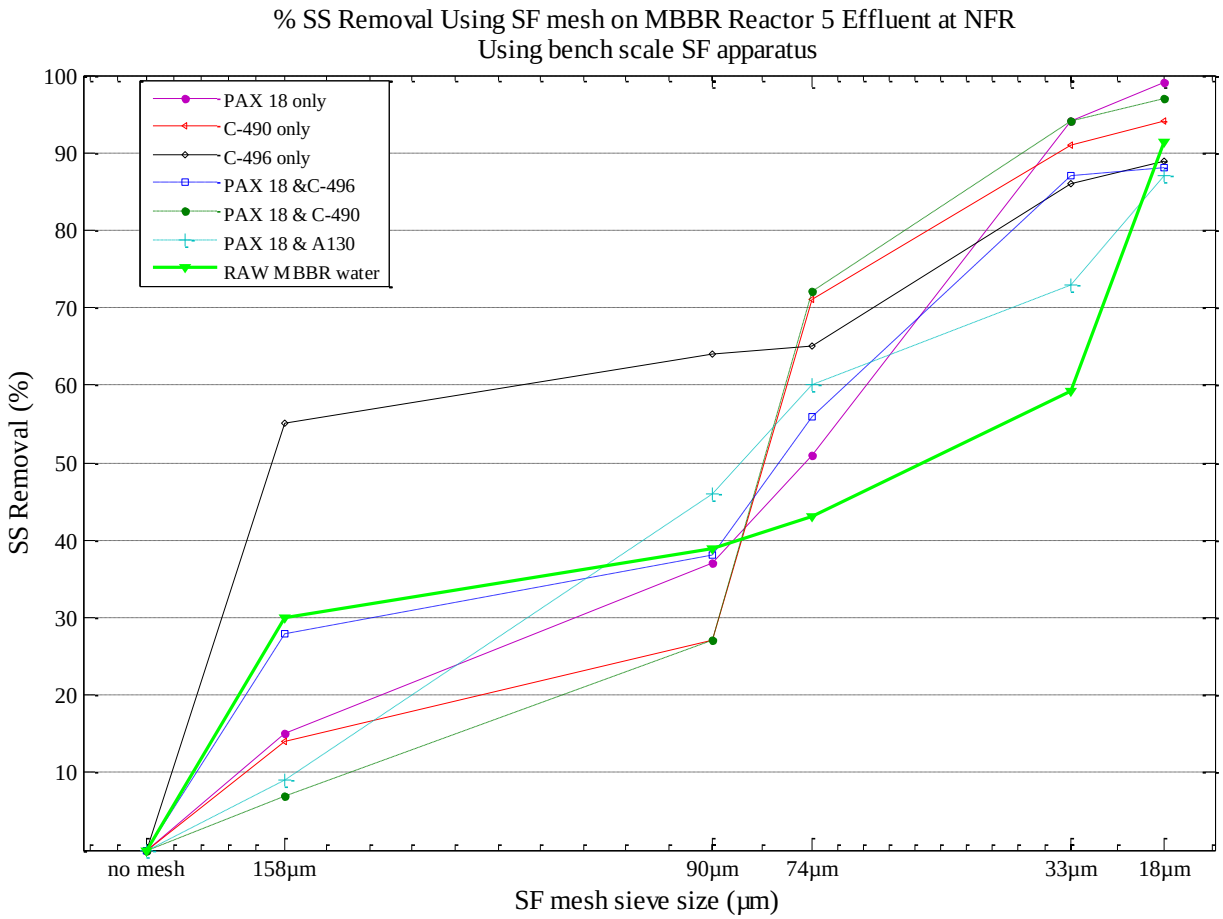

Figure 4-1: Percentage SS removal using settled turbidity optimum dose on bench scale SF apparatus

SS removal results from SF fine mesh sieve 33 µm were then used, to make a decision in selecting PAX-18 and C-490 for any further analysis, based on the following reasons;

- From Figure 4-1, 33 µm mesh sieve provided all filtrate samples with percentage SS removal above 50% and also showed a clear distinction between raw MBBR water and using chemical precipitation.
- Though mesh sieve 18 µm gave excellent results, based on its lower filtration rate, it was considered not economical for commercial use.
- PAX-18 & C-490 combination (sample 4) provided 94% SS removal and was the highest among all samples with respect to 33 µm mesh sieve.

PAX-18 and C-490 were selected for further bench scale SF screening test as described in Section 3.6 and Figure 3-11 to determine various optimum doses to be used on the pilot scale coagulation/flocculation experiment.

4.1.2 PAX-18 optimization

PAX-18 chemical with dosing range from 3.65 mg Al/L to 19.44 mg Al/L was studied using both jar test and bench scale SF apparatus according to Section 3.6. Results obtained are presented in Figure 4-2 below.

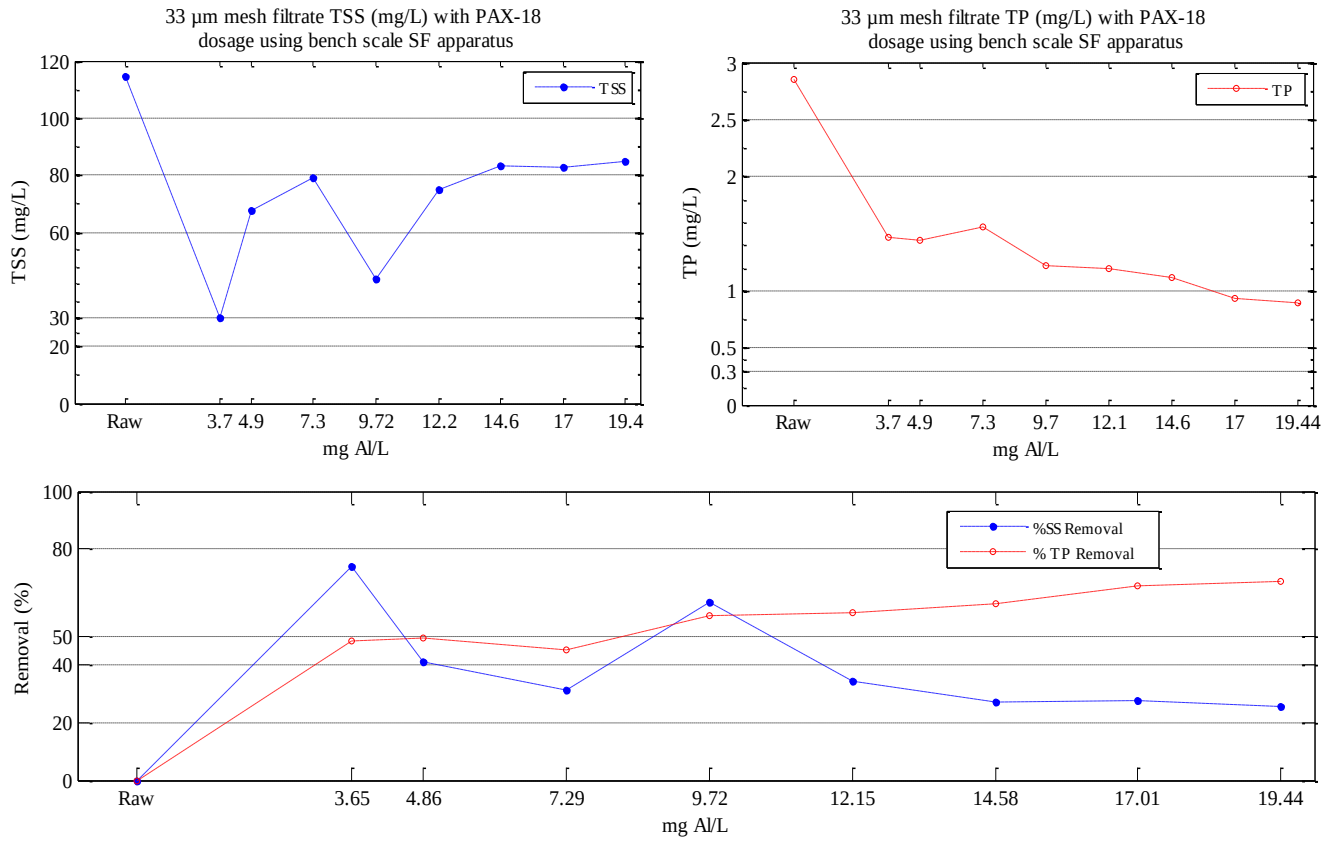

Figure 4-2: TSS against PAX-18 (top left), TP against PAX-18 (top-right) and removal efficiency against PAX-18 (down) using 33µm mesh sieve

From Figure 4-2, 9.72 mg Al/L and 17.0 mg Al/L were selected as optimum doses for PAX-18. These two (2) doses were selected based on results obtained and visual observations of flocs during the process. 9.72 mg Al/L had both %SS and %TP removal above 50%. 17.0 mg Al/L formed bigger flocs on visual observations, however due to the limitations (pouring of flocs) of bench scale SF apparatus, the TSS results showed otherwise. Again 17.0 mg Al/L from previous settled turbidity test was as the optimum dose. 17.0 mg Al/L can again be seen from Figure 4-2, to have high phosphorus removal since phosphorus removal was critical for the study, this dosage was selected. Though 19.44 mg Al/L had a better phosphorus removal, based on chemical cost, using more chemicals was not an option.

4.1.3 C-490 optimization

Polymer C-490 with dosing range from 0.05 mg/L to 1.0 mg/L was studied using both jar test and bench scale SF apparatus according to Section 3.6. Results obtained are presented in Figure 4-3 below.

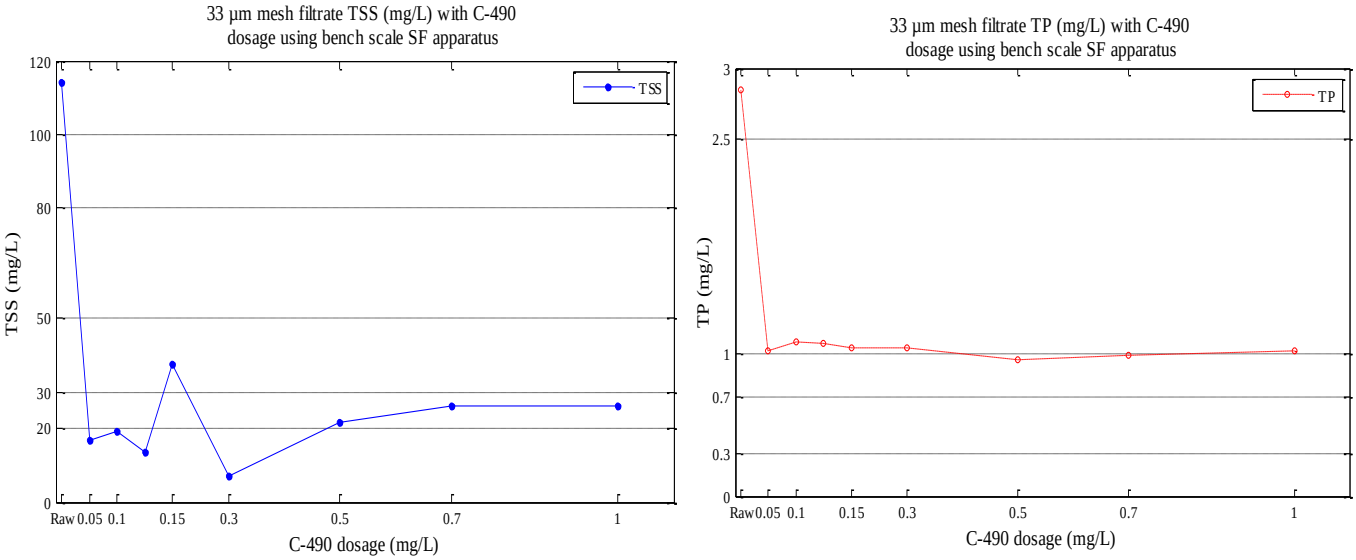

Figure 4-3: TSS against C-490 (left) and TP against C-490 (right) using 33µm mesh sieve

From Figure 4-3 below, 0.3 mg C-490/L provided a filtrate with the lowest residual TSS. Though from the right of Figure 4-3, phosphorus removal showed no significant removal with varying doses of C-490, 0.5 mg C-490/L provided filtrate with the lowest residual TP. Based on the above reasons provided, 0.3 mg C-490/L and 0.5 mg C-490/L were selected for further studies based on the assumption that, error in the procedure and measurement was constant throughout the experiment and negligible.

4.1.4 PAX-18 and C-490 optimization

From Section 4.1.3 and Section 4.1.4 above, two (2) selected doses of PAX-18 were combined with two selected doses of C-490. This provided four sample combinations as shown in Table 4-2 below. Further bench scale SF screening tests were performed using PAX-18 and C-490 combinations according to Section 3.6. Sample 1 with 9.72 mg Al/L & 0.3 mg C-490/L was finally selected as a final optimum dose combination. This was because it was the only sample, which had a filtrate with above 90% removal for both SS and TP.

Though sample 3 had almost equal better results with respect to TSS removal, its TP removal was the worst among all samples.

Table 4-2: PAX-18 and C-490 combination to determine the final Optimum chemical/polymer dose

Sample	PAX-18 and C-490 combination Dose	Filtrate TSS (mg/L)	% SS Removal	Filtrate T-P (mg/L)	% TP Removal
1	9.72 mg Al/L & 0.3 mg C-490/L	16.12	92	0.31	93
2	9.72 mg Al/L & 0.5 mg C-490/L	34.38	82	0.36	92
3	17.0 mg Al/L & 0.3 mg C-490/L	13.33	93	0.56	87
4	17.0 mg Al/L & 0.5 mg C-490/L	35.29	82	0.33	93

4.1.5 G – Value optimization

Now using the above selected optimum dose combination, jar test experiments were performed before transferring to bench scale SF apparatus according to Section 3.6. This time, slow mixing speed of the jar test device was varied from 10 rpm to 50 rpm. Rapid mix speed was maintained at 400 rpm for 20 s. A slow mixing time of 10 min was used before transferring to bench scale SF apparatus for filtration. The sequence of coagulant (PAX-18) and polymer (C-490) was kept the same as outlined in Section 3.2. Only TP analysis was performed on the filtrate from this experiment using 33 µm mesh sieve, to determine the optimum G-value. Results obtained for this experiment are presented in Table 4-3.

Table 4-3: Determination of Optimum G-value

Speed (rpm)	**G-value (s^{-1})**	**% TP Removal**
Raw	Raw	0
50	74.52	70
40	53.32	68
30	34.63	67
20	18.85	68
10	6.67	66

From Table 4-3 above, TP removal efficiency did not show any significant difference, when the sample was filtered with the bench scale SF apparatus. However at 74.52 s^{-1} (50 rpm), maximum removal of 70% was achieved. Therefore the theoretical jar test device G-value of 74.52 s^{-1} was selected as the optimum G-value, on the assumption that mistakes or errors occurred during the experiment and in measurements were constant and negligible throughout.

4.1.6 Flocculation time optimization

Lower flocculation time was a critical parameter during the thesis period. It was a specific objective to use flocculation time not more than 10 min. Kemira Kemwater flocculator 90 had only two slow mixing times (10 min and 5 min), which were within the range of achieving this objective. Again using the above optimum parameters obtained (PAX-18 & C-490, optimum dosage, optimum G-value), screening test experiments were performed according to Section 3.2 and Section 3.6. 400 rpm rapid mix for 20 s and 50 rpm (74.52 s^{-1}) slow mixing speed were used. This time, only slow mixing time was varied (5 min and 10 min) before transferring to bench scale SF screening tests with 33 µm mesh sieve. Both TSS and TP analysis were performed on the filtrate and presented in Table 4-4.

Table 4-4: Optimum flocculation time using already determined optimum parameters

Flocculation time	% SS Removal	%TP Removal
5 min	59	40
10 min	82	80

From Table 4-4, it is obvious that flocculation time 10 min gave better result as compared to 5 min. Both SS and TP removal efficiencies were above 80% at 10 min flocculation time. Therefore flocculation time of 10 min was selected as the optimum slow mixing time to be used on the pilot scale coagulation/flocculation studies.

4.1.7 Mesh sieves predictions using optimum flocculation parameters

The above obtained optimum coagulation/flocculation parameters (9.72 mg Al/L, 0.5 mg C-490/L, 74.52 s^{-1} and 10 min flocculation time) were used on 1 L jar test experiment before transferring to bench scale SF apparatus with a particular selected mesh sieve, as described in Section 3.2 and 3.6 and Figure 3-11.. From 158 to 33 micron mesh openings were used to predict their removal efficiency with regards to the optimum parameters obtained. Figure 4-4 describes the results obtained.

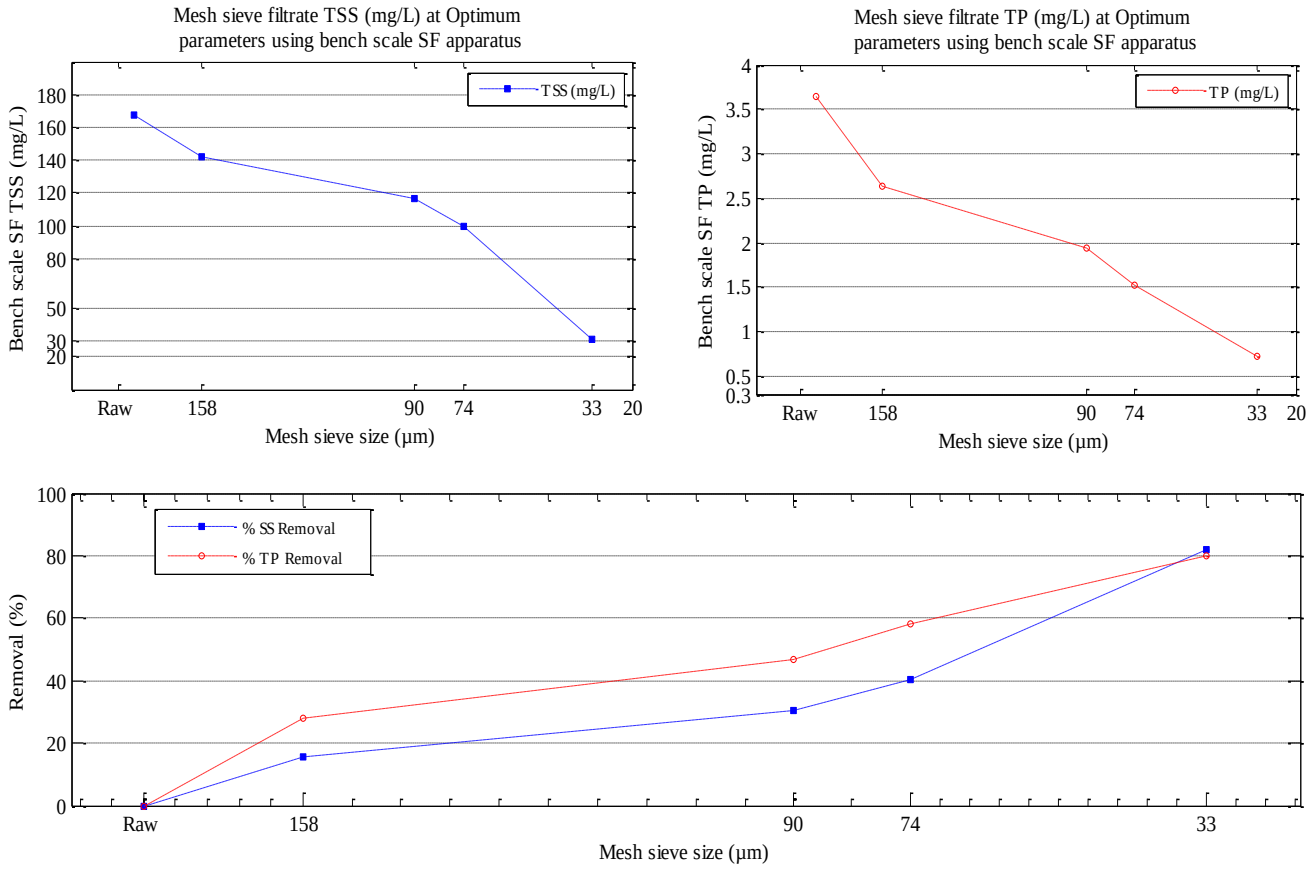

Figure 4-4: Mesh sieves TSS and TP removal efficiencies with respect to optimum parameters obtained.

From Figure 4-4, both filtrated TSS and TP had similar looking curves and therefore a similar relationship. Filtrate TSS and TP had a direct relationship with mesh sieve size. As the mesh sieve size decreases, the filtrate TSS and TP also decreased. From Figure 4-4, target TSS (below 30 mg TSS/L) was only achieved on the 33 µm mesh sieve. Though 0.3 mg TP/L (target) was not achieved on the mesh 33 µm, it was still below 1mg TP/L which was possible to meet the EU discharge permit (BlöcH, 2005) and Norwegian discharge permit (Al Nabelsi and Ganesh, 2013). Considering the remaining mesh sieves, both TSS and TP removal were below 60%, but mesh sieve 33 µm had both results above 80%. Figure 4-4 also shows the effect one should expect as one moves from a mesh sieve size far less than the previous mesh sieve. From Figure 4-1 and Figure 4-4, an indication that, about 50% of the particle sizes in the MBBR biofilm water are below 74 µm can be derived or estimated.

4.2 Pilot Scale Coagulation/Flocculation

The above optimum parameters ((9.72 mg Al/L, 0.5 mg C-490/L, and 10 min flocculation time) were used on the pilot scale coagulation/flocculation tanks as described in Section 3.7 and Figure 3-14. However the exact optimum G-valve obtained with bench scale apparatus could not be used, due to the inability of the pilot scale flocculation set-up speed regulator to provide that same G-value. Therefore the closest G-value possible of 65.84s-1 was used on pilot scale. It was observed that floc sizes obtained were not good enough to meet the expected targets, based on the indications of the expected particle size of MBBR wastewater obtained from Section 4.1.1 and 4.1.7. Forming a good, strong, and big floc was critical for the study. Upon further reference from Ng (2012), visual observations and second look at Figure 4-1 above, Superfloc C-496 was selected to be tried. A second reference of Figure 4-1 showed that Superfloc C-496 was able to form bigger floc sizes which were capable of removing above 50% and 60% SS with 158 µm and 90 µm mesh sieves respectively. Superfloc C-496 was then tried on the pilot scale. Figure 4-5 shows a visual comparison of floc size, using C-490 and C-496 with PAX-18 at jar-test optimum parameters. It also formed bigger floc sizes on the pilot scale flocculation tanks upon the first trial, using the above optimum parameters (except C-490). Figure 4-6 shows a first trial of C-496 with PAX-18 at jar test optimum parameters on pilot scale coagulation/flocculation tanks.

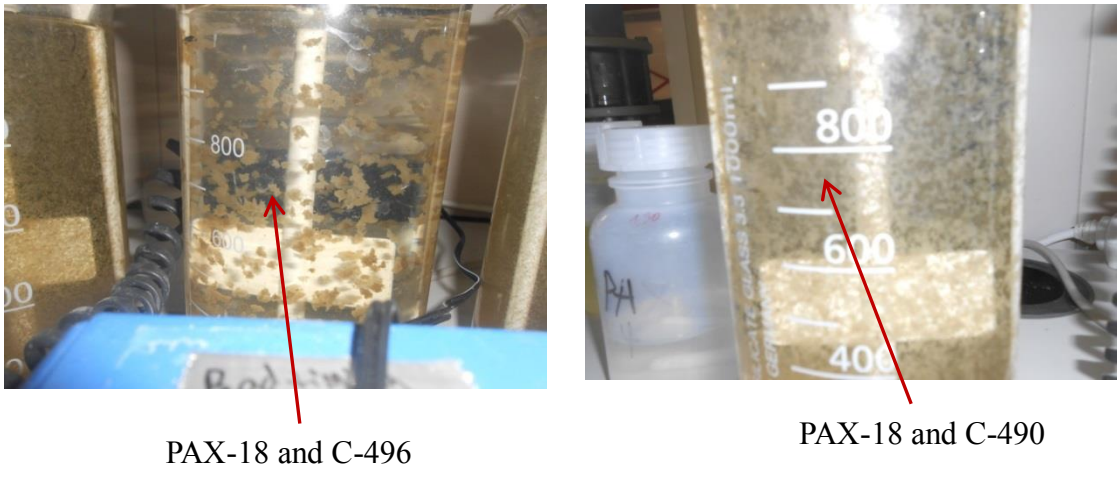

Figure 4-5: Visual comparison of C-496 and C-490 with PAX-18, using jar-test optimum parameters

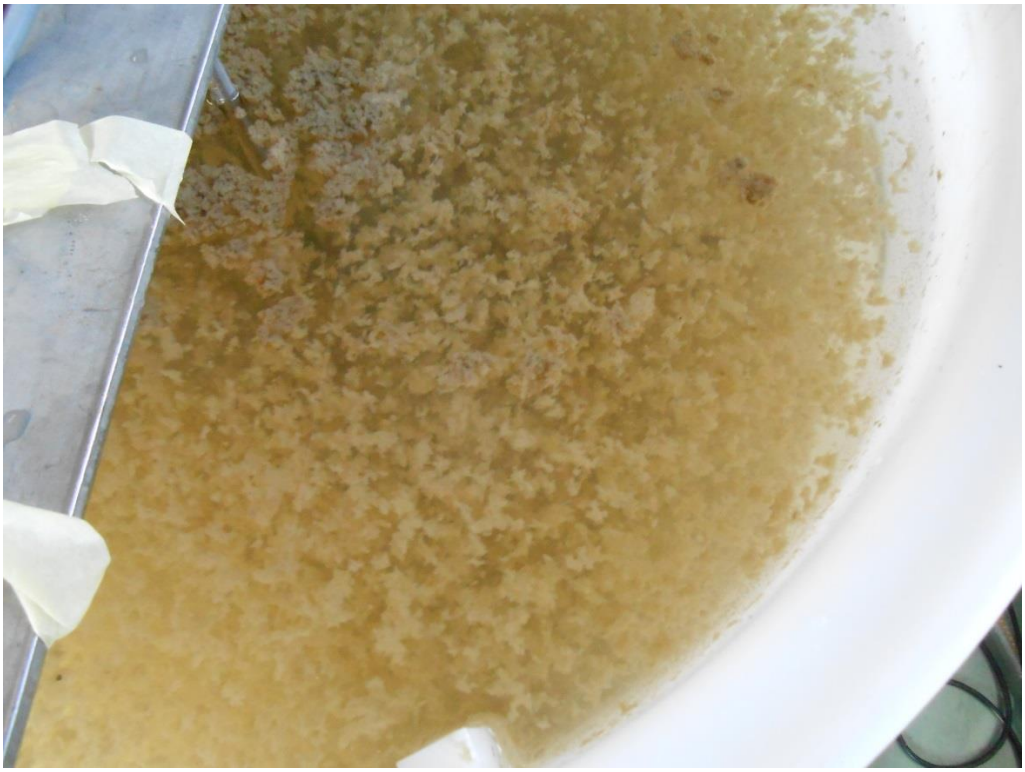

Figure 4-6: First trial of C-496 with PAX-18 doses at jar-test optimum parameters on pilot scale coagulation/flocculation tank.

A decision was further made to determine the critical coagulation concentration of PAX-18 and to know how negative the MBBR water surface charge was. This decision was made based on, how unreliable the bench scale SF apparatus was with respect to this study, though it works best for ordinary municipal primary (degritted) wastewater.

This section presents results on determining the CCC and the MBBR biofilm solid surface charge using zeta potential analysis. This section also presents results obtained during the pilot scale coagulation/flocculation and SF500 filtration study. It includes the chemical dose and polymer dose combination used on the pilot scale coagulation/flocculation process before SF500 filtration. However during these experiments there was a problem with the flow meter, which logs data to the PLC device. Therefore flow rate to the SF500 was estimated using Equation 4-1.

Equation 4-1: Influent SF500 flow rate

$$\text{SF500 influent flow rate} = (\text{Tanks influent flow rate}) - (\text{By-pass flow rate})$$

The above equation however was expected to contain some errors that could not be accounted for during the thesis period. This is because, based on the level at the point of by-pass, the by-pass hose had to be lifted a little above its normal discharge position, before by-passed water measurements could be taken. This estimated SF500 flow rates were made for experiments presented in Section 4.2.2 to Section 4.2.8.

However, this problem with the SF500 flow meter was later rectified. Therefore experiments performed later and presented in Section 4.2.9 presents the actual flow rate to the SF500 machine recorded using the electromagnetic flow meter shown in Figure 3-19.

4.2.1 Zeta potential analysis

Zeta potential analysis on MBBR reactor 5 effluent wastewater was performed to determine the range of critical coagulation concentration (CCC) according to procedure outlined in Section 3.12. Figure 4-7 presents the results obtained. The zeta potential of the MBBR Reactor 5 effluent wastewater was -14.8±3.83 mV. The initial recorded pH was 5.95 at 15.9°C. PAX-18 concentration dosing range of 4.86 – 19.44 mgAl/L was studied on the MBBR wastewater. Results obtained are presented in Figure 4-5 below.

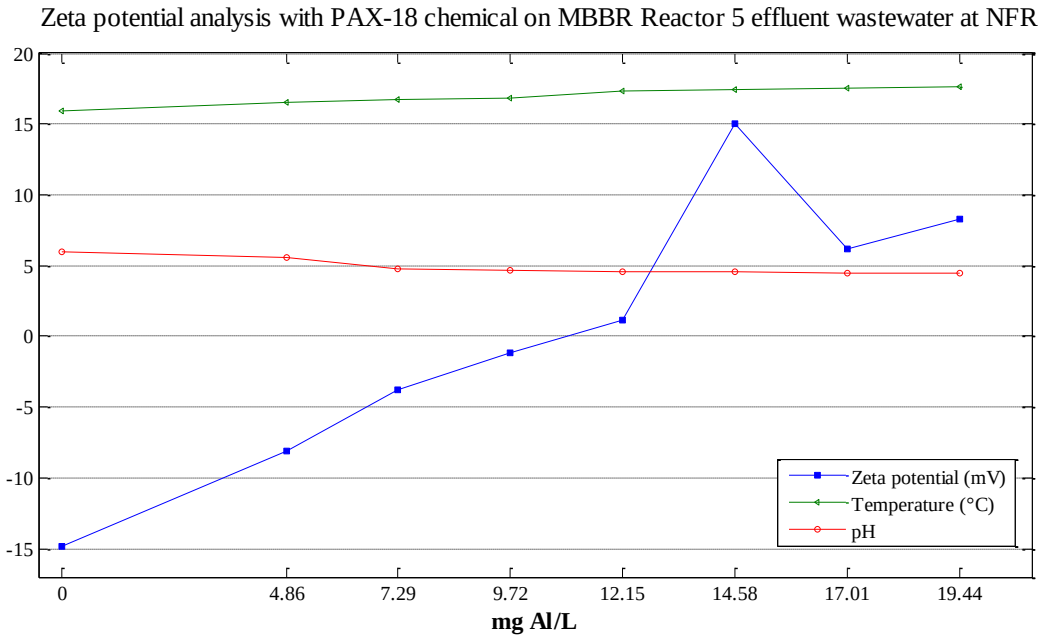

Figure 4-7: Zeta potential analysis on MBBR wastewater using PAX-18

From Figure 4-7, temperature remained almost constant during the study. The pH changed from 5.95 to 4.46 at 19.44 mg Al/L, representing 1.49 pH decreases from initial. The initial zeta potential showed that MBBR wastewater was outside the critical range (±10 mV) (Fairhurst, 2014). From Figure 4-7 a range of 9.72 – 12.15 mg Al/L brought MBBR wastewater zeta potential close to zero (0 mV).

A decision was therefore made to use a range of 9.7 ± 2.0 mg Al/L to 12.1±2.0 mg Al/L for usual daily jar-test experiments to determine optimum dose, before pilot scale coagulation experiments, in order to minimize the errors with the varying wastewater composition.

4.2.2 C-496 optimization using PAX-18 on bench scale SF apparatus with 33 µm

Superfloc C-496 and chemical PAX-18 were used to perform bench scale screening test according to the procedure outlined in Section 3.6, in order to verify and confirm the chemical and polymer selections. PAX-18 dose was kept at 12.34 mg Al/L and C-496 dose varied from 0.3 to 1.5 mg/L. Mesh sieve 33 µm was used on the bench scale SF apparatus. The results obtained are presented in Figure 4-8;

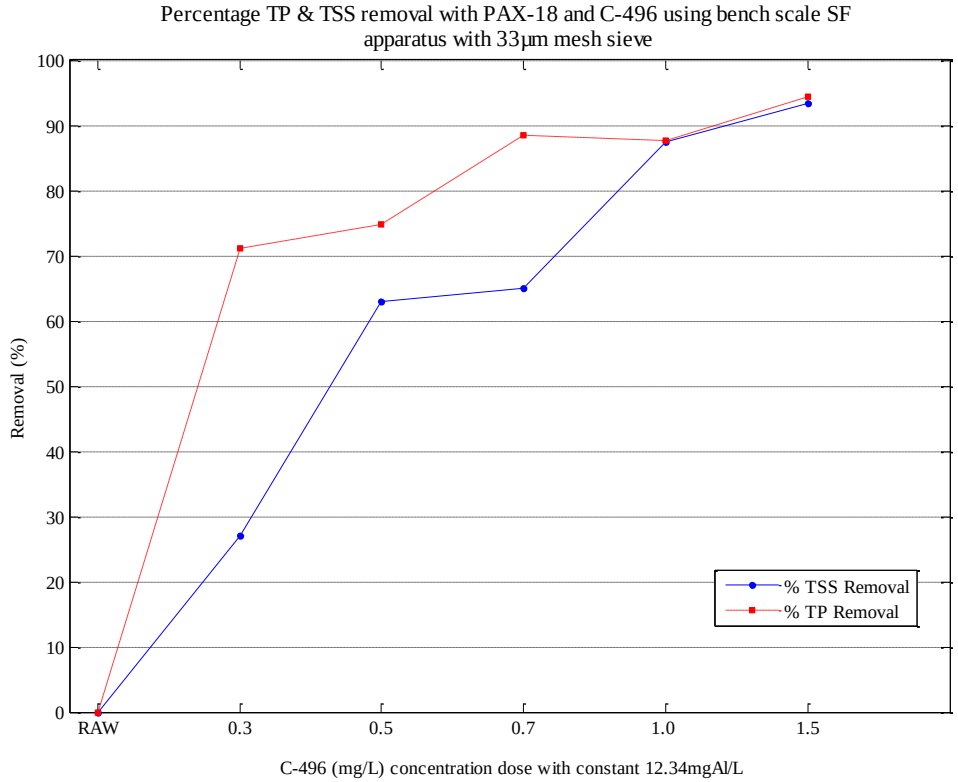

Figure 4-8: Polymer C-496 optimization with PAX-18 for MBBR Reactor 5 effluent wastewater at NFR

From Figure 4-8**,** it is observed that both SS and TP percentage removal looked alike and increased as C-496 concentration was increased. Both curves began to converge at 1.0 mg C-496/L with a percentage removal above 85% for both TSS and TP. 1.5 mg C-496/L concentration dose gave a better result. It also shows an increase in floc size as more polymer dose (C-496) was added. From the results obtained, 0.5 mg C-496/L to 1.5 mg C-496/L provided filtrates with TP from 1mg/L to 0.23 mg/L which again meets the EU discharge permit (BlöcH, 2005). Therefore a range of 0.5 to 1.5 mg C-496/L was selected for pilot study with any critical PAX-18 concentration selected.

4.2.3 Pilot scale SF500 filtration with 33µm mesh sieve

Optimum parameters obtained and selected above were used on the pilot scale coagulation/flocculation tanks and filtered using SF500 with 33 µm mesh sieve according to procedure described in Section 3.7 and Section 3.8.1 above. 0.5 mg/l, 0.7 mg/L and 1 mg/L C-496 were used as polymer doses with constant PAX-18 dose of 13.24 mg Al/L. 1380 rpm speed was used on the rapid mix tank for 20 s retention time and a constant G-value of 64.84 s^{-1} used on the two flocculation tanks. An estimated SF500 influent flow rate of 0.3 L/s was used. SF500 was operated in automatic mode with filter level set-point, stop filter level, belt cleaning speed and filter speed set on the PLC to 45 mm, 45 mm, 20% and 4% respectively. SF500 with 33 µm mesh sieve size was used and the filtrate samples were collected right from the SF500 cartridge at 30 mins interval. Filtered samples were evaluated for TSS, TP, COD, and turbidity. Results obtained are presented in Figure 4-9 and Table 4-5 below.

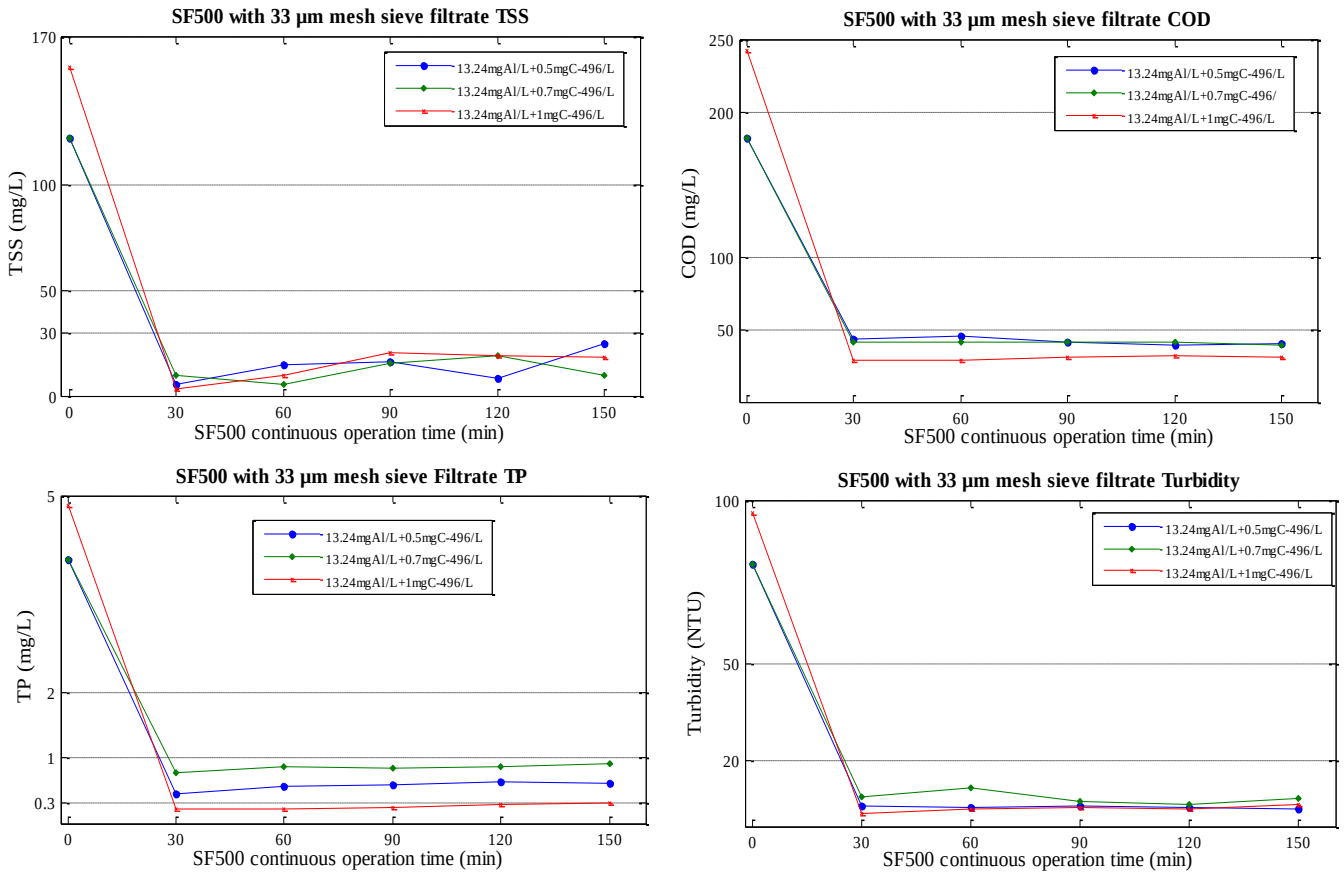

Figure 4-9: SF500 with 33 µm mesh sieve effluent parameters at 30 min sampling interval with influent parameters of 132.8±19.4 mg TSS/L and 4.3±0.5 mg TP/L

An assumption that each dosing pair was the optimum dose for each day was made. SF500 was operated continuously for 2.5 hours on scraper and water wash cleaning for 4 times. Its flow rate of 0.3 L/s (24.63 m^3/m^2-h) was used. From Figure 4-9 filtrate TSS for all cases was below the target 30mg/L. The target TP (< 0.3 mg/L) was achieved with dosing combination of 13.24 mg Al/L and 1 mg C-496/L. Though the remaining dosing combinations could not attain the target TP, their filtrates TP were below EU discharge permit (1 mg TP/L). COD at all instances was below target 50 mg/L. Filtrate turbidity was always below 20 NTU. From Table 4-5 a maximum of 98% SS removal and above 93% TP removal was achieve with 13.24 mg Al/L and 1 mg C-496/L combination dose. Looking at Table 4-5, a constant percentage removal above 75% was achieved, for all cases with respect to TSS, TP, COD, and Turbidity.

Table 4-5: SF500 with 33 µm mesh sieve percentage removal efficiencies

SF500 Time (min)	13.24 mg Al/L + 0.5 mg C-496/L				13.24 mg Al/L + 0.7 mg C-496/L				13.24 mg Al/L + 1 mg C-496/L			
	%SS	%TP	%COD	%NTU	%SS	%TP	%COD	%NTU	%SS	%TP	%COD	%NTU
30	95	89	76	93	92	81	77	89	98	96	88	96
60	88	86	75	93	96	78	77	86	94	96	88	95
90	87	85	78	92	88	79	78	90	87	95	87	94
120	93	84	78	93	85	79	77	92	88	94	87.	94
150	80	85	78.	93	92	78	79	89	88	93	87	93

4.2.4 Pilot scale SF500 filtration with 54 µm mesh sieve

This experiment was performed same as the procedure described in Section 4.2.3 with the same SF500 operation set points and PLC settings. Flow rate was 0.35 L/s (28.74 m^3/m^2-h) was used. Mesh sieve 54 µm was however used. A constant PAX-18 dose of 13.24 mg Al/L was used to pair various C-496 doses. These experiments were conducted on four (4) different days, with different MBBR Reactor 5 effluent parameters at each day as shown in Figure 4-10 below. These changes in MBBR wastewater composition affected the results for same polymer dose of 0.8 mg C-496/L. None of the C-496 concentration dose was able to achieve the target 0.3 mg TP/L. However all SF500 filtrate were below 1.0 mg TP/L and met the EU discharge permit. 0.5 mg C-496/L could not achieve the target TSS of 30 mg/L on average over 2.5 hours study. All experiments performed had filtrate COD and turbidity below 50 mg/L and 20 NTU respectively.

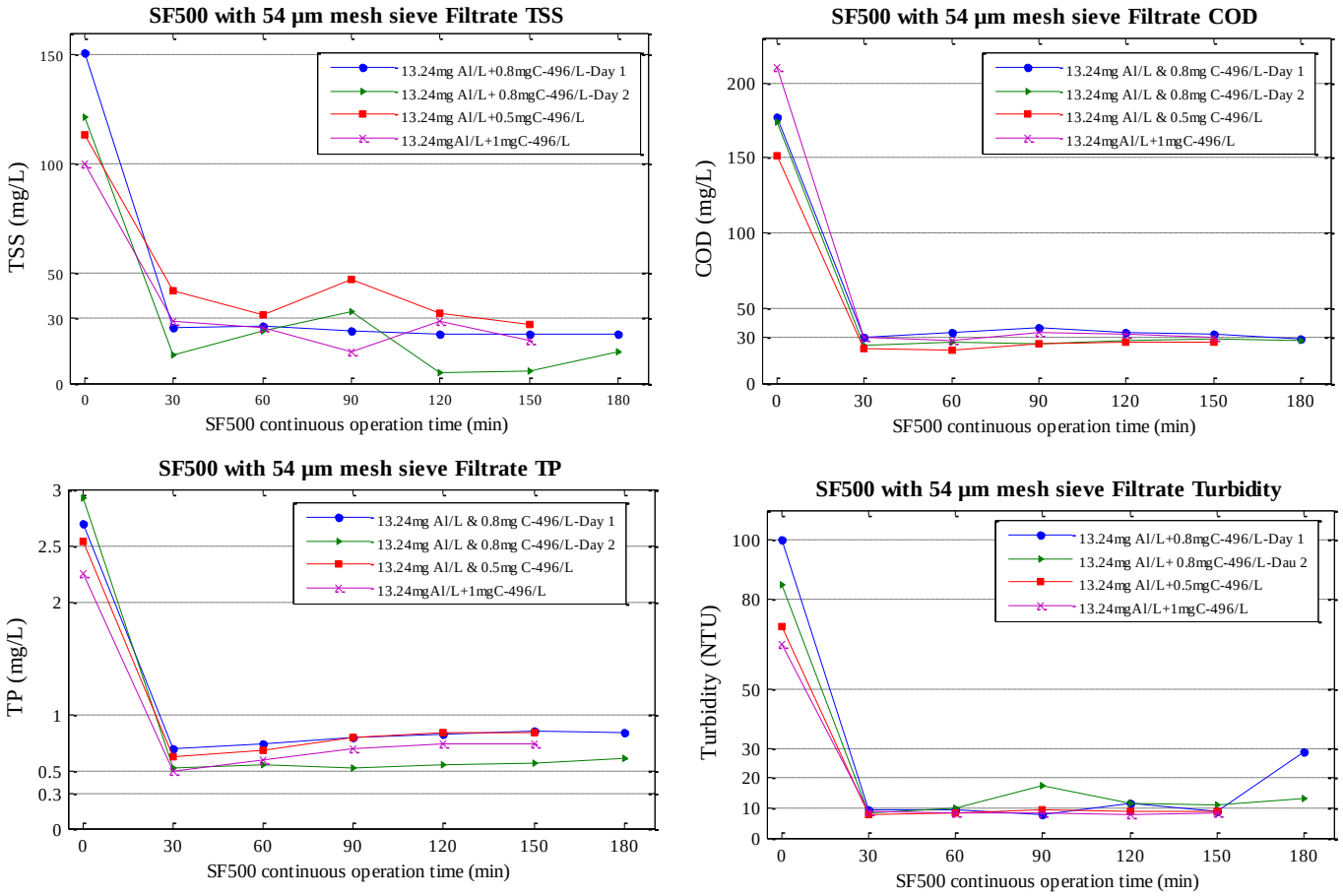

Figure 4-10: SF500 with 54 µm mesh sieve filtrate parameters at 30 min sampling interval with influent parameters of 121.3 ± 21.6 mg TSS/L , 2.6 ± 0.3 mg TP/L, 178±24 mg COD/L and 80±63 NTU

Though 1 mg C-496/L was expected to perform better, its influent parameters were the lowest among the four measurements studied with respect to TSS, TP, and Turbidity from Figure 4-10. This might be the reason. It also gives an indication that, when the initial TSS is low, one should avoid using more polymer dose. Another reason could be that higher polymer dose already indicated in Section 4.2.2, forms bigger floc sizes, and due to the by-pass junction, bigger and weak floc breaks forming tiny particles less than 54 µm and therefore making their way through the mesh sieve. The highest SS and TP removal of 87±9% and 81±1% respectively were achieved using 13.24 mg Al/L and 0.8 mg C-496/L combination.

4.2.5 Pilot scale SF500 filtration with 90 µm mesh sieve

This experiment was performed the same way, as previously described in Section 4.2.3 however the SF500 filtration was performed by using 90 µm mesh sieve. Flow rate of 0.4 L/s

(32.84 m^3/m^2-h) was used. Dosing was performed according to daily optimum chemical and polymer doses. The results obtained are presented in Figure 4-11 and 4-12.

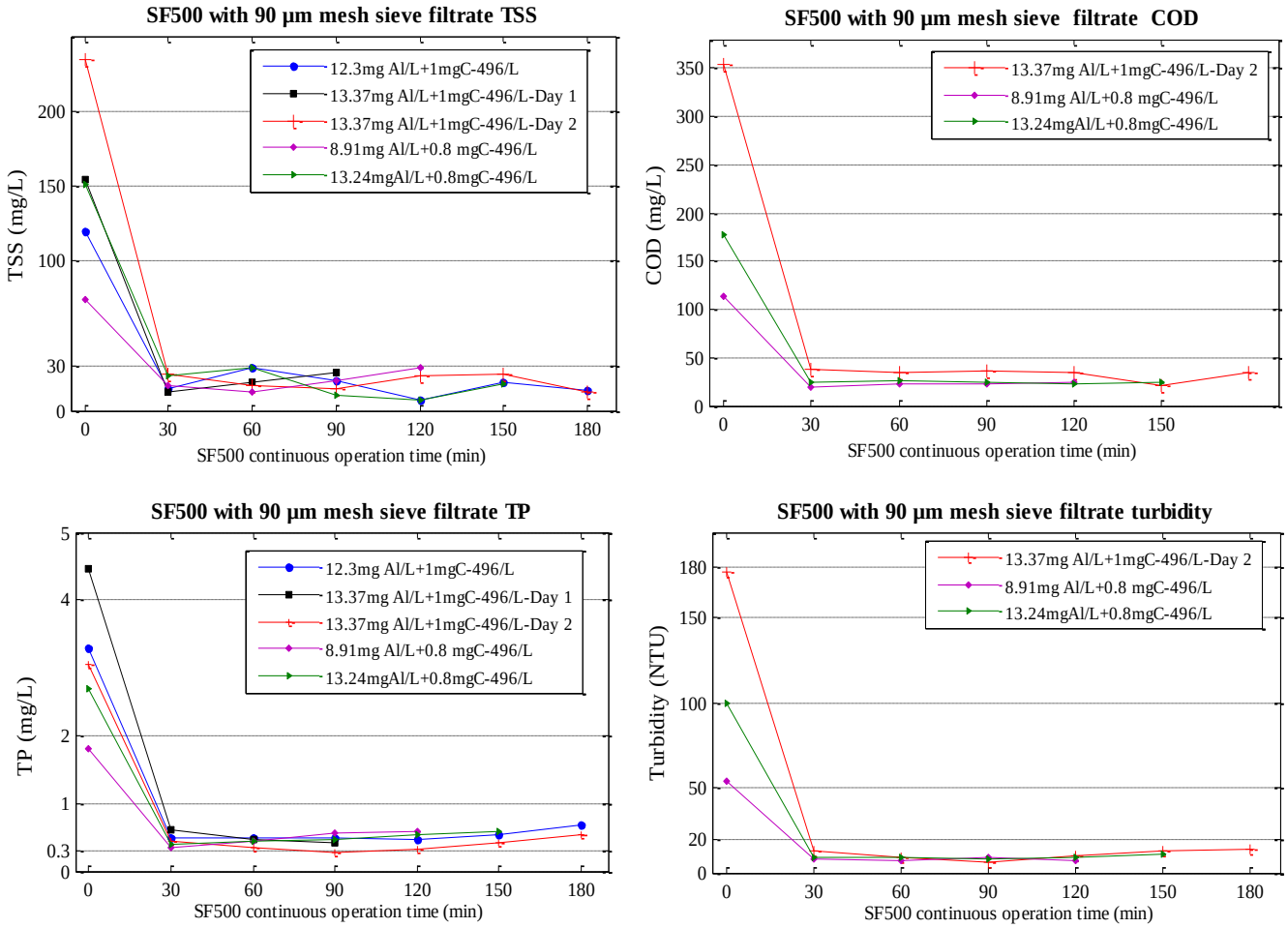

Figure 4-11: SF500 with 90 µm mesh sieve effluent parameters at 30 min sampling interval with influent parameters of 146.7± 58.67 mg TSS/L and 3±1 mg TP/L

It can be observed that all target parameters were achieved with regards to TSS, COD, and Turbidity. Though the target of 0.3 mg TP/L was not achieved, all filtrate TP were far less than 1 mg TP/L and therefore met the EU discharge permit. All filtrates TSS and COD for various optimum doses were below 30 mg/L and 50 mg/L respectively. Also its can be seen that, due to the minimum TSS and turbidity of MBBR biofilm wastewater, minimum PAX-18 (8.91 mg Al/L) and C-496 (0.8 mg/L) dose combination was required to ensure a better coagulation/flocculation processes therefore obtaining the expected filtrate parameters. On Day 2 from Figure 4-11, initial TSS and turbidity were very high, therefore 13.37 mg Al/L+1

mg C-496/L combination performed very well and gave effluent water with the minimum residual TP.

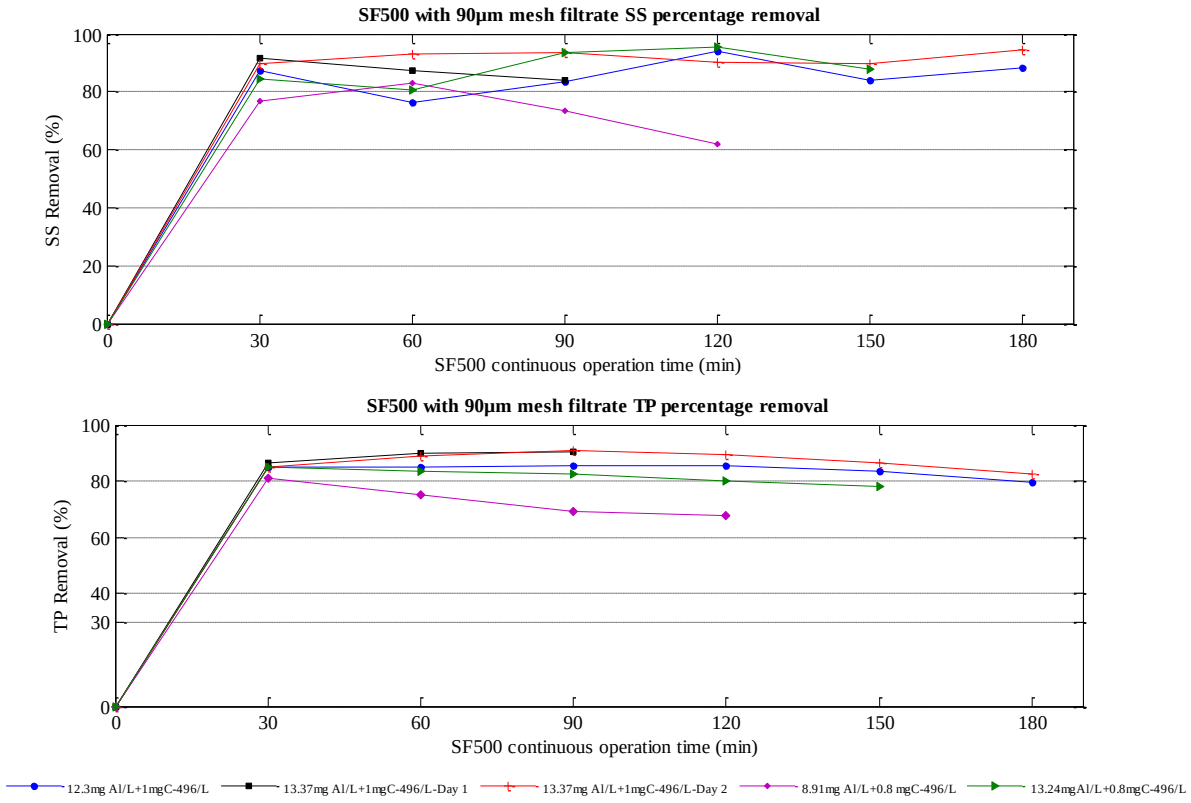

Figure 4-12: SF500 with 90 µm mesh sieve removal efficiency at 30 min sampling interval with influent parameters of 146.7± 58.67 mg TSS/L and 3±1 mg TP/L

From Figure 4-12, it is observed that, on average all dosing combinations provided an effluent with more than 80% removal for SS and TP except for 8.91 mg Al/L + 0.8 mgC-496/L. This is because, as already pointed out its initial or influent parameters were too low. Though it performed very well almost throughout, the percentage removal provided a different indication. This also indicates that at times, percentage removal alone do not always provide the true performance of a wastewater treatment. However considering both effluent and percentage removal gives more reliable information on the performance of a treatment technology.

4.2.6 Pilot Scale SF500 filtration with 158 µm mesh sieve

This experiment was performed for two days with the longest SF500 operation time of 2 hours. However some of the filtration processes lasted for an hour. The experiment was performed according to Section 3.7 and 4.2.3 by using 158 µm sieves. Flow rate of 0.5 L/s (41.05 m^3/m^2-h) was used. Filter level set-point and stop filter level were increased to 65 mm and 60 mm respectively. Results obtained are presented in Figure 4-13 below. Only TSS and TP analysis were performed during the process. An assumption that the influent parameters remained constant for entire day was made. Due to the pore size of the 158 µm mesh sieve, bigger floc size was required. Therefore higher polymer dose of 1 mg C-496/L and 1.5 mg/L were used with constant PAX-18 dose of 12.34 mg Al/L. SF500 cleaning with the scraper was not good enough to clean all captured solids from the mesh. Therefore more water wash cleaning was used in the process. Again an assumption was made that, SF500 was operated under the best operating condition and the dilution factor throughout measurement was constant and negligible.

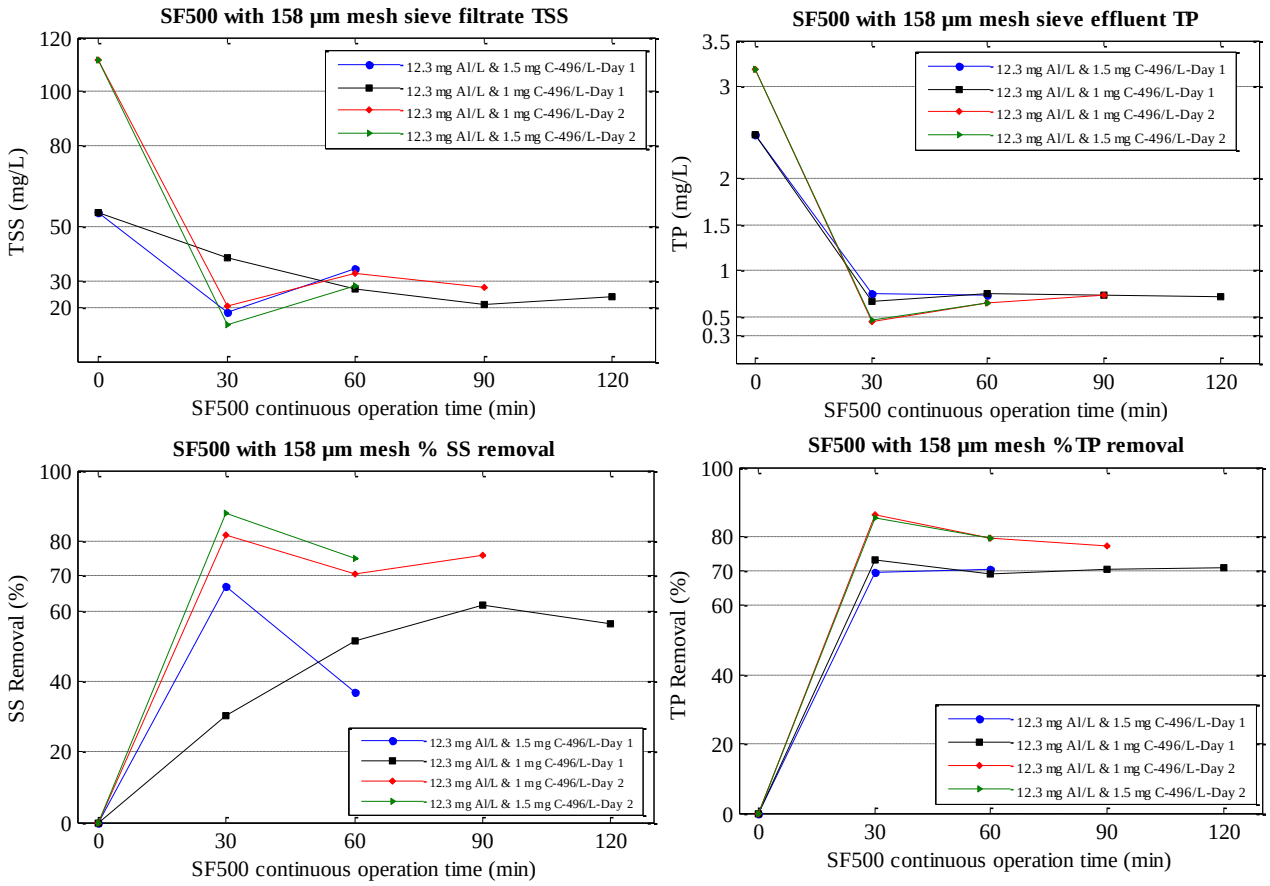

Figure 4-13: SF500 with 158 µm mesh sieve effluent parameters at 30 min sampling interval with influent parameters of 83.4±32.9 mg TSS/L and 2.8±0.4 mg TP/L

From Figure 4-13 it is observed that, the target TP was not achieved, though all effluent TP were below 1mgTP/L. Again eight (8) out of eleven (11) data points had TSS below the target TSS (30 mg/L) representing about 72%. From Day 1, initial TSS was very low and therefore resulted in poor removal efficiency for that particular day. As already pointed out, when the influent parameters are low, it requires one to use less chemical and polymer dose for a better performance. However, TP removal remained almost constant for each day, though the polymer concentration dose was not the same. TP removal for all cases was above 70%. The best TSS result was achieved with 1.5 mg C-496/L only in the first 30 min but increased with time. This might be that, as the polymer concentration addition increased, floc sizes increased and became too big and weak with time. These weak flocs then break-off when subjected to shear forces usually at the point of by-pass and forms tiny floc sizes which are capable to move through the mesh sieve.

4.2.7 Pilot scale SF500 filtration with 210 µm mesh sieve

This experiment was performed according to procedure described in Section 3.7, and 4.2.6 above. SF500 was however used with 210µm mesh sieve for filtration. Flow rate of 0.5 L/s (41.1 m^3/m^2-h) was used. Results obtained are presented in Figure 4-12 below. The optimum dose for that day was used. The cleaning of the 210 µm mesh sieve was not enough with only the scraper and therefore multiple water wash cleaning was used in the process. The samples taken were expected to be diluted. An assumption was made that, SF500 with 210 µm mesh over 2.5 hours was operated under the best operating condition for that particular day and dilution factor was constant and negligible.

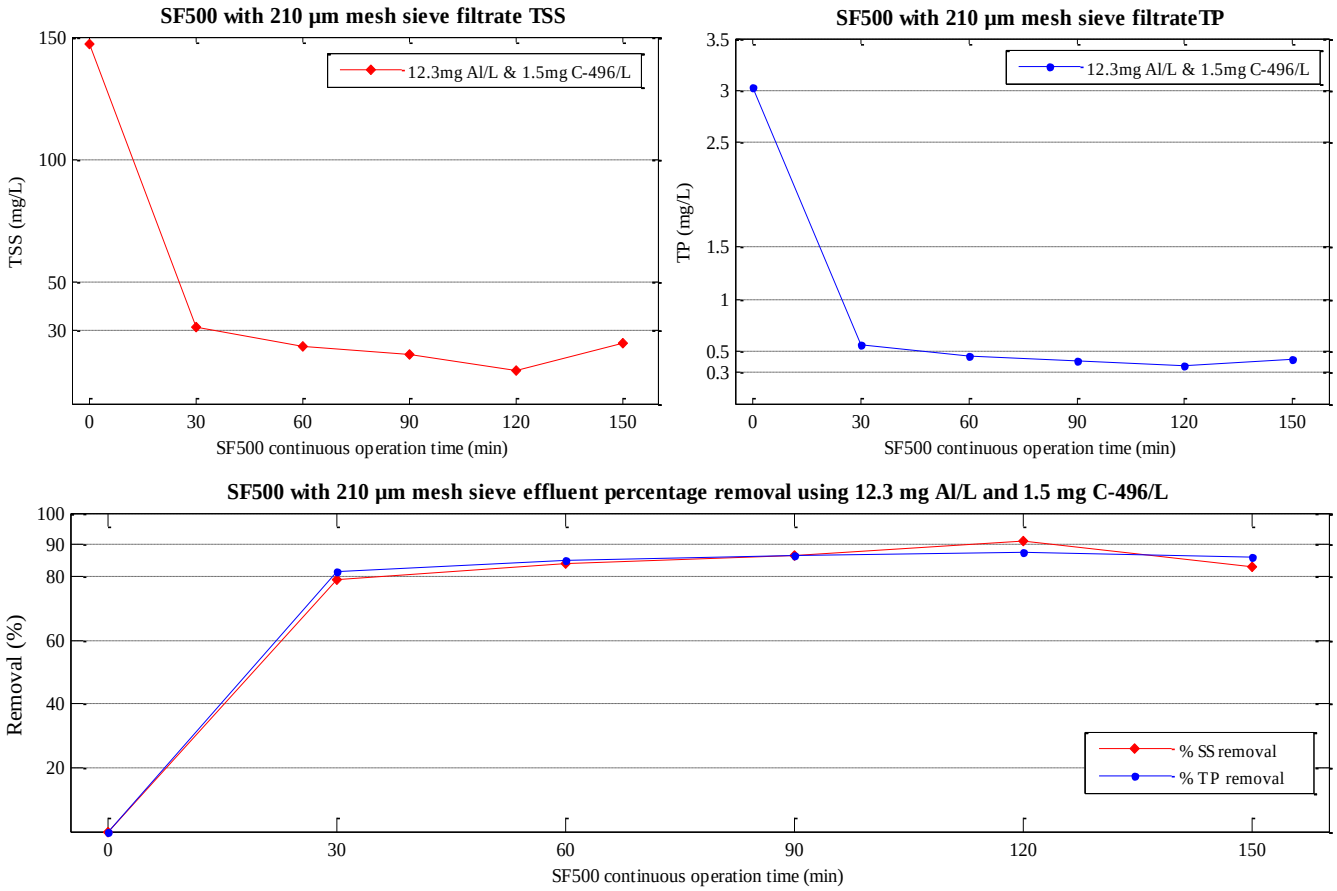

Figure 4-14: SF500 with 210 µm mesh sieve effluent parameters at 30 min sampling interval with influent parameters of 147 mg TSS/L and 3 mg TP/L

From the top right of Figure 4-14, effluent TSS decreased consistently below 30 mg/L from the first 30 min. Target TP of 0.3 mg/L was not achieved over the 2.5 hour study. However all effluent TP were below 1mg/L which makes 250 µm mesh sieve capable of meeting the EU permit only if the assumption made above holds. From the percentage removal graph, it can be observed that above 80% was achieved with respect to both SS and TP for the last 2 hours.

4.2.8 Pilot scale SF500 filtration with 250 µm mesh sieve

This experiment was performed with the same procedure as described in Section 3.7, and 4.2.6. SF500 was operated with 250 µm mesh sieve. Flow rate of 0.52L/s (42.69 m^3/m^2-h) was used. Two polymer doses of 1 mg C-496/L and 1.5 mg C-496/L were used with a constant PAX-18 dose of 12.34 mg Al/L. In order to reduce captured solids finding their way to the effluent, more water wash cleaning was used. This was used because, the air blower

was not working at that time. It is however expected that test samples taken for analysis were diluted. On the assumption that, this was the best way to operate the machine, results obtained are presented in Figure 4-15. From the top left, the combination with 1.5 mg C-496 showed a consistent decrease of TSS over an hour and began to increases above 30 mg/L. This is however attributed to the fact that, floc became too big and weak, which broke up at the point of maximum shear, especially at by-pass and higher flow rate. The combination with 1 mg C-496/L though showed a consistent decrease of filtrate TSS with time, the target of 30 mg/L was not achieved over 90 min of SF500 operation time.

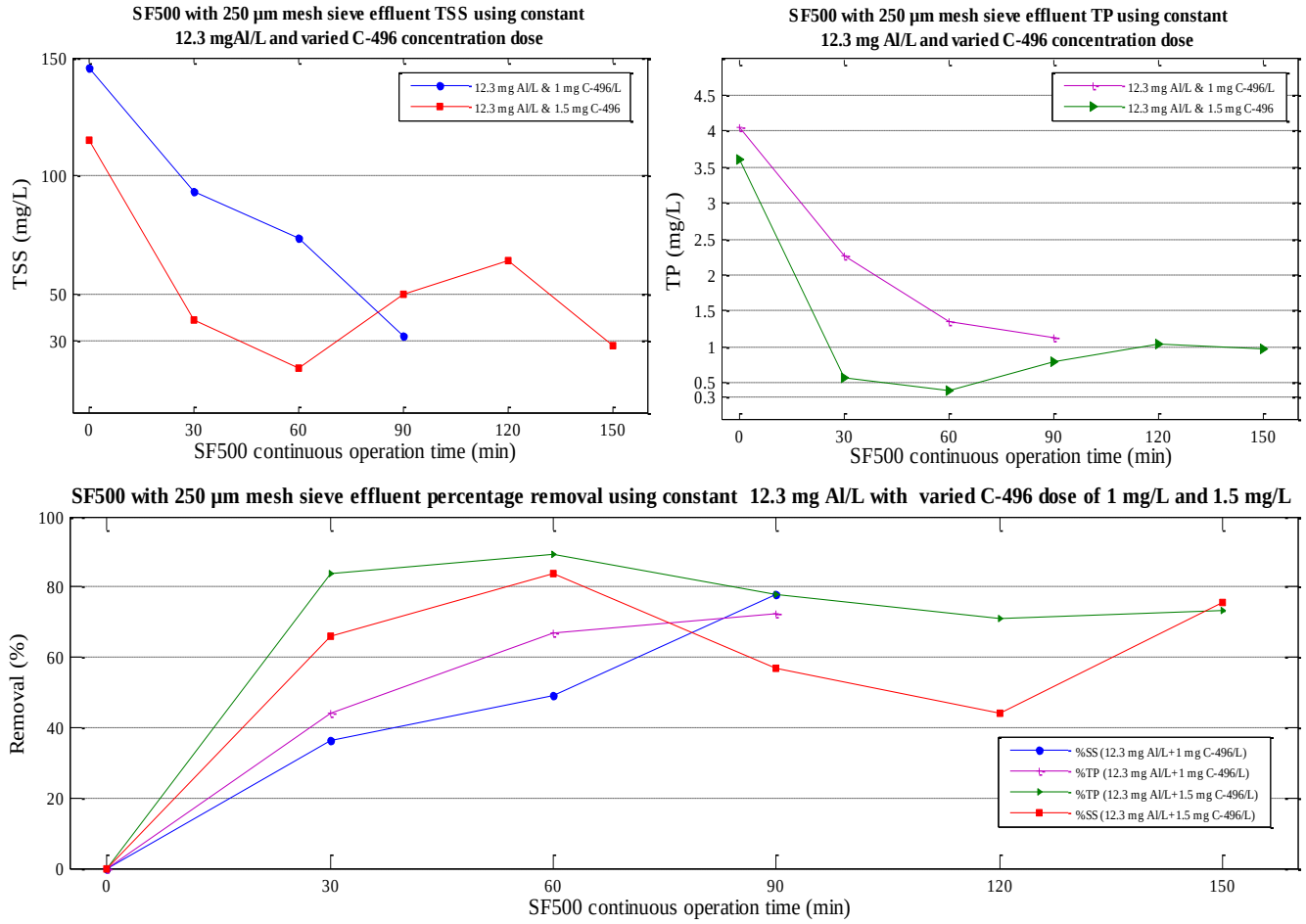

Figure 4-15: SF500 with 250 µm mesh sieve effluent parameters at 30 min sampling interval

From the top right, the combination with 1.5 mg C-496/L could not achieve the target of 0.3 mg TP/L. Again it could not maintain a consistent filtered TP below 1 mg TP/L over 2hours. Same observation is made for the combination with 1 mg C-496/L, though there was a consistent decrease of filtrate TP, all filtrate measurements were above 1 mg/L. On the bases

of this, 250 µm operations could not provide filtrate capable of meeting the EU discharge permit. From the removal efficiency graph of Figure 4-15, though at some point TP removal was above 80% was achieved with 1.5 mg C-496/L this was not consistent over a long period. 1 mg C-496/L on the other hand, could not achieve 80% removal for both TSS and TP on all cases.

4.2.9 SF500 filtration with constant coagulation/flocculation condition, constant SF500 operation for all mesh sieves

This experiment was performed as already described in Section 3.7, and 4.2.3. Same coagulant dose of 13.24 mg Al/L, flocculant dose of 1 mg C-496/L, 10 min flocculation and 65.84 s^{-1} G-value was used throughout with each mesh sieve size for a particular day. A total of 5 days were used for the entire experiment. SF mesh sieve openings 210, 158, 90, 54, and 33 µm were used. SF500 was operated on the flocculated biofilm solids for an hour, for each mesh sieve. Samples were taken at 15 min interval. Two sample points were studied, thus sample directly from mesh sieve (filtrate sample) and that from the actual design SF500 effluent (actual effluent sample). SF500 PLC settings were made to run on wash water at every 15 min, if the set-point was not reached before the 15mins cleaning time. Settings on the PLC were made according to Table 4-6. SF500 PLC mesh belt speed was converted from percentages (%) to belt rotation per min and attached in Appendix E.

Table 4-6: SF500 PLC settings for automatic operation for 1hour flocculated biofilm solids filtration

Level set point in filter (mm)	53	Maximum standby time cleaning (min)	15
Start level filter cloth (mm)	55	Rotation of cloth to be cleaned (belt rotation)	1
Stop level filter cloth (mm)	52	Cloth travel time per revolution at 50% (s)	34
Start delay filter cloth when cleaning (s)	1	Belt speed during cleaning (belt rotation/min)	1.72
Belt speed threshold to begin cleaning (belt rotation/min)	4.81	Manual speed filter cloth (belt rotation/min)	2.07
Cleaning delay when above speed threshold (s)	15	Minimum speed filter cloth (belt rotation/min)	0.59

This experiment lasted for five (5) days, and distribution of the influent MBBR biofilm wastewater parameters to coagulation/flocculation tanks are presented in Table 4-7 below.

Table 4-7: Raw MBBR Reactor 5 effluent parameters over 5 days

TSS(mg/L)	TP (mg/L)	COD (mg/L)	Turbidity (NTU)	PH
140±21	4.34±0.72	212.84±28.72	93.26±8.48	6.40±0.17

Both filtrate sample and actual design effluent were taken at the same time with about 20 s time lag. TSS and turbidity analysis were performed on all samples collected. However, only the last sample (60 min) was taken from the five (5) filtrate samples for TP and COD analysis. All samples from actual design effluent were analysed for TP, COD and pH. Results obtained during these five days experimental study are presented in Table 4-8.

Table 4-8: SF500 filtrate and actual design effluent parameters

Mesh sieve size (um)	TSS (mg/L)		TP (mg/L)		COD (mg/L)		Turbidity (NTU)		
	Filtrate sample	Actual design effluent	Filtrate sample	Actual design effluent	Filtrate sample	Actual design effluent	Filtrate sample	Actual design effluent	Effluent pH
33	14.17±1.05	24.24±4.35	0.45	0.66±0.04	26.3	38.23±3.07	9.60±3.20	18.10±1.69	4.65±0.13
54	10.28±1.25	31.03±2.77	0.63	0.86±0.05	26.3	46.85±4.26	7.74±0.34	24.30±3.54	4.49±0.15
90	15.73±5.32	22.96±3.57	0.84	0.90±0.10	38.8	45.90±1.90	9.50±2.05	18.93±3.88	4.61±0.10
158	36.85±3.22	59.01±2.84	1.28	1.57±0.10	57	79.85±6.83	23.00±2.94	31.75±4.43	4.47±0.22
210	51.35±6.39	67.46±11.09	1.31	1.26	58.3	65.3	22.25±1.26	25.75±3.30	4.59±0.14

The actual design effluent removal efficiencies of SF500 were evaluated. The wash water during the hour operation time was collected in a tank, and a sample taken after 60 min SF500 operation time for TSS analysis. A sample of the sludge after the 60 min operation time was also taken for TSS analysis. Flow rate (m^3/m^2-h), power consumption (kWh/m^3) and number of water wash per hour, were calculated based on the data logged on the PLC device during the entire hour study. Power consumed by both coagulation stirrer and flocculation stirrers were included in the power calculations. A mesh sieve area of approximately 0.043 m^2 was used in the SF500 filtration process for each mesh sieve. The distribution of data obtained for the 5 days is presented in Table 4-9.

Table 4-9: Actual design SF500 efficiencies

Mesh sieve (µm)	**Actual design SF500 efficiencies**			**Filtration rate** (m^3/m^2-h)	**Power consumed** (kWh/m^3)	**No of water wash per hour**	**Wash water TSS** (mg/L)	**Sludge** TS (g/L)
	% SS removal	%TP removal	%COD removal					
33	80±4	80±1	79±2	24.62	0.19	4	40	16
54	73±2	77±1	75±2	21.01	0.21	4	66	17
90	86±2	82±2	81±1	40.96	0.11	3	167	20
158	63±2	68±2	67±3	35.95	0.13	3	368	18
210	54±8	73	70	39.68	0.11	4	275	20

4.2.9.1 Possible measurement errors

Some errors are expected on the values provided in Table 4-9 above due to the following reasons;

1. It was difficult to maintain a constant or reasonable flow rate for some mesh sieves (54 µm, 158 µm and 210 µm) therefore affecting their filtration rate (m^3/m^2-h), though one would expect a higher filtrate rate as the mesh sieve increases. One possible reason was that, the valve control for by-passed water was difficult to adjust at each time. Another reason was, the PLC recorded almost zero (0) flow rate (L/s) when filter mat was being formed on the mat, though flocculated biofilm water were filtered during that process.
2. Air blower was connected to the PLC device, which consumed more than 25 W, though it was not used in the process. Again power consumption by the feed pump, polymer preparation and dosing pumps were unaccounted for in the power consumption calculations.
3. The chemical (PAX-18) and polymer (C-496) doses used were constant and did not represent the optimum treatment for that particular day. Therefore mesh sieve sizes are not compared on the same optimum coagulation/flocculation of the biofilm solids for the effective filtration on the SF500 mesh sieves.

The discussion of the results obtained in Table 4-8 and Table 4-9 are therefore made on the assumption that, the possible errors listed in Section 4.2.9.1 are constant and negligible throughout with all mesh sieves studied.

From Table 4-8 and 4-9, 33 μm and 90 μm had both filtrate and actual design effluent TSS below the 30 mg/L with a removal efficiency of above 80%. This shows that the chemical and polymer were optimum for that particular day. Mesh sieve sizes 33 μm, 54 μm and 90 μm were the only mesh sieves capable of achieving less than 1 mg TP/L for both filtrate and actual effluent. As it stands, 90 μm mesh sieve can only achieve EU discharge permit only when daily optimum dose is used in the coagulation/flocculation process. Wash water TSS was always above 30 mg/L and therefore cannot be discharge without treatment. the wash water solids increased as the mesh size increased, due to the inefficiency of using just scraper on bigger mesh sieve sizes (> 33 μm)

4.2.9.2 SF500 PLC data Log Analysis

PLC device that came with SF500 was programmed to log data of the usual SF500 operation for every 5s. Data logged on the device were;

1. Operation ID
2. Time
3. Filter Level (mm)
4. Filter flow rate (L/s)
5. Filter power (W)
6. Filter cloth speed (%)
7. Cleaning (True/False)

Operation ID basically represents the excel row for logging a sequence of data at a time. *Time* column records date and time of operation. The time is logged in seconds (s). *Filter level* is the colume that indicates the level of water on the mesh sieve during SF500 filtration process. It is usually recorded and stored in mm. *Filter power* column logs the overall power consumption of all devices attached to the PLC device. It is usually recorded in watts (W). *Filter cloth speed* logs the speed of belt rotation at every instances of operation. It is recorded and stored in percentage (%). *Cleaning* is logged and stored with either True or False. True indicates the period where cleaning of the mesh sieve took place. False on the other hand is stored, when SF500 is operating without either air or water cleaning.

Figure 4-16 below presents the distribution of PLC log data during an hour operation of SF500 with all fine mesh sieve sizes. Individual mesh sieve PLC data distribution is attached in Appendix F.

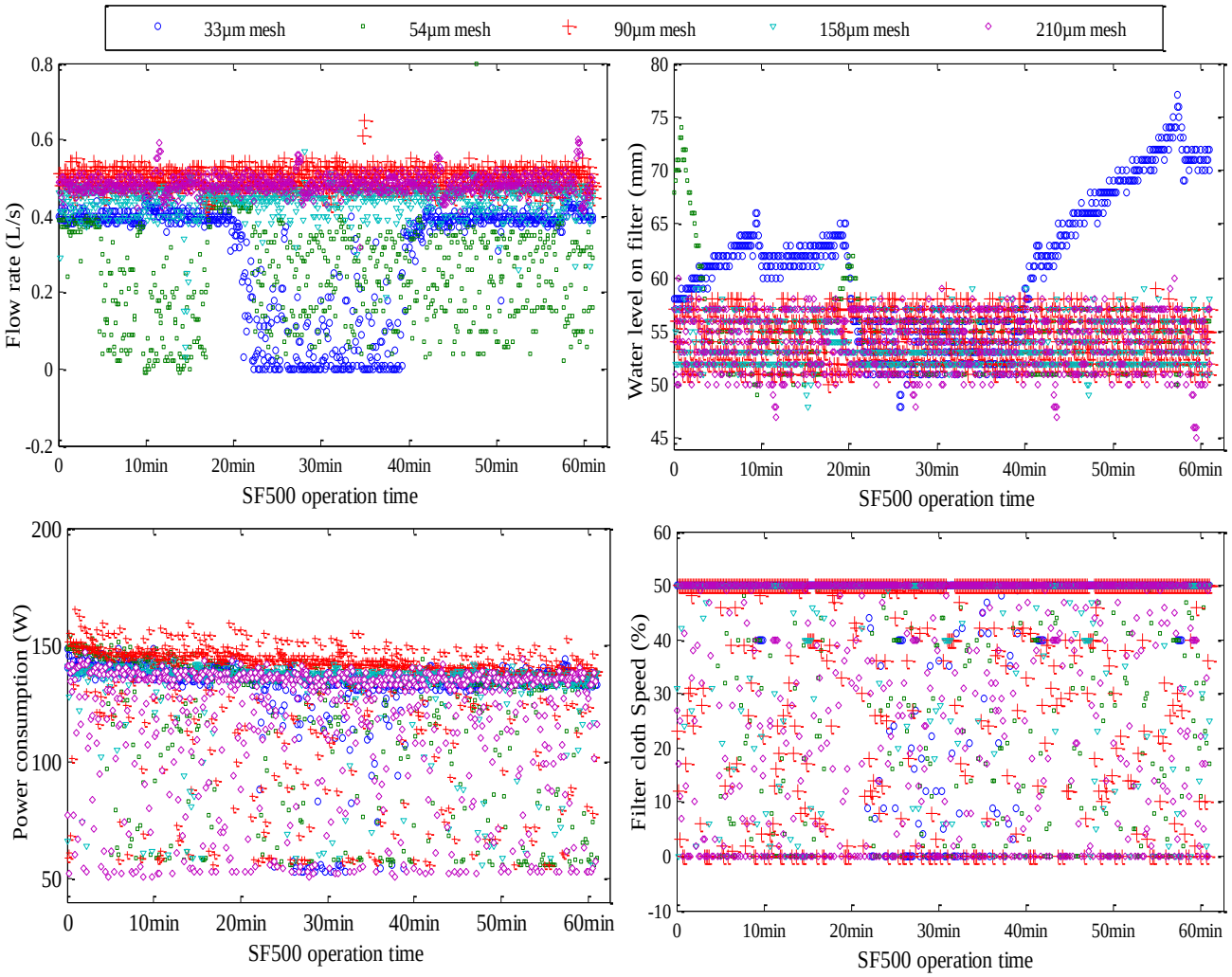

Figure 4-16: PLC data log distribution for the 1 hour SF500 operation time

From Figure 4-16 top left, the order of decreasing flow rate is 90 µm > 210 µm > 158 µm > 33 µm > 54 µm. This order also relates to Table 9 above. The straight decrease in flow rate for 33 µm mesh is attributed to the difficulty in trying to stabilize the level of water on the mesh sieve with the by-passed valve. This is because when a flow rate is reduced below a certain value, the flow velocity of the flocculated biofilm water is not enough for the electromagnetic flow meter to read and log data. This is also observed on the top right graph, the same dip is seen between the same periods for 33 µm mesh. Again from the top right, the

flow meter was able to record only when the water level on the 33 µm mesh was allowed to stay within 55 mm and 75 mm. The same problem was also experienced during 54 µm mesh operation. The valve control was done manually and therefore accurately by-passing a required volume of wastewater was difficult to achieve. Both 33 µm and 54 µm operation experienced the problem due to their small pore sizes, which did not allow much water to flow in the carrying hose to generate the needed flow velocity for the flow meter to log data into the PLC.

Again from the top right of Figure 4-16, much of the data points for 210 µm mesh sieve is observed below 50 mm than other sieves due to its ability to form filter mat. This again can be seen on the power consumption graph where most of 210 µm mesh data points are observed between 50 W and 100 W. It also has much data points with filter cloth speed of almost 0%. This is usually seen when filter mat begins to form, where the motor stops its operation. The water level then increases from zero (0) to the level set-point in filter, before the rotating motor is triggered to begin operation to rotate the filter cloth. From the bottom left, 90 µm mesh consumed more power due to the high flow rate through the SF500 during the filtration process.

4.3 Bench scale SF screening test for wastewater particle characterization

This Section presents results and discussions on using bench scale SF apparatus on both NFR primary wastewater and MBBR Reactor 5 effluent wastewater. These experiments were performed as already outlined in Section 3.13 and Section 3.14.

4.3.1 Bench scale SF screening test for NFR primary (degritted) wastewater particle size characterization test

As part of this thesis, bench scale SF screening test was performed on the primary wastewater at NFR using bench scale SF apparatus. Mesh sieve sizes 350 µm, 250 µm, 150 µm, 90 µm, 74 µm, 55 µm, 33 µm and 18 µm were used in the process. This experiment was performed as described in Section 3.13 and Figure 3-37 (Experiment 1). TSS, COD and TP analysis were performed according to Section 3.4 and Section 3.5 on each sample collected. Filtration rate of each mesh sieve was measured. PSD analysis on each sample was also performed using Malvern Mastersizer 3000 and FlowCAM according to procedure outlined in Section 3.10 and Section 3.11. Results obtained are presented in Table 4-10, Figure 4-17 and Figure

4-18. The results are discussed on the assumption that, pouring of samples through bench scale SF apparatus was performed under the same conditions without forcing particles through the mesh sieve. Again an assumption made, is that all measurements were performed with a constant and negligible error.

Table 4-10: SF mesh sieve removal efficiency and filtrate rate using bench scale SF screening test on NFR primary wastewater

Mesh Sieve (µm)	Percentage Removal (%)				**Filtration Rate** (m^3/m^2-h)
	% SS	**% COD**	**% TP**	**% SS** Removal (upper mesh to lower mesh)	
350	48	47	11	0	174
250	49	50	12	2	256
150	54	53	13	9	151
90	59	55	15	11	167
74	59	56	18	2	150
55	64	56	18	12	161
33	80	69	37	45	50
18	90	75	49	51	49

From Table 4-10, SS removal increased from 350 µm to 18 µm. This is already expected as mesh pore size decreases. However, not much removal difference is observed from mesh 350 µm to 74 µm with respect to SS, COD and TP. From Figure 4-17, 350 µm mesh is expected to remove less than 20% SS, since less than 18% of NFR primary wastewater particle by volume were above 350 µm particle size. However a higher TSS removal of 48% was observed due to the inefficiency of trying to avoid filter mat formation on the mesh sieve during 350 µm mesh filtration process. This is due to the toilet papers which formed greater part of the 18% of particles above 350 µm. These particles further decreased the pore size as they settled on the mesh and also captured some of the smaller size particles. Therefore after 350 µm mesh filtration, less removal was expected for the next mesh sieve 250 µm representing 1.6% SS removal.

Though it is expected for the filtrate rate to decrease as the mesh sieve size reduces, from Column 6, the filtration rate increased from 174 m^3/m^2-h to 256 m^3/m^2-h. This filtration rate increase shows that almost all 350 µm mesh effluent water were filtered by 250 µm mesh and at a faster rate. This is because of the filter mat that was formed on the 350 µm mesh. At 74 µm mesh, only 1.5% SS removal was achieved when 90µm mesh effluent water was filtered

with 74 µm mesh, this is because these mesh sieve sizes are too close, with just 16µm size difference, therefore less removal was achieved as expected.

From Table 4-10 column 5, less than 12% SS removal difference is observed as 350 µm effluent water is filtered through various meshes to 74 µm. The removal efficiency however increases significantly from mesh size 55 µm to 18 µm. This is expected because looking at Figure 4-17 below, about 50% of the NFR primary wastewater volumetric particle size are approximately above 55 µm. Therefore filtering with 55 µm, 33 µm and 18 µm mesh sieves without filter mat formation on NFR primary wastewater is expected to remove above 50% SS.

From Table 4-10 it is also observed that, the mesh sieve did not have significant effect on the removal of TP (< 50%). However its effect on COD removal was good and above 50% from 250 µm mesh to 18 µm mesh, with the highest removal of 75% COD removal achieved with 18 µm mesh. From Column 6 of Table 4-10, it is also observed that the filtration rate can be maintained, if the right mesh sieve sizes are selected to be operated in series to provide the expected SS removal.

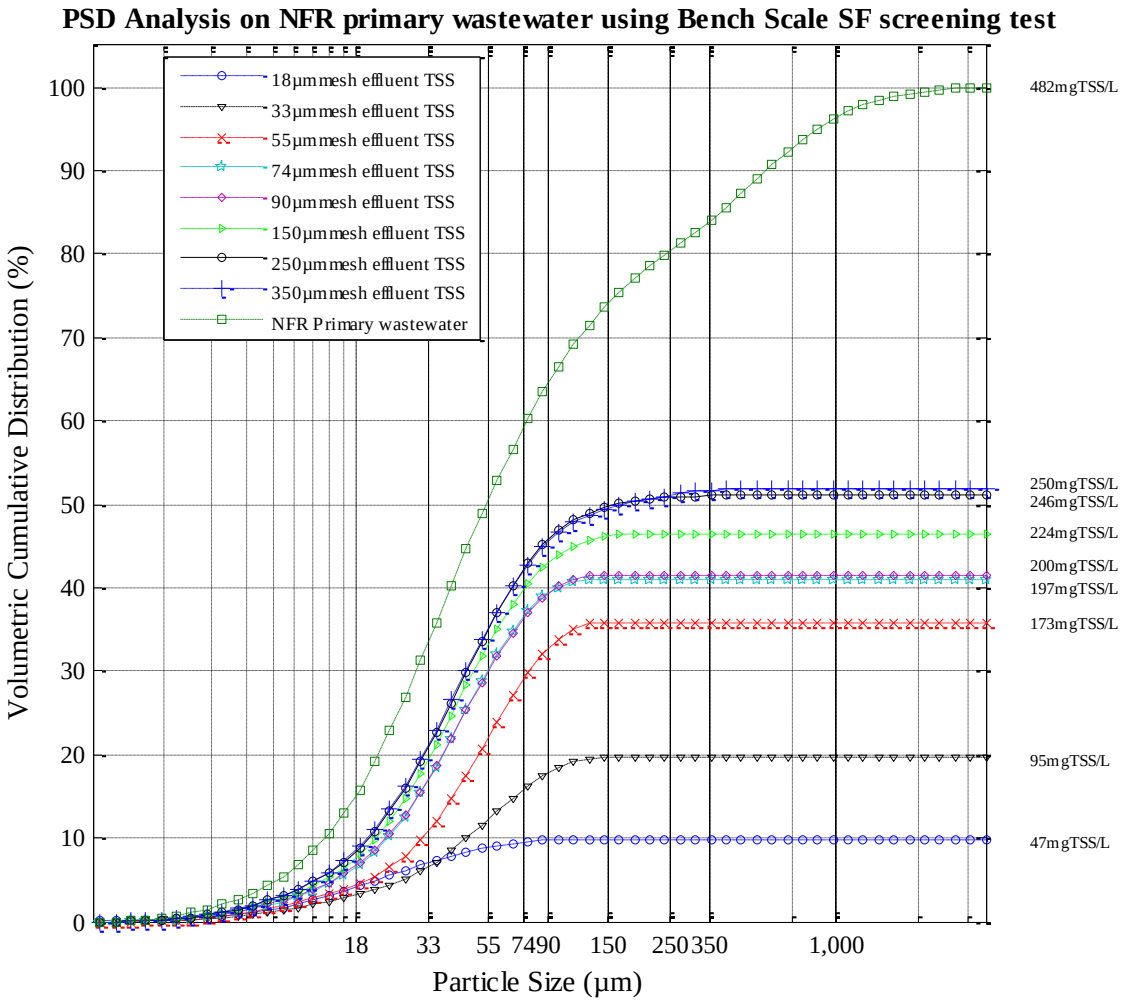

Figure 4-17: PSD of NFR primary wastewater and mesh filtrate using Malvern Mastersizer 3000

Figure 4-17 presents the volumetric particle size distribution for raw NFR primary wastewater and all mesh sieve effluent samples. Each of the mesh effluent distribution represents the volume of particle sizes retained in the mesh filtrate. As already explained above, the significant difference in NFR primary wastewater and 350 µm mesh is due to the toilet papers which progressively reduced mesh pore size. For this same reason, there was only a small difference in the volumetric cumulative distribution for 350 µm & 250 µm meshes. The small difference between 90 µm and 74 µm is again due to the small pore size (16 µm) difference. However a significant difference in the distribution is observed from mesh sieve 55 µm to 33 µm. From mesh 33 µm to 18 µm, a difference of 10% volumetric cumulative distribution representing about 50% SS removal is observed. This means that,

when 18 µm mesh sieve is used on 33 µm mesh filtrate, about 50% SS removal will be achieved and at the same time maintaining the filtrate rate as shown in Table 4-10.

Figure 4-18 below shows the volumetric cumulative distribution of the NFR primary wastewater using FlowCAM and Malvern Mastersizer 3000. It also shows the respective filtrate particle volumes based on filtrate TSS measurements.

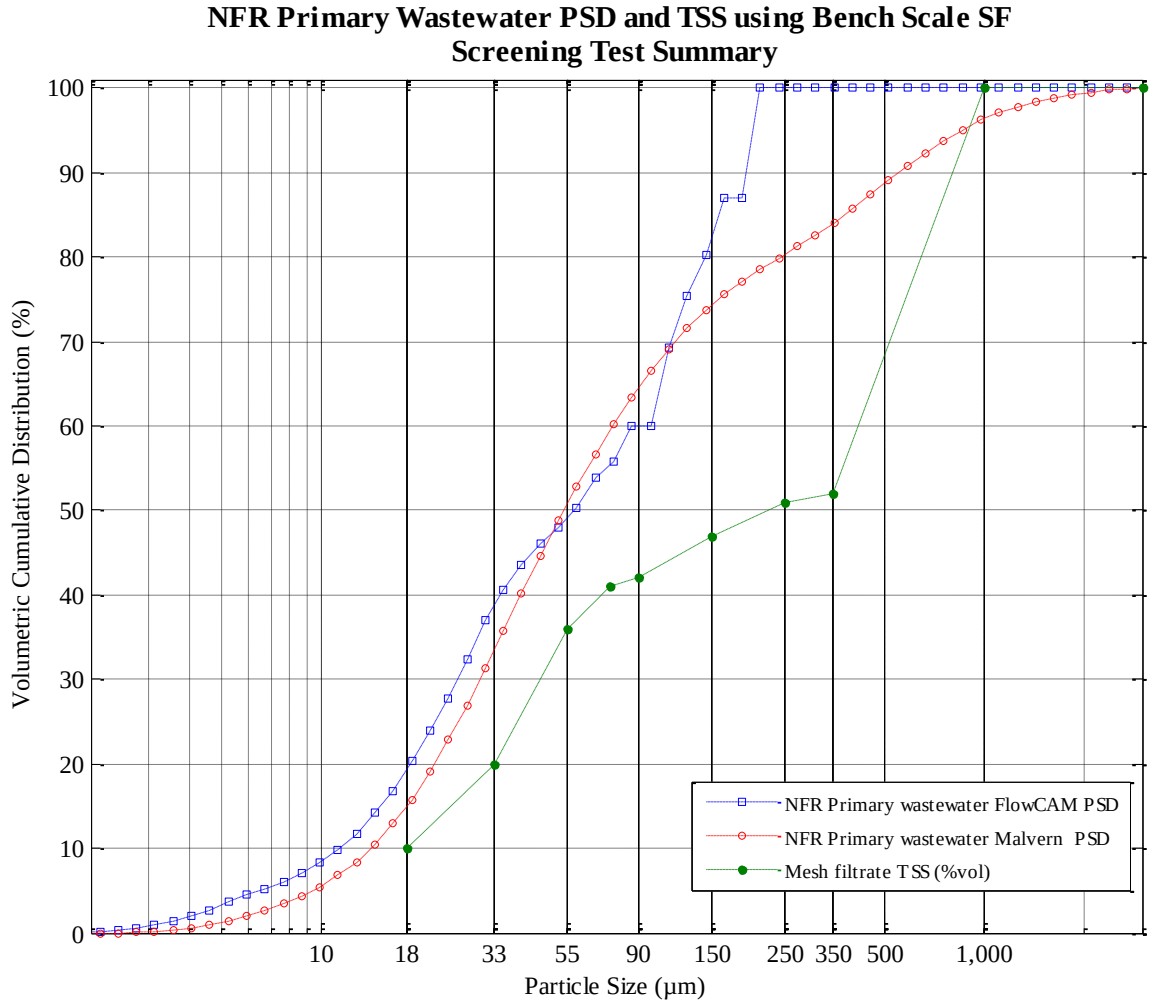

Figure 4-18: PSD of NFR primary wastewater using TSS measuremen, Malvern Mastersizer 3000 and FlowCAM

All three curves look alike and showed the same trend from 0% to 50%, then deviated after 50%. The mesh filtrate distribution showed less retained volumetric particles, due to a greater number of small particles captured by the toilet papers (350 µm mesh screening) and the smaller particles (< 1.2 µm) that made their way through GF/C filter. These particles were not

accounted for in the cumulative filtrate particle volume based on TSS measurements. The deviation in FlowCAM, measurements might be that, the dilution factor used on the samples above 90 µm mesh sieve was not enough, to ensure accurate measurements. Again it could be that, there were errors in the FlowCAM measurements. The distribution obtained by Malvern is assumed to show the true distribution with minimum error, since only a dilution factor of 2 was used to obtain an obscuration less than 20% for all sample measurement from the raw NFR primary wastewater to 18 µm filtrate water sample.

From Figure 4-18**,** both Malvern and FlowCAM shows that approximately 50% (Dv 50) of the particle volume in the raw NFR primary wastewater are below 55 µm. Malvern distribution shows that about 90% (Dv 90) are below 571 µm and 10% (Dv 10) below 16 µm. Finally from the above explanations and Figure 4-18, in order to achieve SS removal above 50% on NFR primary water with 350 µm mesh sieve, it has to be operated with filter mat. Attach in Appendix G is the PSD for each mesh sieve filtrate collected.

4.3.2 Bench scale SF screening test for NFR MBBR Reactor 5 effluent wastewater particle characterization

Bench scale SF screening test was performed again on NFR MBBR Reactor 5 effluent wastewater. The experiment was performed according to procedure described in Section 3.13 and Figure 3-37 (Experiment 2). MBBR wastewater was filtered using mesh sieve sizes 350 µm, to 18 µm. The filtrate of one mesh was used as influent for its corresponding lower mesh size to obtain the filtrate sample for that lower mesh sieve. Results obtained are presented in Table 4-11, Figure 4-19 and Figure 4-20 below. Same assumptions made in Section 4.3.1 above are considered applicable to this section.

Table 4-11: SF removal efficiency and filtrate rate using bench scale SF apparatus on NFR MBBR Reactor 5 effluent wastewater

Mesh Sieve (µm)	Percentage Removal (%)				**Filtration Rate** (m^3/m^2-h)
	% SS	**% COD**	**% TP**	**% SS** Removal (upper mesh to lower mesh)	
350	6	2	2	0	293.1
250	22	12	8	16	247.5
150	45	14	14	29	222.7
90	47	24	38	4	164.1
74	62	31	36	28	135.0
55	66	45	46	11	140.1
33	95	65	58	84	37.4
18	96	67	61	22	85.5

From Table 4-11, SS, COD and TP removal efficiencies increased from 350 µm mesh sieve to 18 µm mesh sieve as already expected. The lowest SS removal by 350 µm is also expected because from Figure 4-19 below, less than 6% of the raw MBBR volumetric particle sizes are above 350 µm. This made it possible for all raw MBBR wastewater to move through the 350 µm mesh sieve, resulting in the highest filtration rate recorded. Again for the same reason, looking at Figure 4-19 almost 50% of the volumetric particles sizes is above 90 µm. Therefore more than 50% SS removal was also expected for the 74 µm mesh. Again from the same graph, more than 85% of the volumetric particle sizes are above 33 µm, therefore above 85% SS removal for both 33 µm and 18 µm mesh sieves was expected. The volumetric cumulative distribution for the raw MBBR water is less steep as compared to NFR primary water for 33 µm to 18 µm; therefore not much %SS removal difference was expected between both mesh sieves. This is again confirmed in Column 6 of Table 4-11, where the filtration rate for 18 µm fine mesh increased from 37.4 m^3/m^2-h (33 µm mesh sieve) to 85.5 m^3/m^2-h, indicating that 33 µm mesh sieve effluent was filtered at a faster rate using 18 µm mesh. From Table 4-11, though all mesh sieves had less effect on COD and TP, above 50% removal was achieved with 33 µm and 18 µm mesh sieves.

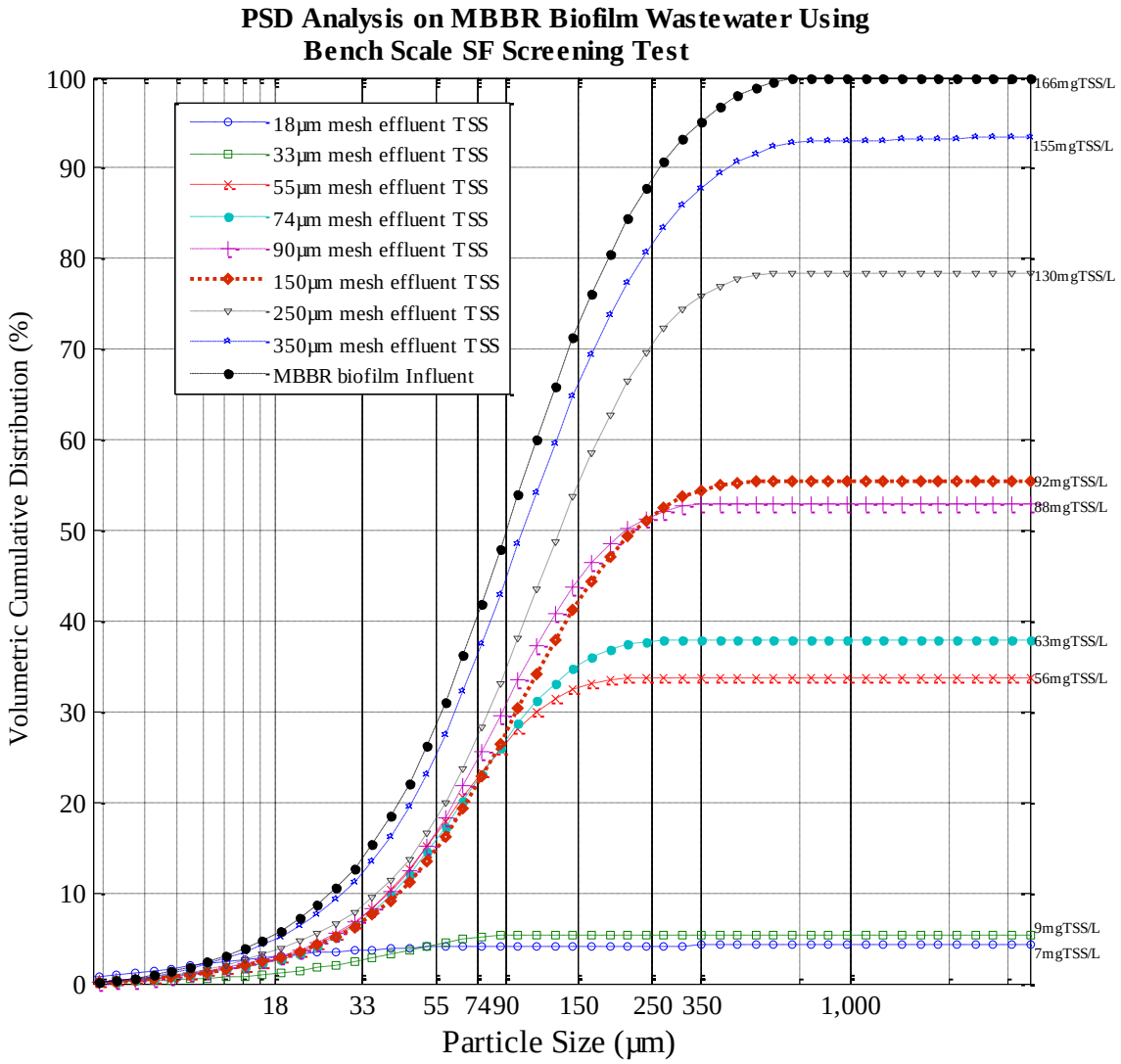

Figure 4-19: PSD of MBBR Reactor 5 wastewater and mesh filtrate using Malvern Mastersizer 3000

From Figure 4-19 above, about 50% (Dv 50) of the raw MBBR wastewater are below 90 µm, therefore 90 µm mesh filtrate TSS showed a little above 50% of the cumulative volumetric particle sizes. Though the difference in pore size between 74 µm and 90 µm meshes is very small (16 µm), there is a significant difference in terms of volumetric particle size. This is because, 90 µm mesh filtrate still contains greater volume (50%) of the raw MBBR total particle sizes, which may also have significant volume of particle sizes between 90 µm and 74 µm. Again the largest difference in volumetric particle size is observed between 55 µm and 33 µm mesh sieve sizes. This is because, from Table 4-11 above, the highest SS removal of 84% was achieved with the filtration of 55 µm mesh effluent on 33 µm mesh sieve.

Effluent from 33 µm mesh sieve to be used on 18 µm mesh showed less removal difference because, the raw MBBR cumulative curve is less steep at 33 µm to 18 µm particle sizes.

Figure 4-18 below, shows volumetric cumulative distribution of the raw MBBR Reactor 5 effluent wastewater using FlowCAM and Malvern Mastersizer 3000. It also shows the respective filtrate particle volume from various mesh sieves.

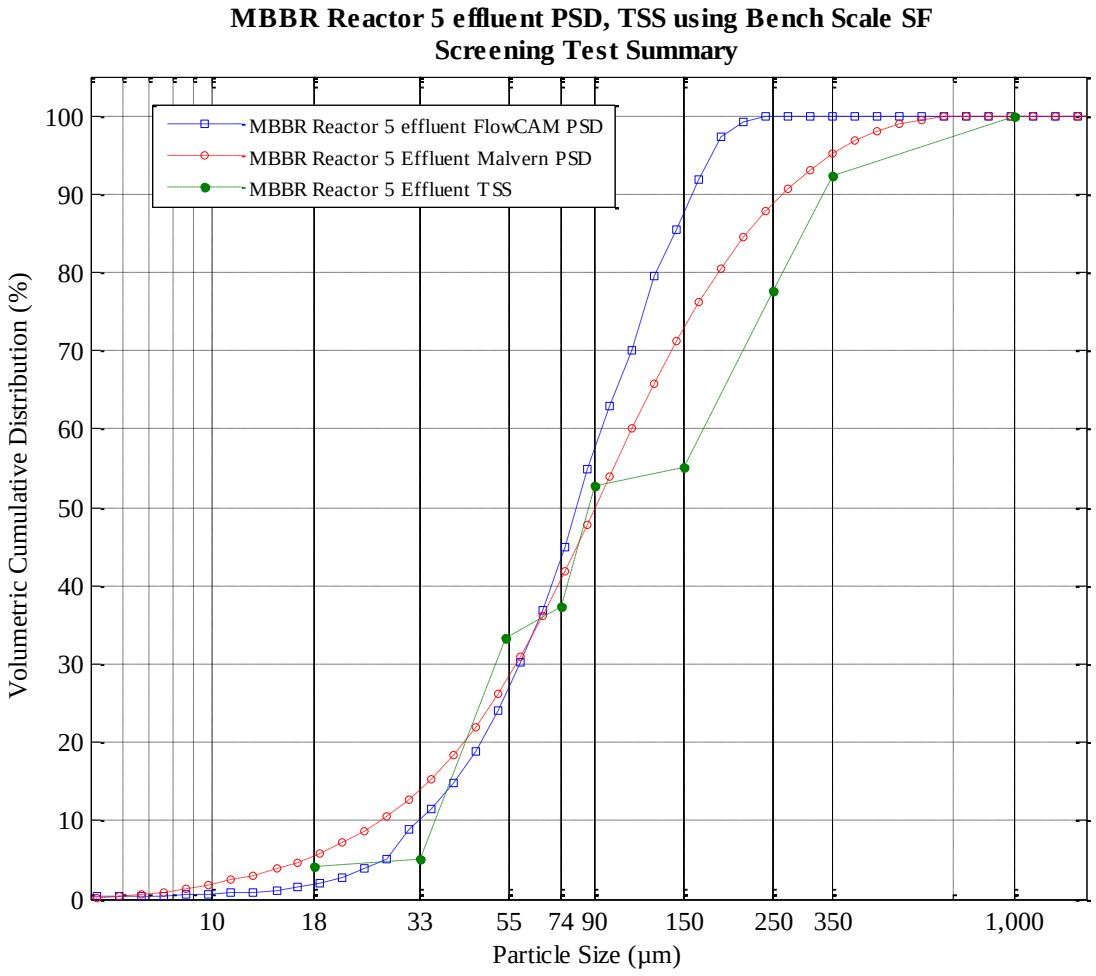

Figure 4-20: Filtrate volumetric SS and PSD of NFR MBBR Reactor 5 effluent wastewater using Malvern Mastersizer 3000 and FlowCAM

All three curves show a similar trend with a little difference compared to Figure 4-18 above. This is because problems with filter mat were not experienced with this experiment due to the fact that, about 6% volumetric particle sizes were above 350 µm with respect to Malvern. FlowCAM distribution was as expected. This might be that there was lower volume of particles in the samples or dilutions made were enough to ensure less number of particles

through the flow cell. This makes it possible for the FlowCAM camera to have a good focus on particles. Again looking at the Malvern distribution, about 94% of the particle sizes were below the flow cell (300 µm) used for PSD measurement.

The difference in the filtrate distribution may be attributed to the smaller particle sizes (< 1.2 µm) which are unaccounted for during TSS (GF/C filter) measurements. From Figure 4-20, it is obvious that, above 50% SS removal can only be achieved on MBBR Reactor 5 effluent, by operating with a mesh with sieve below 90 µm. This mesh (< 90 µm) will be capable of forming filter mat when need to improve SS removal. Finally, from Table 4-11 and Figure 4-20, it can be observed that, operating the mesh sieves in series with a good mesh sieves selections can result in a better SS removal and at the same time ensuring higher filtrate rate (33 µm to 18 µm). Attach in Appendix H is the PSD of the filtrate from each fine mesh sieve.

4.4 SF1000 particle characterization test with 33µm and 350µm mesh sieves on NFR Primary wastewater

As part of this thesis, SF1000 was operated on the raw NFR primary wastewater using mesh sieves 33 µm and 350 µm. This experiment was performed according to procedure outlined in Section 3.14 above. SF1000 was operated with varying filter cloth speeds (Hz). The machine with 33 µm mesh was operated without forming filter mat, while 350 µm mesh was operated with filter mat formation. This experiment was performed based on previous experiments with bench scale SF, on raw NFR primary wastewater, which determined 33 µm mesh sieve to deliver a better effluent particle size volume, suitable for biological nutrient removal (Razafimanantsoa et al., 2014) and same time providing sludge for biogas production . However, 350 µm mesh sieve is usually used on full scale treatment plants before biological treatment (Rusten and Ødegaard, 2006). Therefore this experiment seeks to determine, a particular SF1000 filter cloth speed, with 350 µm mesh sieve, capable of producing effluent water with similar particle size volume as that of 33 µm mesh sieve. Due to the low filtrate rate of 33 µm mesh sieve, SF1000 was operated with influent rate of 1.5 L/s for both mesh sieves. TSS, COD, TN and TP analysis were performed according to Section 3.4, and 3.5. An assumption that, SF1000 PLC was operated with optimum parameters for both sieves is made in the discussion of the results obtained. The raw NFR primary wastewater parameter is also assumed to be constant during the experimental period for both mesh sieves. The experimental error encounted for all measurements is assumed to

be constant and negligible. Table 4-12 and Figure 4-21 presents the results obtained during the experimental period.

Table 4-12: SF1000 screening test with 33µm and 350µm mesh sieves on NFR Primary wastewater

SF1000 Operation		Percentage Removal (%)			
Mesh sieve	Speed (Hz)	% SS	% COD	% TN	% TP
33um mesh (no filter mat)	10	34	24	6	0
	20	11	19	8	5
	30	15	17	5	2
350um mesh (filter mat)	10	48	24	15	2
	20	38	18	3	6
	30	30	22	12	2

From Table 4-12 above, SS removal decreased when both mesh sieves were operated with an increasing cloth speed (Hz) representing a high retain volume of particles in SF1000 effluent. COD, TN and TP did not show significant changes in parameters with varying cloth speed (Hz). It is also observed that a higher SS removal was observed when SF1000 was operated with filter mat at the very low speed of 10 Hz. As already stated in Section 4.3.1, higher removal can be achieved if 350 µm is operated slowly to allow significant filter mat formation.

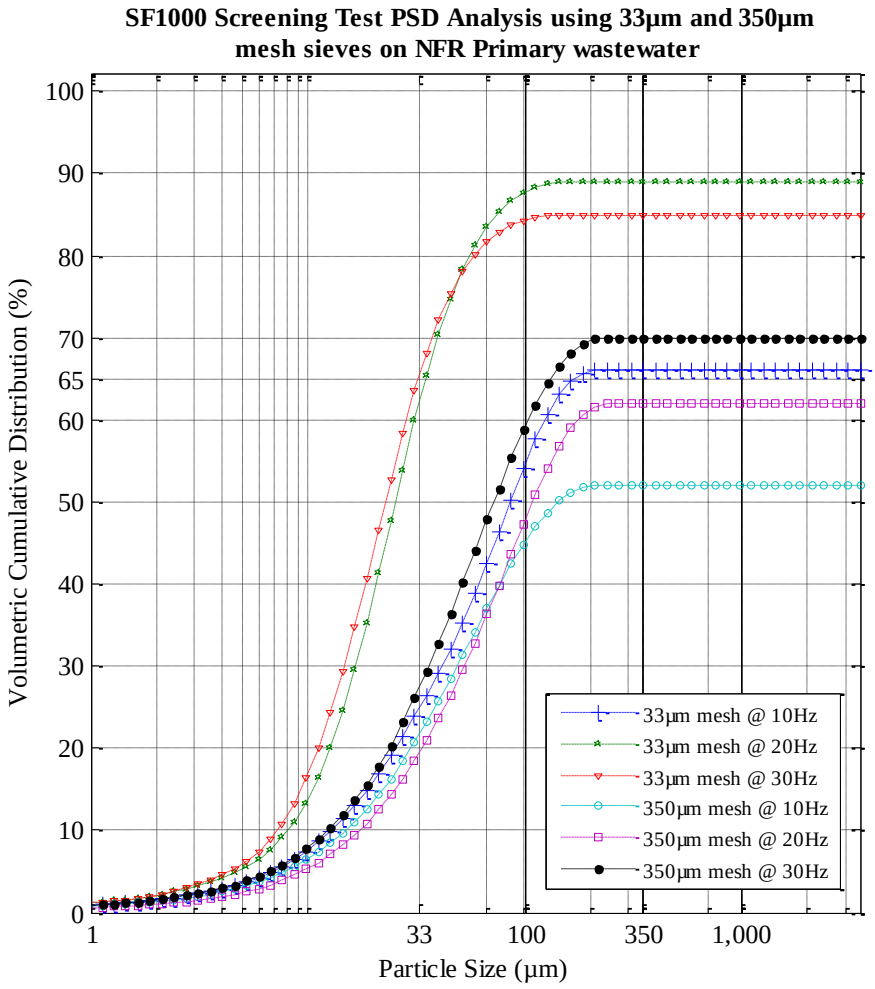

Figure 4-21: PSD of SF1000 effluent water on NFR Primary wastewater

Figure 4-21 above shows a PSD distribution of the volume of particles in the effluent of all samples collected. 350 µm mesh sieve at 10 Hz is observed to have the least volume of particles retained in its filtrate. 33 µm mesh at 20 Hz is observed to have the highest volume of particles in its filtrate, followed by 33 µm at 30 Hz. Again, it is observed that 350 m mesh sieve at 20 Hz and 30 Hz are the only curves close to 33 µm mesh operated at 10 Hz. Therefore both speeds (20 Hz and 30 Hz) with 350 µm mesh can be operated with SF1000 to obtain a similar particle size volume as 33 µm mesh. Finally looking at the COD removal, 350 µm mesh operated at 20 Hz, had the minimum COD removal, and also ensured a reasonable SS removal. This therefore shows that, at 20 Hz, there will still be excess COD for biological processes to be effective downstream SF1000.

CHAPTER V

5.0 CONCLUSION

NFR MBBR biofilm wastewater coagulation/flocculation before SF500 filtration experimental results obtained from this thesis showed prototype SF500 is very efficient in achieving a high removal for TSS, TP, COD, and Turbidity. PAX-18 and Superfloc C-496 formed the best biofilm floc for SF filtration. 13.24 mg Al/L + 1 mg C-496/L was able to achieve below 0.3 mg TP/L consistently over 2 hours of SF500 operation time, with 33 µm fine mesh sieve. Filtrate TSS, TP , COD and turbidity remained below 30 mg/L, 1 mg/L, 50 mg/L and 20 NTU respectively, for SF fine mesh sieve size 90, 54 and 33µm. The highest SS, TP, COD, and turbidity removal achieved were 98%, 96%, 88%, and 96% respectively, with 33 µm fine mesh sieve. These results were achieved with an average filtrate rate of 24.63 m^3/m^2-h. A pH of 4.6 ±0.2 was recorded in all filtrate samples using 13.24 mg Al/L+1 mg C-496/L. Flocculation time of 10 min was adequate to form dense and correctly sized flocs for SF500 filtration. A G-value of 65.84 s^{-1} was capable of achieving adequate floc size with 10 min of flocculation time. Power consumption (including coagulation/flocculation stirrers) between 0.1 – 0.2 kWh/m^3 was used. The power consumption could be reduced if the problems identified with SF500 are rectified in order to allow a higher flow rate into SF. The best removal was observed when.

An average dosage of 94.57 mg Al/g TSS + 7.14 mg C-496/g TSS, 10 min flocculation time with a G-value of 65.84 s^{-1}, and a SF 33 µm mesh running in auto-mode, on MBBR biofilm wastewater will meet the EU discharge permit. Higher mesh sieve sizes (54µm to 90µm) can be used to achieve the same expected results expected results as long as, optimal parameters are determined with daily jar tests. SF wash water cannot be discharged, and should be recycled for treatment.

Particle characterization of NFR primary wastewater and MBBR Reactor 5 effluent wastewater characterisation showed that the knowledge on PSD of a specific wastewater was crucial in selecting the appropriate mesh sieves. This allows delivery of the desired SS removal and same time ensuring high filtration rate.

Particle characterization of NFR primary (degritted) wastewater showed that SF1000 with 350 µm mesh can be operated in automatic mood with filter mat, with a PLC manual speed setting of 20 Hz to provide a similar particle volumetric cumulative distribution to that of 33µm mesh sieve. The effluent from this setting (20 Hz in automatic mode) with 350 µm mesh will be best for SF primary wastewater treatment before biological nutrient removal (BNR) reactor. SF1000 with 350 µm at these parameters will remove adequate solids, which will be helpful for biogas generation, and at same time containing the required particle size volume or organic carbon in its effluent. This effluent organic carbon will be adequate for BNR and also reduce the energy demand (lower oxygen demand).

CHAPTER VI

6.0 RECOMMENDATION

Experiments performed in this thesis showed the SF500 prototype to be very effective in removing flocculated biofilm solids. However, SF removal efficiency could be improved with further study and updates to the design.

A. Recommendations for NFR wwtp

1. Any of the studied dosage combinations studied will meet the EU discharge permit with 33 µm mesh. However, it is recommended when using a higher mesh size (54 µm to 90 µm), daily optimum dosages of coagulants and flocculants must be used to reach discharge limits.
2. It is also recommended to conduct daily jar test experiment on the MBBR biofilm wastewater to achieve the optimal performance for SF filtration. The range of 85.71±14.38 mg Al/g TSS and 5±2 mg C-496/g TSS is recommended for daily monitoring.
3. SF500 flow meter should be changed if it is to be operated at low flow rate (<0.4 L/s). However, if the SF500 capacity (exposed mesh area or mesh size) can be increased to ensure a high flow rate, which is capable of providing adequate flow velocity for proper data logging and appropriate monitoring, then it is sufficient.
4. Only water wash cleaning is effective in cleaning the porous mesh with the current prototype with MBBR solids, therefore efforts should be made to include a recycle pump which can be programmed to recycle the wash water to the flocculation tanks. This wash water contains a high concentration of polymer, which could help reduce polymer dosage in tanks if recycled.

B. Recommendation for any researching institution

1. There should be a newly designed bench scale SF apparatus for studies on flocculated solids which can provide a more accurate and reliable predictions on the SF.
2. Further studies in line with this experiment should have properly sized flocculation tanks, capable of transferring flocculated biofilm to SF without

by-passing, to help minimize the breakage of flocs, and to provide more continuous flow, while ensuring flocs get to the SF without breakage for efficient filtration.

3. Studies should be carried out on SF mesh plastic support locations; relocate them to locations which will avoid build-up of solids beneath the mesh sieves, which eventually falls into effluent water.
4. A cost benefit analysis should be done to decide, whether it is worth using more or less of a polymer dose. Higher polymer dosing form bigger flocs, which allows use of a larger mesh sieve size, increases the maximum flow rate, and also reduces power consumption.
5. Further studies should be performed on using technology capable of auto sampling for jar tests and laser diffraction monitoring of floc formation, in order to automatically regulate dosing pumps for optimum dosage of coagulants and flocculants. This could reduce operator presence, while ensuring effective performance of SF. This will require partnership with other institutions which are already involved with this sort of technology.

C. Recommendation for Salsnes Filter AS

1. Design modifications should be carried out on the cartridge design to avoid a gap between the lower roller and the inner plate, which allows filtered water to wash solids from the back side unclean mesh to effluent water. This will in effect avoid the shear of flocs at the inlet of SF. Possible design modification has been provided in Figure 6-1.
2. It is also recommended that more tests be performed to determine the best air knife design with optimal air pressure capable of removing biofilm flocs from mesh sieve.
3. From the study, water wash cleaning will at any time be needed once a while and this water can't just be discharge to effluent. Therefore SF should consider incorporating a recycle pump for wash water to flocculation thanks.

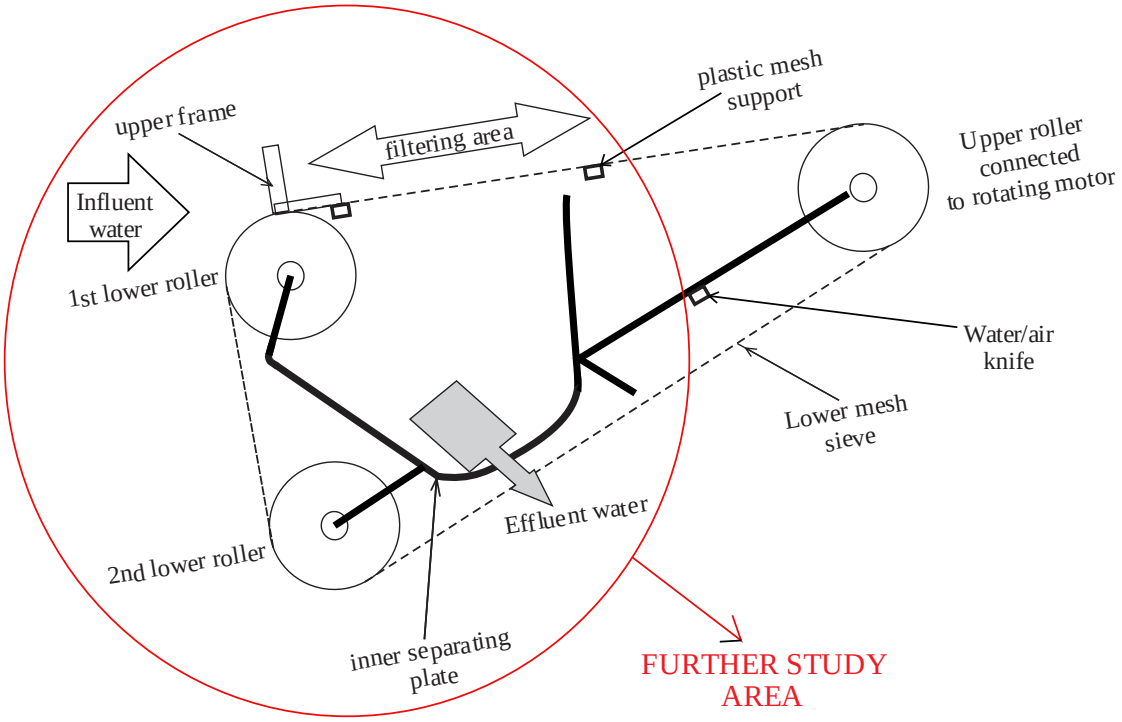

Figure 6-1: Possible SF cartridge/frame modification

4. SF1000 lower roller is currently positioned to rotate through outgoing filtered water. This makes it necessary for the mesh to be completely cleaned before repeating another cycle. It therefore requires continuous cleaning, which will not be energy efficient and also more fresh water will be needed. Again the design is made in way (high inclined angle) that directs all cleaning water to effluent water. It is therefore recommended to raise the lower roller a little above effluent discharging hole to avoid rotating mesh sieve contact with filtered water.
5. SF1000 machine design should be reconsidered to have a compartment to receive any washwater.

CHAPTER VII

7.0 REFERENCES

Alemayehu, Z. (2010) *Dissolved air flotation*. School of Civil & Environmental Engineering, AAU.

AL NABELSI, S. & GANESH, R. 2013. *On-site wastewater treatment system in Høyås farm, Ås Norway*. Ås: Masters Thesis, Norwegian University of Life Sciences.

American Water Works Association (2000) Water Quality and Treatment: A Handbook of Community Water Supplies. *AWWA*, 5th edition**,** McGraw Hill, New York.

Artiga, P., Oyanedel, V., Garrido, J. M., Méndez, R. (2005) An innovative biofilm-suspended biomass hybrid membrane bioreactor for wastewater treatment. *Desalination*, 179**:** 171-179.

ASTM (2003) Standard Practice for Coagulation - Flocculation Jar Test of Water.

AWWA (1999) Standard Methods For The Examination of Water and Wastewater. *In:* Lenore S. Clesceri, A. E. G., Andrew D. Eaton (ed.) 20th ed.: American Water Works Association.

Barragán, G. R. (2014) *Performance of Salsnes Water to Algae Treatment (SWAT) Technology in a Continuous Mode for High Algae Recovery*. Masters' Thesis, University of Stavanger.

Blöch, H. (2005) European Union legislation on wastewater treatment and nutrients removal. European Commission,Foundation for Water Research (FWR), B-1049 Brussels

Bolto, B., Gregory, J. (2007) Organic polyelectrolytes in water treatment. *Water Research*, 41**:** 2301-2324.

Brandy, N.,Soros, A., Mroz, A., Rusten, B. (2006) Removal of particulate and organic matter from municipal and industrial wastewaters using fine mesh rotating belt sieves. *WEFTEC*, Dallas, Texas, USA .

Bratby, J. (2006) Coagulation and Flocculation in Water and Wastewater Treatment. 2nd Edition 407.

Bratby, J. (2006) *Coagulation and Flocculation in Water and Wastewater Treatment*, Alliance House, 12 Caxton Street, London SW1H 0QS, UK, IWA.

Bratby, J. (2007) Coagulation and flocculation in water and wastewater treatment. *IWA*, 2nd edition.

Camp T.R (1955) *Flocculation and flocculation basins*.

Casson, L. W., Lawler, D. F. (1990) Flocculation in turbulent flow: measurement and modelling of particle size distributions. *AWWA*, 82**:** 54-68.

Crittenden, J. C., Trussell, Hand, D. W., Howe, K. J. & Tchobanoglous, G. (2012) *MWH's Water Treatment: Principles and Design: Third Edition*.

DAVIS, M. L. 2010. *Water and wastewater engineering: design principles and practice*, New York, McGraw-Hill.

Dougherty, G. M., Rose, K. A., Tok, J. B. H., Pannu, S. S., Chuang, F. Y. S., Sha, M. Y., Chakarova, G., Penn, S. G. (2008) The zeta potential of surface-functionalized metallic nanorod particles in aqueous solution. *electrophoresis*, 29**:** 1131-1139.

Duan, J., Gregory, J. (2003) Coagulation by hydrolysing metal salts. *Advances in Colloid and Interface Science*, 100–102**:** 475-502.

Ebeling, J. M., Welsh, C. F., Rishel, K. L. (2006) Performance evaluation of an inclined belt filter using coagulation/flocculation aids for the removal of suspended solids and

phosphorus from microscreen backwash effluent. *Aquacultural Engineering,* 35**:** 61-77.

Ekama, G. A. (2011) 4.14 - Biological Nutrient Removal. *In:* WILDERER, P. (ed.) *Treatise on Water Science.* Oxford: Elsevier.

Fairhurst, D. (2014) *An Overview of the Concept, Measurement, Use and Application of Zeta Potential* [Online]. Horiba Scienctific. Available: http://www.horiba.com/fileadmin/uploads/Scientific/Documents/PSA/AP014.pdf [Accessed 6th June 2014].

Fluid Imaging Technologies, I. (2011) FlowCAM Maual.

Fu, F., Wang, Q. (2011) Removal of heavy metal ions from wastewaters: A review. *Journal of Environmental Management,* 92**:** 407-418.

Geoffrey, I. G. (2010) Interfacial Science. 2nd edition**:** 241-284.

Gough, R., Holliman, P. J., Willis, N., Freeman, C. (2013) Dissolved organic carbon and trihalomethane precursor removal at a UK upland water treatment works. *Science of the Total Environment,* 468-469**:** 228-239.

Hach (2008) Portable Turbidimeter Model 2100P manual, USA.

Hach (2010) DR 2800 TM UV-Vis Laboratory Spectrophotometer. USA: Hach Company.

Hatt, J. W., Germain, E., Judd, S. J. (2011) Precoagulation-microfiltration for wastewater reuse. *Water Research,* 45**:** 6471-6478.

Headworks, B. (2014) *BIOLOGICAL NUTRIENT REMOVAL* [Online]. Texas Available: http://www.headworksinternational.com/biological-wastewater-treatment/bnr.aspx [Accessed 11th July 2014].

Hopkins, D. C., Ducoste, J. J. (2003) Characterizing flocculation under heterogeneous turbulence. *Journal of Colloid and Interface Science,* 264**,** 184-194.

Horiba, S. (2012) A GUIDEBOOK TO PARTICLE SIZE ANALYSIS. Irvin, CA 92618 USA: Horiba Istruments, Inc.

Hunter, R. J. (1993) Foundations of Colloid Science. 2nd edition**:** 239-255.

Jang, W., Nikolov, A., Wasan, D.T., (2004) Effect of depletion force on the stability of food emulsions. 817- 821.

Jarvis, P., Jefferson, B., Parsons, S. A. (2005) Breakage, regrowth, and fractal nature of natural organic matter flocs. *Environmental Science and Technology,* 39**:** 2307-2314.

Jiang, B. & Zheng, J. T. (2013) Electrical plasma technology for dye decolorization in a continuous reactor system. Guilin.

Kan, C., Huang, C., Pan, J. R. (2002) Coagulation of high turbidity water: the effects of rapid mixing. *Water Supply: Research and Technology - AQUA,* 51.2**:** 79 - 85.

Kan, C., Huang, C. & Pan, J. R. (2002) Time requirement for rapid-mixing in coagulation. *Colloids and Surfaces A: Physicochemical and Engineering Aspects,* 203**:** 1-9.

Kemwater 2008. Kemwater Pax-18. (2008) ed.: Kemwater Chemical AS.

Kleimann, J., Gehin-Delval, C., Auweter, H., Brokovec, M., (2005) Super-stoichiometric charge neutralization in particle-poly-electrolyte systems . 8**,**

Kurniawan, T. A., Chan, G. Y. S., Lo, W. H., Babel, S. (2006) Physico-chemical treatment techniques for wastewater laden with heavy metals. *Chemical Engineering Journal,* 118**,** 83-98.

Lange H. (2001) *LCK 349. Procedure manual,* USA patent application.

Lange, H. (2001). LCK 314. *Procedure manual,* Germany: HACK LANGE.

Langelier, W. F. (1921) Coagulation of Water with Alum by Prolonged Agitation. *Engineering News Record,* 86**:** 924 - 928.

Luo, Y., Guo, W., Ngo, H. H., Nghiem, L. D., Hai, F. I., Zhang, J., Liang, S., Wang, X. C. (2014) A review on the occurrence of micropollutants in the aquatic environment and

their fate and removal during wastewater treatment. *Science of the Total Environment,* 473-474**:** 619-641.

Machenbach, I. (2007) *Drinking water production by coagulation and membrane filtration,* Trondheim, Norges teknisk-naturvitenskapelige universitet.

Malvern (2011). Hydro series wet dispersion units manual. M. I. (ed.). United Kingdom: Malvern Instruments Ltd.

Malvern (2011) Malvern Mastersizer procedure for analysing solids and oil droplet sizes, Malvern Instruments Ltd,User Manual, United Kingdom.

Malvern (2014) Malvern Zetazizer Nano ZS operation Manual.

Malvern. (2014) *ZATASIZER NANO Series Brochure* [Online]. Available: http://www.malvern.com/Assets/MRK1839.pdf [Accessed 5th June 2014].

Mainstone, C. P., Parr, W. (2002) Phosphorus in rivers — ecology and management. *Science of The Total Environment,* 282–283**:** 25-47.

Mccurdy, K., Carlson, K., Gregory, D. (2004) Floc morphology and cyclic shearing recovery: comparison of alum and polyaluminum chloride coagulants. *Water Research,* 38**:** 486-494.

Mukherjee, M., Swami, A., Ramteke, D. S., Moghe, C. A., Sarin, R. (2004) Role of conventional and non-conventional coagulants with and without polyelectrolyte in treatment of refinery wastewater. *Pollution Research,* 23**:** 417-426.

Ng, H. Q. (2012) *Removal of MBBR Biofilm Solids by Salsnes Filter fine mesh sieves,* Masters thesis, University of Stavanger, Stavanger, Norway.

Nordre Follo Renseanlegg, (NFRA). (2014) *Biological Nitrogen Removal* [Online]. Hoyengsletta 19, 1407 Vinterbro. Available: http://www.nfra.no/ [Accessed 25th June 2014].

Ntalikwa, J. W., Bryant, R., Zunzu, J. S. M. (2001) Electrophoresis of colloidal α-alumina. *Colloid and Polymer Science,* 279**:** 843-849.

Ødegaard, H., Cimbritz, M., Christensson, M. & Dahl, C. P. (2010) Separation of biomass from moving bed biofilm reactors (mbbrs). *In:* FEDERATION, W. E., ed. WEF/IWA Biofilm Reactor Technology Conference 2010. Water Environment Federation, 22.

Ødegaard, H., Liao, Z., Melin, E., Helness, H. (2004) Compact high-rate treatment of wastewater.

Razafimanantsoa, V. A., P. A. Vargas Charry, T. Bilstad, L. Ydstebø, A. K. Sahu & B. Rusten (2014) Impact of selective size distribution of influent suspended solids on downstream biological processes. IWA Conference on Pretreatment of Water and Wastewater "The status and progress on Water Pretreatment Technology", , 2014 Shanghai, China. IWA, 8.

Rubin A.J , B. H. (1979) Coagulation of montmorillonite suspensions with aluminum sulfate. *J. AM. Water Works Science Technology* 41.

Ruiken, C. J., Breuer, G., Klaversma, E., Santiago, T., Van Loosdrecht, M. C. M. (2013) Sieving wastewater – Cellulose recovery, economic and energy evaluation. *Water Research,* 47**:** 43-48.

Rusten, B. (2004) Development of a simple test apparatus and procedure to predict the full scale treatment performance of Salsnes filter fine mesh sieves preliminary testing. *Aquateam Report No. 04-002.*

Rusten, B., Ødegaard, H. (2006) Evaluation and testing of fine mesh sieve technologies for primary treatment of municipal wastewater.

SALSNES. (2014) *Brochure* [Online]. Available: http://www.salsnes-filter.com/wp-content/uploads/sites/3/2013/06/Salsnes-detailer-13.pdf [Accessed 20th May 2014].

Salsnes Filter. 2014. *About Salsnes Filter* [Online]. Salsnes Filter. Available: http://www.salsnes-filter.com/ [Accessed 26th June 2014].

Santo, C. E., Vilar, V. J. P., Botelho, C. M. S., Bhatnagar, A., Kumar, E., Boaventura, R. A. R. (2012) Optimization of coagulation-flocculation and flotation parameters for the treatment of a petroleum refinery effluent from a Portuguese plant. *Chemical Engineering Journal,* 183**:** 117-123.

Shammas, N. K. (2004) Coagulation and flocculation. 3**:** 103 - 140.

Smoluchowski, M. (1917) Verrsuch einer mathematischen Theorie der KoagulationsKinetic Kolloider Losunger. *Zeit. Phys. Chemie,* 92**:** 129-168.

Spicer, P. T., Pratsinis, S. E. (1996) Coagulation and Fragmentation: Universal Steady-State Particle-Size Distribution. *AIChE Journal,* 42**:** 1612-1620.

Thomas, D. N., Judd, S. J. Fawcett, N. (1999) Flocculation modelling: A review. *Water Research,* 33**:** 1579-1592.

Tzfati, E., Sein, M., Rubinov, A., Raveh, A., Bick, A. (2011) Pretreatment of wastewater: Optimal coagulant selection using Partial Order Scaling Analysis (POSA). *Journal of Hazardous Materials,* 190**:** 51-59.

University Of Arizona. (2014) *Filtration* [Online]. Available: http://quiz2.chem.arizona.edu/vip/filtration/ [Accessed 27th June 2014].

Verma, S., Prasad, B., Mishra, I. M. (2011) Thermochemical Treatment (Thermolysis) of Petrochemical Wastewater: COD Removal Mechanism and Floc Formation. *Industrial & Engineering Chemistry Research,* 50**:** 5352-5359.

Webster, E. (2001) Cost-effective wastewater treatment now in SA. *Water Sewage and Effluent,* 21**:** 13.

Woisetschläger, D., Humpl, B., Koncar, M., Siebenhofer, M. (2013) Electrochemical oxidation of wastewater - Opportunities and drawbacks. *Water Science and Technology,* 68**:** 1173-1179.

WTW Gmbh (2004) Multi 340i meter manual, USA.

Wu, T. Y., Mohammad, A. W., Jahim, J. M., Anuar, N. (2010) Pollution control technologies for the treatment of palm oil mill effluent (POME) through end-of-pipe processes. *Journal of Environmental Management,* 91**:** 1467-1490.

Yukselen, M. A., Gregory, J. (2004) The reversibility of floc breakage. *International Journal of Mineral Processing,* 73**:** 251-259.

8.0 APPENDICES

Appendix A: PAX-18 Specification and dosing concentration

PRODUKTINFORMASJON

Kemwater™
PAX-18

Kemwater PAX-18, jernfri polyaluminiumklorid, er et flytende fellingsmiddel som inneholder aktive flerverdige aluminiumsforbindelser. PAX-18 egner seg for overflate- og grunnvannrensing i de fleste renseprosesser samt papirhydrofobering og avløpsrensing.

Kjemisk data

Aluminium (Al^{3+})	9,0 0,3	%
Jern (Fe_{tot})	<0,01	%
pH	1,0 ± 0,5	
Tetthet	1,36 ± 0,02	g/cm³ (25°C)
Uløst stoff	<0,05	%
Klorid (Cl^-)	210 ± 2,0	g/kg PAX-18
Sulfat (SO_4^{2-})	<1,0	g/kg PAX-18
Krystallisasjonstemp	-20°C	
Aktiv stoff (Me)	3,3	mol/kg (4,5 mol/l)

Sporstoff Typiske analyseverdier

Bly (Pb)	1,0	mg/kg PAX-18
Kadmium (Cd)	< 0,05	mg/kg PAX-18
Kobolt (Co)	<1,0	mg/kg PAX-18
Kobber (Cu)	<1,0	mg/kg PAX-18
Krom (Cr)	<1,0	mg/kg PAX-18
Kvikksølv (Hg)	< 0,05	mg/kg PAX-18
Nikkel (Ni)	<1,0	mg/kg PAX-18
Sink	<2,0	mg/kg PAX-18

Dosering
Dosering av PAX-18 skjer med pumper i korrosjonsbeskyttet utførelse. Rørledninger og ventiler skal være utført i plast eller gummiert stål. PAX-18 doseres uten fortynning direkte fra lagertank.

Godkjenning
PAX-18 er godkjent av SNT som fellingsmiddel ved drikkevannsrensing.

Kvalitet og miljø
Kemira Chemicals er sertifisert iht ISO9001/PR2 og ISO 14001.

Omregningstabell for dosering

ml PAX-18/m³	g PAX-18/m³	g Al/m³
20	27	2,43
40	54	4,86
60	81	7,29
80	108	9,72
100	135	12,15
120	162	14,58
140	189	17,01
160	216	19,44
180	243	21,87
200	270	24,30
300	405	36,45
400	540	48,60
500	675	60,75

Håndtering
Beskyttelsesbriller skal benyttes ved åpen håndtering av PAX-18.
Personlig verneutstyr benyttes ved behov.

Lagertanker og beholdere skal merkes:

IRRITERENDE VÆSKE
POLYALUMINIUMKLORID-HYDROKSID

Lagring
Holdbarhet minst 12 måneder. Lagertank bør utføres i glassfiber-armert polyester eller gummiert ståltank. Lagertank bør inspiseres og rengjøres 1 gang per år.

Vernetiltak
PAX-18 er irriterende. Kroppsdeler som kommer i kontakt med væsken skal skylles med rikelig mengder vann. Øynene skylles godt med øyenskyllevann fra spyleflaske i minst 5 minutter. Ved varig irritasjon i øynene eller på huden bør lege kontaktes.
Ved søl bør det spyles med vann og nøytraliseres med kalk eller kalkstensmel.

KEMIRA CHEMICALS AS, ØRAVN. 14, 1630 GAMLE FREDRIKSTAD,
TELEFON: 69 35 85 85, TELEFAX: 69 35 85 95
OSLOKONTOR: HAMANG TERASSE 55, 1336 SANDVIKA, TELEFON: 69358585 TELEFAX: 69358577
e-mail: *kemira.no@kemira.com*, website: *www.kemira.no*

KOA 3e 15.05.08

Appendix B: Theoretical G-value calculated for Jar-Test device at each speed

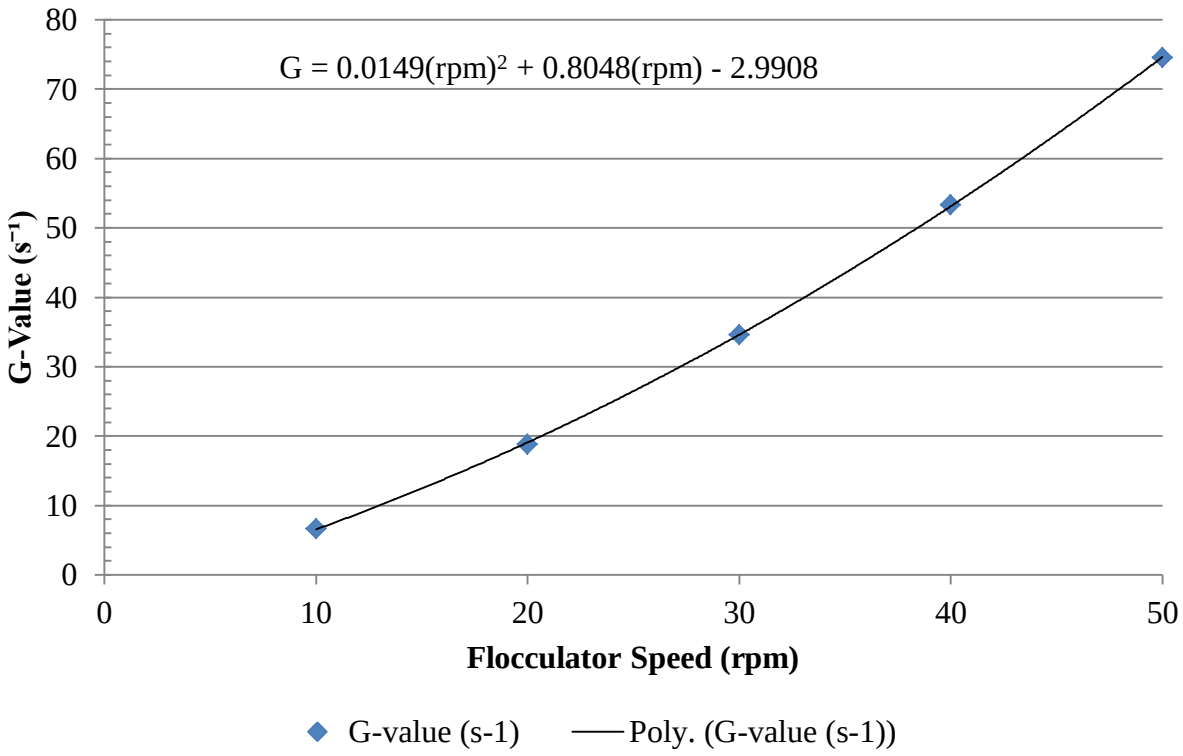

Appendix C: Practical G-value evaluation for pilot scale flocculation tank stirrer

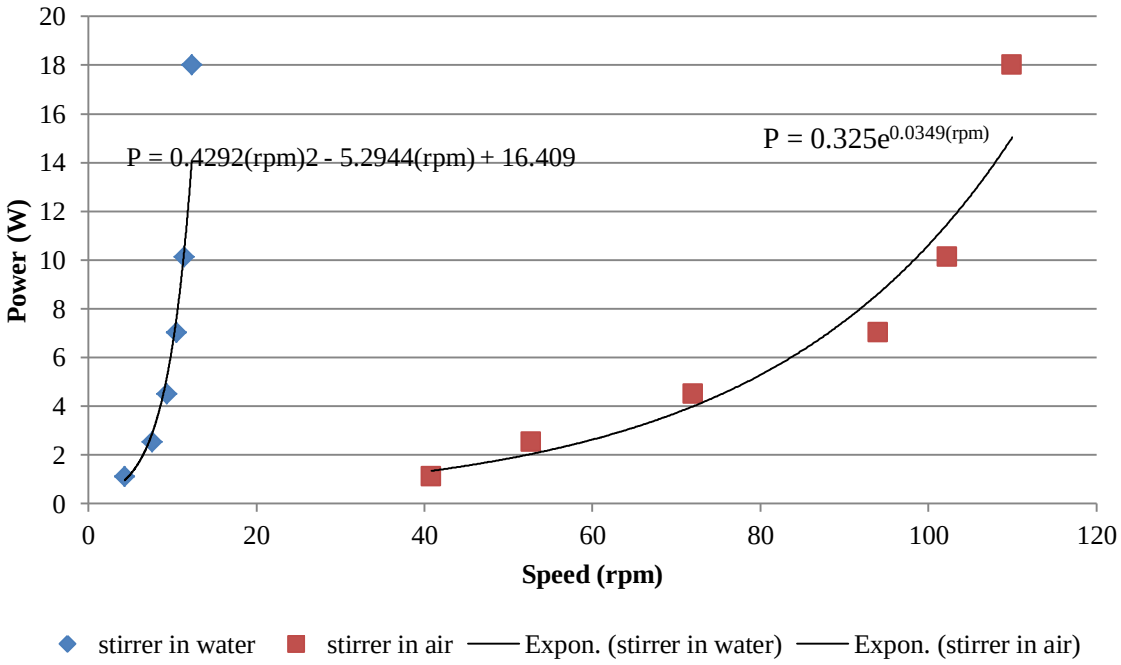

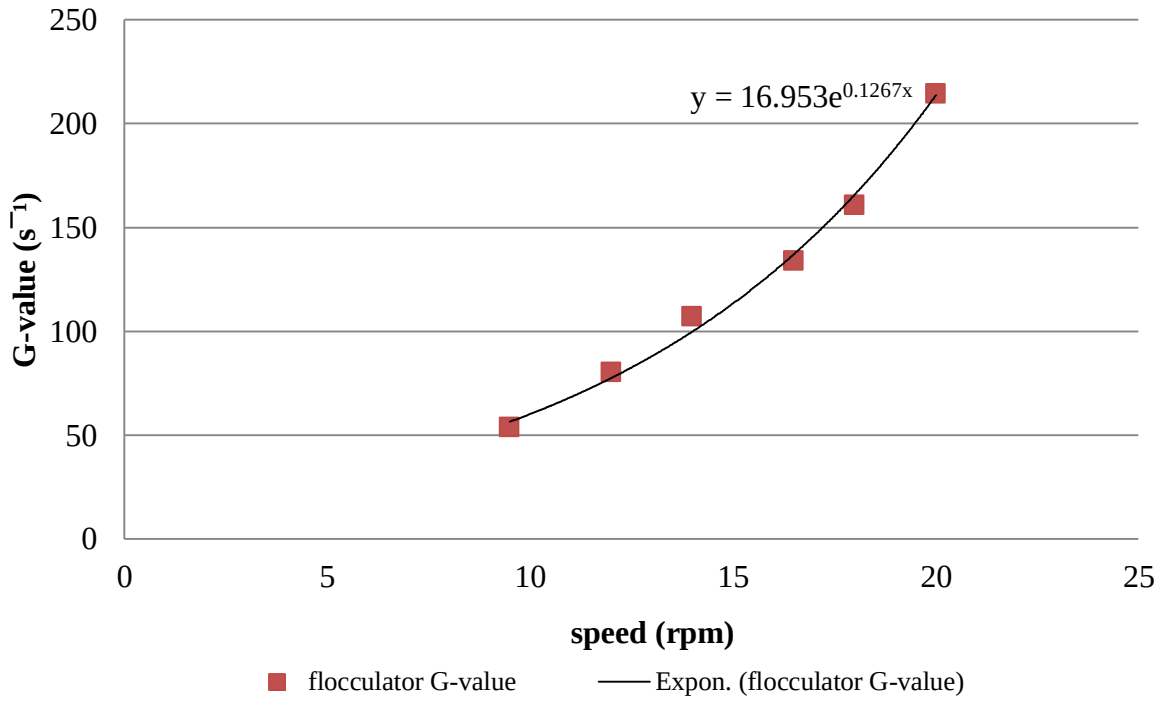

Appendix D: Dilution table prepared for dosing PAX-18

Dilution factor	mg Al/s at each point on dosing pump						
	1	2	3	4	5	6	7
Raw	30.38	53.46	79.46	95.62	122.96	136.78	137.54
2	15.19	26.73	39.73	47.81	61.48	68.39	68.77
3	10.13	17.82	26.49	31.87	40.99	45.59	45.85
4	7.59	13.37	19.87	23.91	30.74	34.20	34.38
5	6.08	10.69	15.89	19.12	24.59	27.36	27.51
6	5.06	8.91	13.24	15.94	20.49	22.80	22.92
7	4.34	7.64	11.35	13.66	17.57	19.54	19.65
8	3.80	6.68	9.93	11.95	15.37	17.10	17.19
9	3.38	5.94	8.83	10.62	13.66	15.20	15.28
10	3.04	5.35	7.95	9.56	12.30	13.68	13.75

Appendix E: SF500 belt speed conversion from percentages (%) to belt rotation/min

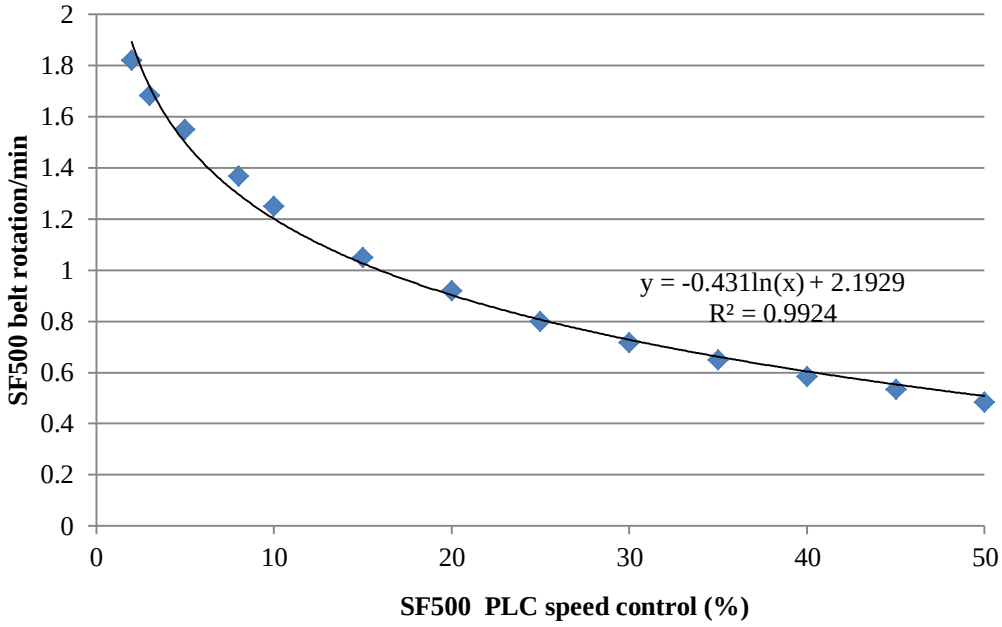

Appendix F : Individual mesh sieve SF500 PLC distribution

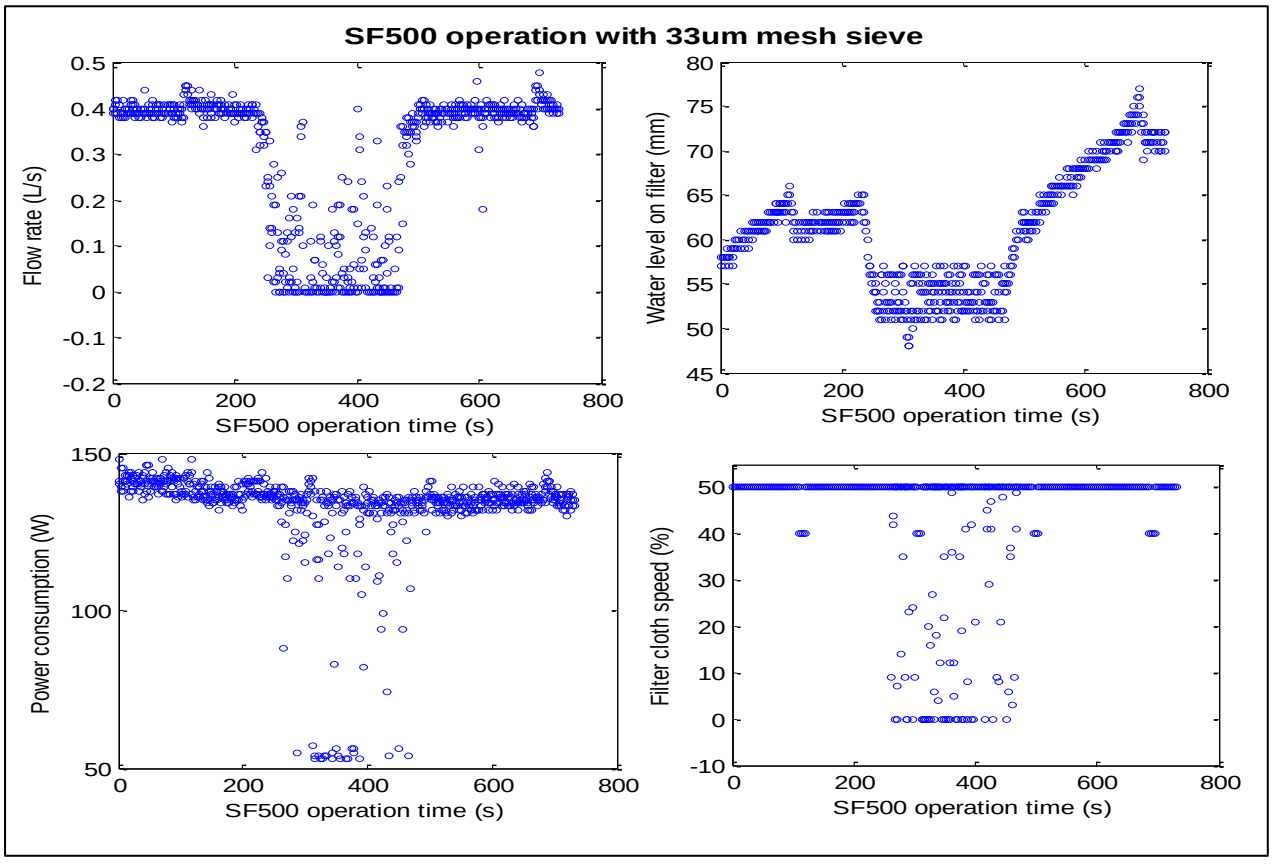

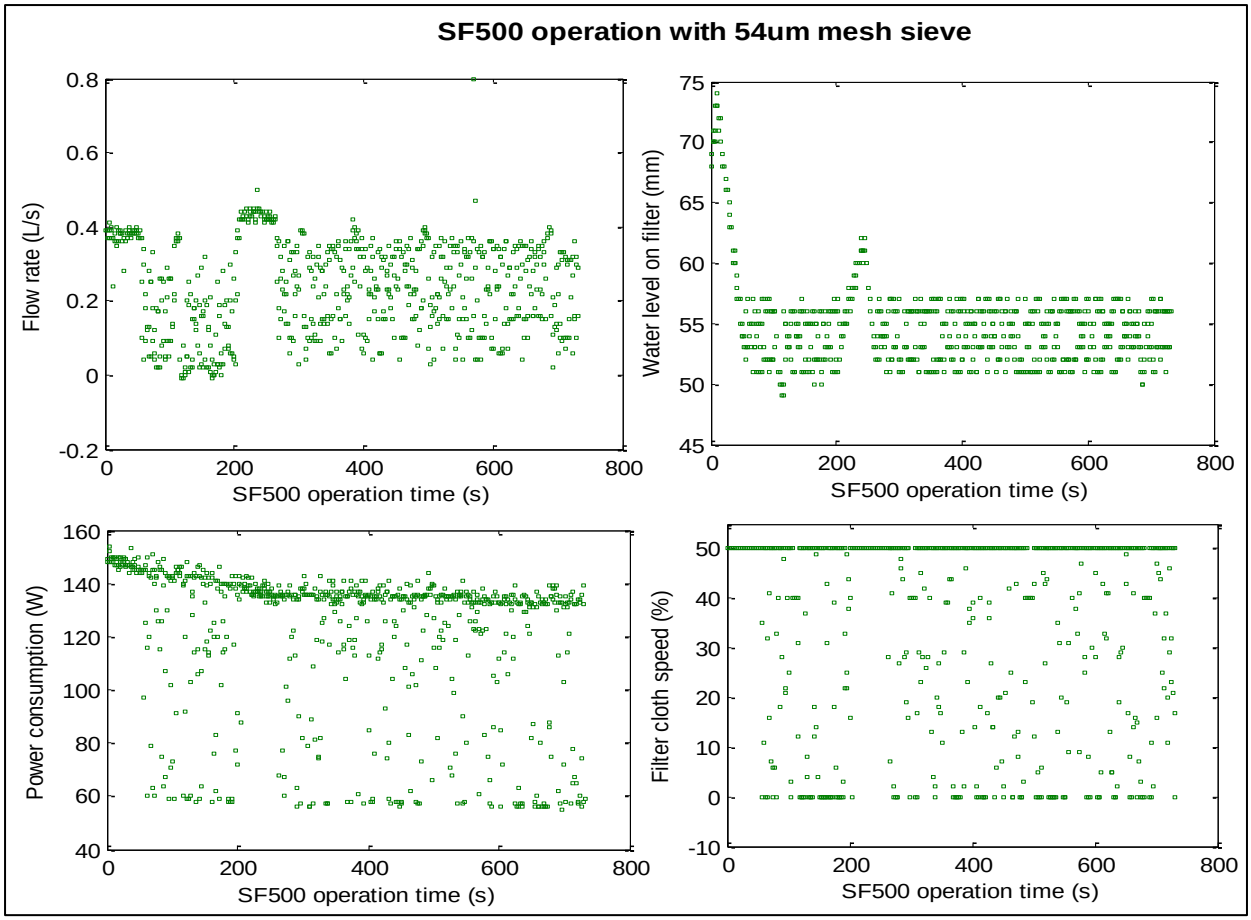
SF500 operation with 54um mesh sieve
Flow rate (L/s)
Water level on filter (mm)
Power consumption (W)
Filter cloth speed (%)
SF500 operation time (s)

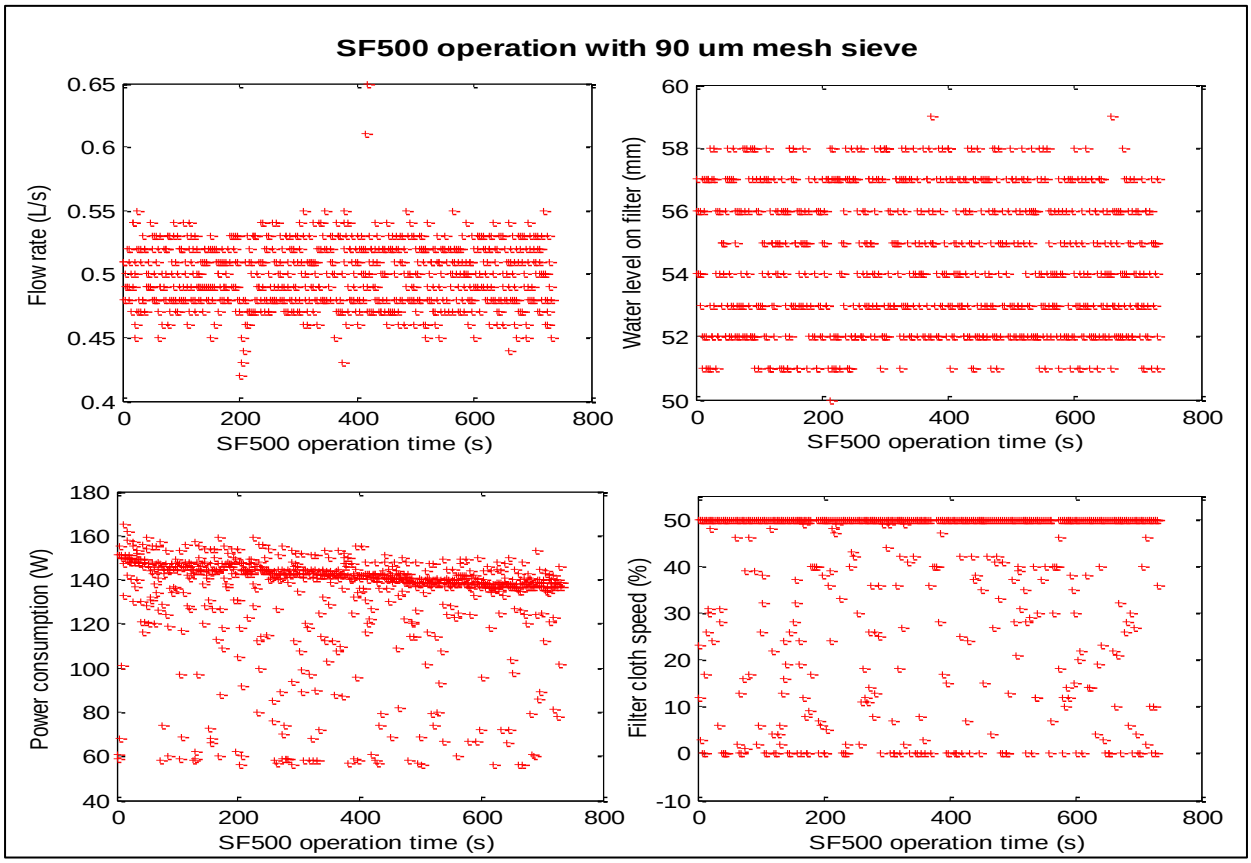
SF500 operation with 90 um mesh sieve
Flow rate (L/s)
Water level on filter (mm)
Power consumption (W)
Filter cloth speed (%)
SF500 operation time (s)

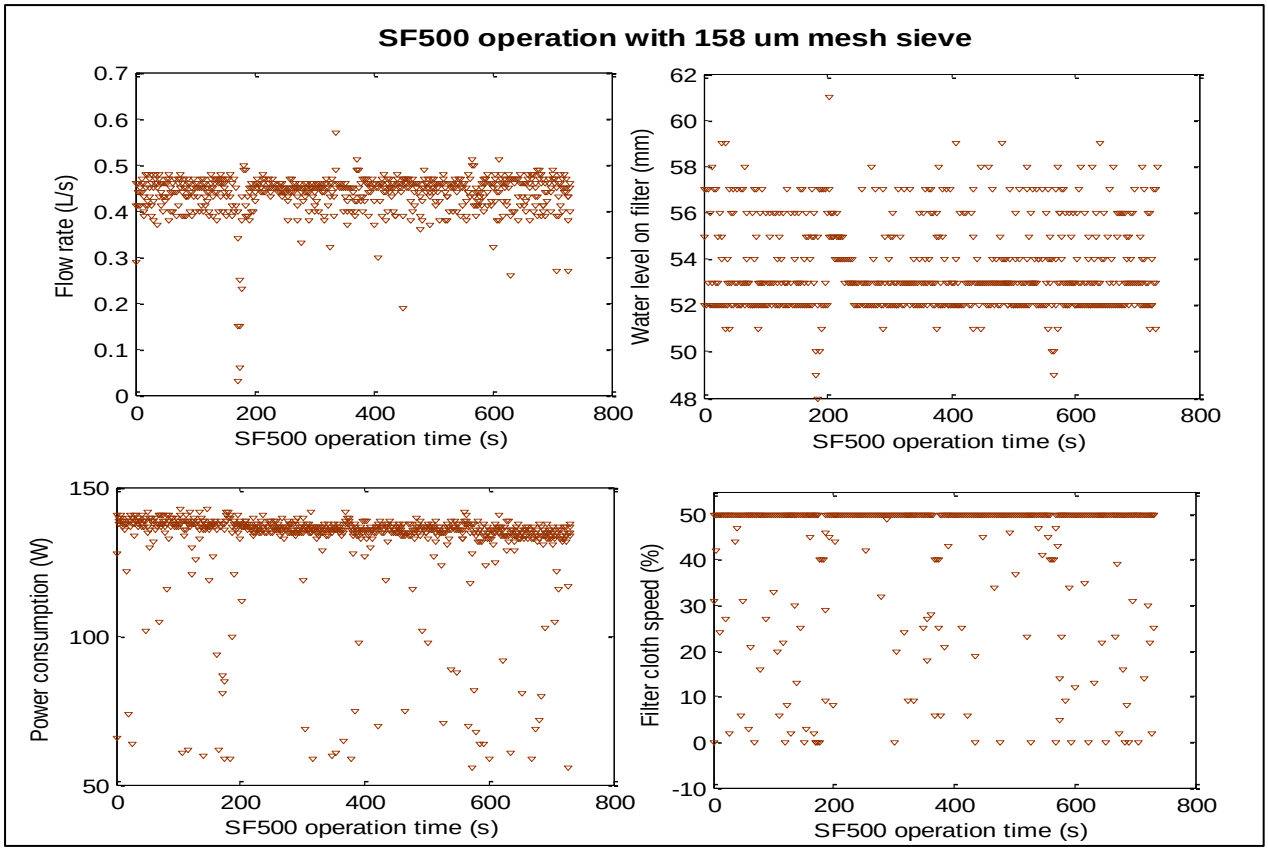
SF500 operation with 158 um mesh sieve
Flow rate (L/s)
SF500 operation time (s)
Water level on filter (mm)
SF500 operation time (s)
Power consumption (W)
SF500 operation time (s)
Filter cloth speed (%)
SF500 operation time (s)

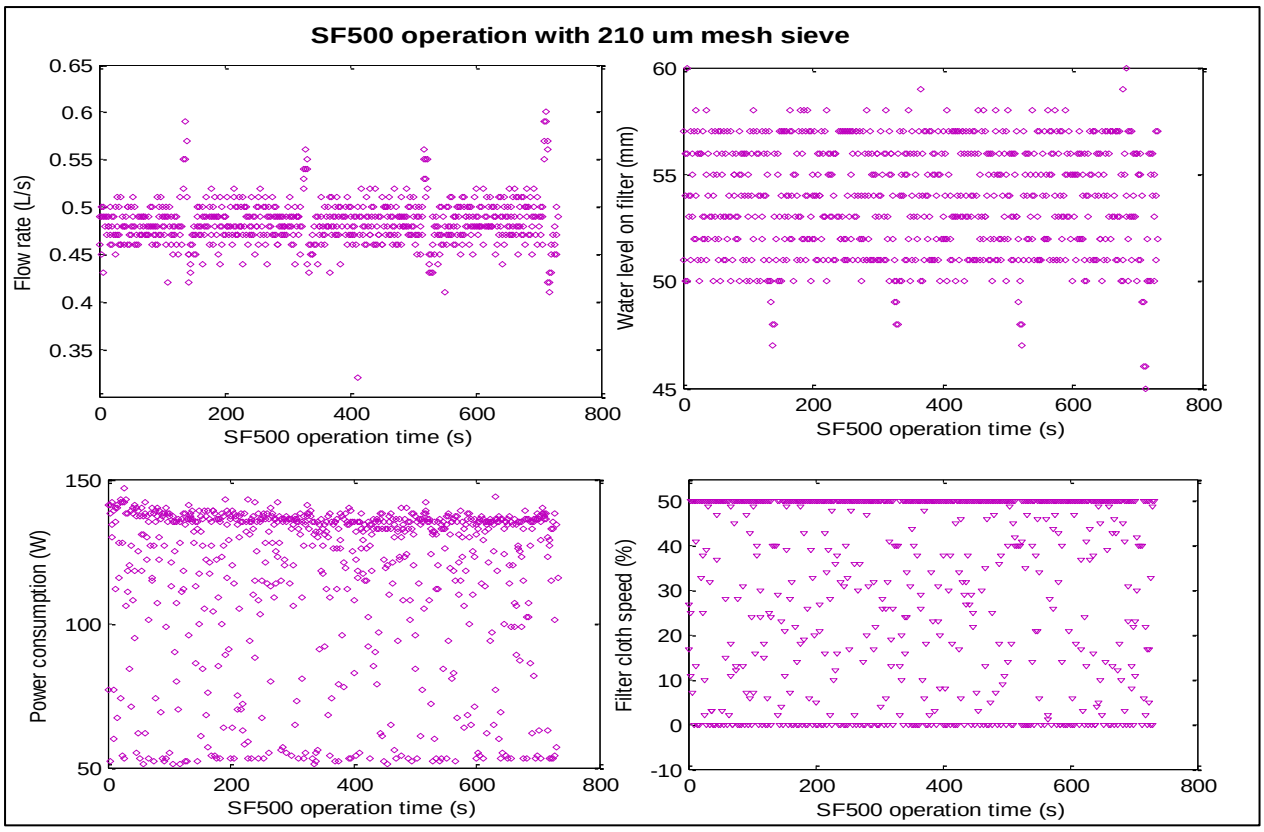
SF500 operation with 210 um mesh sieve
Flow rate (L/s)
SF500 operation time (s)
Water level on filter (mm)
SF500 operation time (s)
Power consumption (W)
SF500 operation time (s)
Filter cloth speed (%)
SF500 operation time (s)

Appendix G: PSD of each filtrate collected from each mesh sieve during NFR primary (degritted) wastewater characterization with Malvern Mastersizer 3000.

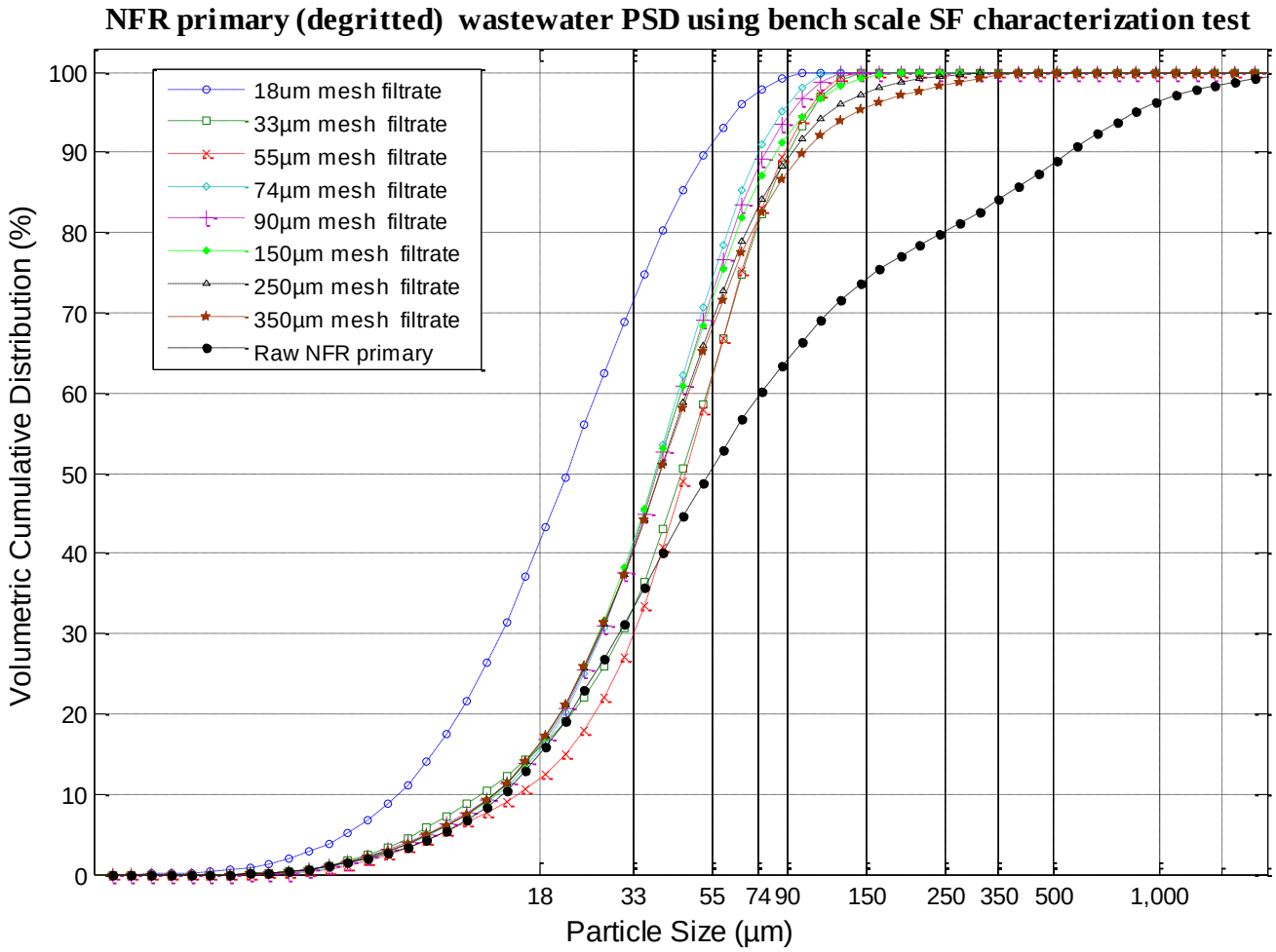

Appendix H: PSD of each filtrate collected from each mesh sieve during NFR MBBR Reactor 5 effluent wastewater characterization with Malvern Mastersizer 3000.